

Unique challenges of clay binders in a pelletised chromite pre-reduction process – a case study

Ernst L.J. Kleynhans
B.Sc. Industrial Science

Dissertation submitted in partial fulfilment of the
requirements for the degree Master of Science in
Chemistry at the Potchefstroom Campus of the
North-West University

Supervisor: Dr JP Beukes

Co-Supervisor: Dr PG van Zyl

November 2011

Potchefstroom

ACKNOWLEDGEMENTS

Since we find ourselves fashioned into all these excellently formed and marvellously functioning parts in Christ's body, let's just go ahead and be what we were made to be. What you are is God's gift to you; what you do with yourself is your gift to God

Romans 12:5 (Msg), Danish proverb

It is my honour and privilege to acknowledge and thank the following people:



My supervisor, Dr. Paul Beukes and co-supervisor, Dr. Pieter van Zyl

Prof. C.A. Strydom, Prof. M. Coetzee, Dr. L.R Tiedt



Paul Kestens, Jabu Langa

My parents, Ernst and Yvette, my family and Anzel, Thank you for your love, support, inspiration and encouragement

CONTENT

LIST OF FIGURES	vi
LIST OF TABLES	xi
ABSTRACT	1
OPSOMMING	3
GRAPHICAL OUTLINE OF THE DISSERTATION	5
CHAPTER 1: MOTIVATION AND OBJECTIVES	6
<hr/>	
1.1. Problem statement and motivation	6
1.2. Objectives	10
CHAPTER 2: LITERATURE STUDY	11
<hr/>	
2.1. General information on chromium	11
2.1.1. Origin and properties	11
2.1.2. Use of chromium	13
2.2. South Africa's ferrochrome industry	14
2.2.1. Economic and market considerations	14
2.2.2. Electricity supply	17
2.2.3. Chromite ore resources	19
2.2.4. Ferrochromium production	20

2.3. Core processes and techniques	23
2.3.1. Mining and beneficiation of chromite ores	23
2.3.2. Ferrochromium production	26
2.4. Chromite pre-reduction	28
2.4.1. Extent of pre-reduction technology commercialisation	28
2.4.2. Strategic advantages of chromite pre-reduction	31
2.4.3. Fundamental aspects of chromite pre-reduction	33
2.4.4. Factors influencing the pre-reduction of chromite	41
2.4.4.1. <i>Effect of time and temperature</i>	41
2.4.4.2. <i>Effects of additives on pre-reduction</i>	42
2.5. Clay binders	45
2.5.1. Basic principles of agglomeration	45
2.5.2. Structure and chemistry of clay binders	47
2.5.2.1. <i>Clay minerals, major constituents of raw clay materials</i>	47
2.5.2.2. <i>Smectites, mineral group of Bentonite</i>	48
2.5.2.3. <i>Palygorskite, mineral group of Attapulgite</i>	55
CHAPTER 3: MATERIALS AND METHODS	57
<hr/>	
3.1. Materials	57
3.2. Methods	58
3.2.1. Chemical and surface analysis	58
3.2.1.1. <i>Scanning Electron Microscopy and Energy Dispersive X-ray Spectroscopy</i>	58

3.2.1.2. <i>Inductively Coupled Plasma Spectrometry</i>	59
3.2.1.3. <i>Proximate analysis</i>	61
3.2.1.4. <i>Elemental analysis</i>	62
3.2.1.5. <i>X-ray Diffraction</i>	62
3.2.2. Sample material preparation	63
3.2.3. Pelletising	64
3.2.4. Pre-reduction and oxidative sintering procedure	65
3.2.5. Abrasion resistance testing	67
3.2.6. Compressive strengths testing	67
3.2.7. Thermo-Mechanical Analysis	69
3.2.8. Ash Fusion Temperature Analysis	69
3.2.9. Analysis of pre-reduction	70
3.3. Statistical handling of data	72
CHAPTER 4: RESULTS AND DISCUSSION	74
<hr/>	
4.1. Raw material characterisation	74
4.2. Characterisation of typical industrial pellets	77
4.3. Compressive strength	81
4.4. Abrasion resistance	83
4.5. XRD and Ash Fusion Temperature Analysis	84
4.6. Thermo-Mechanical Analysis	90
4.7. Pellet pre-reduction	92
4.8. Conclusions	95

CHAPTER 5: PROJECT EVALUATION AND FUTURE PERSPECTIVES	99
<hr/>	
5.1. Project evaluation	99
5.2. Future perspectives	101
5.3. Final remarks	102
BIBLIOGRAPHY	104
<hr/>	

LIST OF FIGURES

CHAPTER 2: LITERATURE STUDY

Figure 2–1:	World production in million metric tons per annum (MMTPA) for 1990-2009 (Ideas 1st Research, 2010)	15
Figure 2–2:	Stainless steel (SS) and FeCr price indexes (CRU, 2010; Ideas 1st Research, 2010)	16
Figure 2–3:	Monthly average exchange rates: South African Rand (ZAR) per U.S. Dollar (US\$) (Pacific exchange rate service, 2011)	16
Figure 2–4:	Electricity demand overview for South Africa (Basson <i>et al.</i> , 2007; Pfister, 2006)	18
Figure 2–5:	Eskom’s tariff adjustment as a percentage of consumer price index (CPI) using 1990 as a basis (Eskom, 2009)	19
Figure 2–6:	High carbon charge grade ferrochromium production 2000-2009 (ICDA, 2010)	21
Figure 2–7:	General process flow sheet for chromite ore beneficiation (Murthy <i>et al.</i> , 2011)	24
Figure 2–8:	A flow diagram adapted by Beukes <i>et al.</i> (2010) from Riekkola-Vanhanen (1999), indicating the most common process steps utilised for FeCr production in South Africa	26
Figure 2–9:	Net energy requirement for the production of 1 ton of FeCr as a function of the degree of pre-reduction achieved and charging temperature (Takano <i>et al.</i> , 2007; Niayesh & Fletcher, 1986)	33

Figure 2–10: The relationship between reduction and metallisation, based on South African LG-6 chromite treated at 1200 °C (Dawson & Edwards, 1986)	36
Figure 2–11: Standard free energies of reduction of metal oxides with carbon and carbon monoxide (Niemelä <i>et al.</i> , 2004)	38
Figure 2–12: Schematic representation of the reduction mechanism of chromite (Ding & Warner, 1997b)	40
Figure 2–13: The effect of time and temperature on the rate of chromite reduction (Barnes <i>et al.</i> , 1983)	41
Figure 2–14: The effect of various salt additives (1 wt% addition) on the reduction rate of Russian chromium ore at 1200 °C (Katayama <i>et al.</i> , 1986)	44
Figure 2–15: Magnitudes of bond strengths for various classes of interparticle bonds in pellets: (A) van der Waals, magnetic, or electrostatic forces; (B) capillary forces from the liquid phase; (C) adhesional and cohesive forces; (D) mechanical interlocking; (E) solid bridges formed by sintering or crystallisation of dissolved materials (Eisele & Kawatra, 2003; Sastry, 1996a; Sastry, 1996b)	46
Figure 2–16: Structure of the smectite crystal (Murry, 1991; Grim, 1968)	49
Figure 2–17: Effect of Ca ²⁺ ions in water on the expansion of sodium bentonite. (A) Water contains no ions, bentonite expands freely. (B) Calcium in the water can displace sodium and increase the bonding between bentonite platelets so that the expansion is reduced (Kawatra & Ripke, 2003)	50

- Figure 2–18: Conventional view of how bentonite platelets bind mineral grains in a pellet. Platelets are initially dispersed in the liquid, and the platelets bond to the mineral grains and each other as the liquid dries. Bonding is enhanced by the electrostatic attraction between the platelet faces (which have a negative charge) and the platelet edges (which are positively charged) (Van Olphen, 1987) 52
- Figure 2–19: Two bonding mechanisms of bentonite on ferrous ore particles. Diagrams A and B show the dispersion mechanism. Diagram C shows the fibre mechanism (Kawatra & Ripke, 2001) 53
- Figure 2–20: Behaviour of bentonite grains that are not completely dispersed in water. The grain expands when moistened and the platelets are lubricated by the interplatelet water. Under shear stress, the grain can then spread into a long fibre in an effect similar to spreading a deck of cards across a table (Eisele & Kawatra, 2003; Kawatra & Ripke, 2001) 54
- Figure 2–21: Scanning electron micrographs of silica sand (A) and of the same sand after bonding with bentonite (B). The bentonite formed strands stretching over and between grains, which is consistent with the bonding mechanism described by Kawatra and Ripke (2001). (A) Sand grains, AFS Fineness No. 55, taken at 250 times magnification. (B) Sand with 6.0% sodium bentonite, mixed 1.5 minutes with 3.2% water, taken at 250 times magnification (Wenninger & Green, 1970) 54
- Figure 2–22: Structure of palygorskite (attapulgite) (Murry, 1991) 55

CHAPTER 3: MATERIALS AND METHODS

Figure 3-1:	Temperature profiles used in pre-reduction and oxidative sintering experiments	66
Figure 3-2:	Graphic representation of compression strength test	68
Figure 3-3:	An example of a typical compressive strength graph	68

CHAPTER 4: RESULTS AND DISCUSSION

Figure 4-1:	SEM micrograph images of the attapulgite clay (4-1A), bentonite clay (4-1B) and chromite ore (4-1C) taken at 200 times magnification as well as the anthracite (4-1D) taken at 60 times magnification	75
Figure 4-2:	Partial SEM micrograph image taken at 45 times magnification of a polished section of an industrial pre-reduced pellet split in two (4-2A), a micrograph of an unpolished section zoomed in (650 times) on the transitional zone and showing part of the core area (4-2B), a micrograph taken at 550 times magnification of the outer layer of a polished section (4-2C), a micrograph taken at 300 times magnification of the inner core of an unpolished section (4-2D) and micrographs of the surface of an industrial pre-reduced pellet taken at 800 times (4-2E) and 650 times (4-2F) magnification	78
Figure 4-3:	Compressive strength (kN) of pre-reduced (primary axis) and oxidative sintered (secondary axis) pellets for the temperature profile up to 1250 °C and hold time of 20 min	81

Figure 4–4:	Compressive strength (kN) of pre-reduced (primary axis) and oxidative sintered (secondary axis) pellets for the temperature profile up to 1300 °C with no hold time	82
Figure 4–5:	Abrasion resistance strength indicated in weight percentage remaining above 9.5 mm versus abrasion time (note error bars were removed, since they were smaller than the markers)	84
Figure 4–6:	Qualitative XRD analysis of the attapulgite clay	86
Figure 4–7:	Qualitative XRD analysis of the bentonite clay	87
Figure 4–8:	Average percentage dimensional changes of <i>in-situ</i> pre-reduced of pellets as a function of temperature for both clays investigated at 3.5 and 10% additions	91
Figure 4–9:	Percentage pre-reduction achieved as function of clay content, for both case study clays with both temperature profiles utilised	92

LIST OF TABLES

CHAPTER 2: LITERATURE STUDY

Table 2–1:	The main commercial grades of ferrochromium according to ISO-standard 5448-81 (Lyakishev & Gasik, 1998; Downing <i>et al.</i> , 1986)	14
Table 2–2:	Production capacity of South African FeCr producers adapted from Jones (2010) by Beukes <i>et al.</i> (2011)	22

CHAPTER 3: MATERIALS AND METHODS

Table 3-1:	Microwave digestion reagents and their ratios according to sample matrix (EPA, 1996)	60
Table 3-2:	Mixing ratios of the recipes for pre-reduced and oxidative sintered pellet mixtures	64
Table 3-3:	Critical values for the rejection of quotient Q (Dean & Dixon, 1951)	73

CHAPTER 4: RESULTS AND DISCUSSION

Table 4–1:	Chemical characterization of the different raw materials utilised, with various techniques	76
Table 4–2:	SEM-EDS analysis performed on selected areas of the industrial pre-reduced pellet	79
Table 4–3:	Quantitative XRD analysis of the attapulgite and bentonite clays utilised	85

Table 4-4:	Ash fusion temperatures for the attapulgite and bentonite clays utilised	89
------------	--	----

ABSTRACT

As a result of increasing cost, efficiency and environmental pressures ferrochrome producers strive towards lower overall energy consumption. Increases in local electricity prices have placed particular pressure on South African ferrochrome producers. Pelletised chromite pre-reduction is likely the currently applied ferrochrome production process option with the lowest specific electricity consumption. In this process fine chromite, together with a carbonaceous reductant and a clay binder is milled, pelletised and pre-reduced.

In this dissertation it is demonstrated that the functioning of the clay binder in this process is not as straightforward as in conventional metallurgical pelletisation processes, since the cured pre-reduced pellets are characterised by an oxidised outer layer and a pre-reduced core. Conventional performance characteristics of clay binders (e.g. compressive strength and abrasion resistance) therefore have to be evaluated in both oxidative sintering and reducing environments. Two clay samples, i.e. attapulgite and bentonite, were obtained from a local ferrochrome producer and investigated within the context of this study. Results indicated that the compressive and abrasion resistance strengths of oxidative sintered pellets for both clays were substantially better than that of pre-reduced pellets. Thus, although the objective of the chromite pre-reduced process is to achieve maximum pre-reduction, the strength of pre-reduced chromite pellets is significantly enhanced by the thin oxidised outer layer. The strength of the bentonite-containing pellets was found to be superior in both pre-reducing and oxidative sintering environments. This is significant, since the attapulgite clay is currently the preferred option at both South African ferrochrome smelting plants applying the pelletised chromite pre-reduction process. Although not quantitatively investigated, thermo-mechanical analysis indicated that the hot strength of the attapulgite pellets could be weaker than

the bentonite-containing pellets. The possible effects of clay binder selection on the level of pre-reduction were also investigated, since it could have substantial efficiency and economic implications. For both case study clays investigated, higher clay contents resulted in lower pre-reduction levels. This has relevance within the industrial process, since higher clay contents are on occasion utilised to achieve improved green strength. The average pre-reduction of the bentonite-containing pellets were also consistently higher than that of the attapulgite-containing pellets. Again, this is significant, since the attapulgite clay is currently the preferred option. In general the case study results presented in this dissertation indicated that it is unlikely that the performance of a specific clay binder in this relatively complex process can be predicted; based only on the chemical, surface chemical and mineralogical characterisation of the clay.

Keywords: Chromite, Ferrochrome, Pre-reduction, Pelletisation, Clay binder, Attapulgite, Bentonite

OPSOMMING

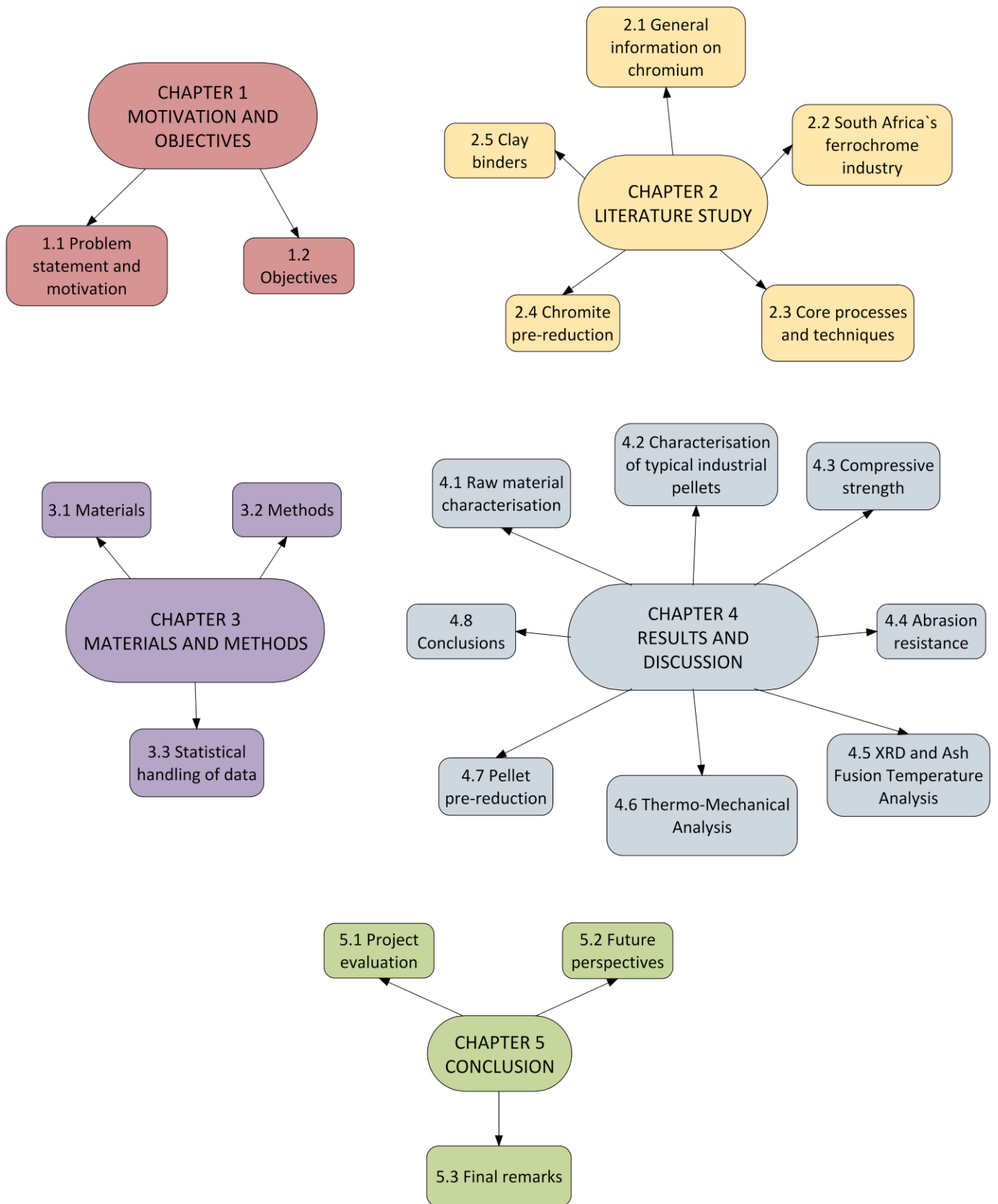
As gevolg van stygende koste, asook verhoogde druk om effektiwiteit te verbeter en omgewingsimpakte te minimaliseer streef ferrochroomprodusente daarna om hul algehele energieverbruik te verminder. Stygende elektrisiteitspryse in Suid Afrika het veral groot druk op die plaaslike ferrochroomprodusente geplaas. Tans is die pre-reduksie van chromiet waarskynlik die ferrochroomproduksieproses met die laagste spesifieke energieverbruik. In hierdie proses word fyn chromiet saam met 'n koolstofreduktant en 'n kleibinder vermaal, geagglomereer om sfeeragtige agglomerate ("pellets") te vorm en daarna geprereduseer.

In hierdie verhandeling is daar bewys dat die werking van 'n kleibinder in 'n pre-reduksie proses nie so eenvoudig is as in konvensionele metallurgiese agglomerasiëprosesse nie, aangesien die verharde geprereduseerde agglomerate gekenmerk word deur 'n geoksideerde buitenste laag en 'n geprereduseerde kern. Dus moet konvensionele vereistes waaraan 'n kleibinder moet voldoen (bv. druksterkte en slytweerstand) in beide oksidatiewe en reduserende omgewings geëvalueer word. Twee kleimonsters, naamlik attapulgië en bentoniet, is vanaf 'n plaaslike ferrochroomprodusent verkry en binne die konteks van hierdie studie ondersoek. Resultate het aangetoon dat die druksterkte en slytweerstand van oksidatief gesinterde agglomerate van albei kleie aansienlik sterker was as dié van geprereduseerde agglomerate. Dus, al is die doel van die industriële pre-reduksieproses om die maksimum pre-reduksie te bereik, word die sterkte van geprereduseerde chromiet agglomerate aansienlik verbeter deur die dun geoksideerde buitenste laag. Daar is ook gevind dat die druksterkte en slytweerstand van agglomerate wat bentoniet bevat het superieur was in beide oksidatiewe en reduserende omgewings. Dit is betekenisvol omdat beide Suid Afrikaanse ferrochroomsmelters wat gebruik

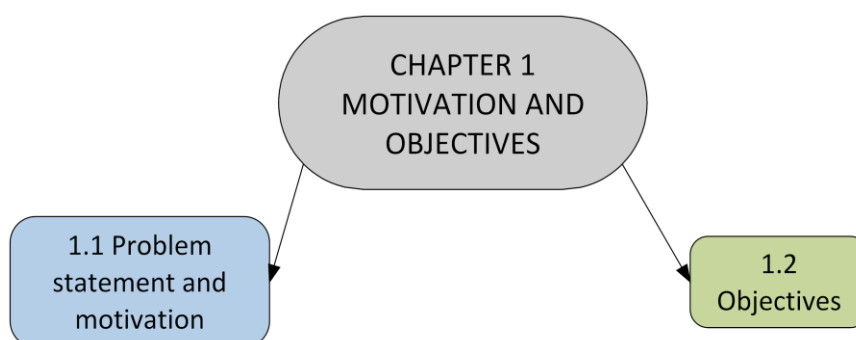
maak van die pre-reduksie proses tans attapulgië as binder verkies. Alhoewel die sterkte van geprereduseerde agglomerate by hoër temperature nie kwantitatief ondersoek kon word nie het termo-meganiese analises wel getoon dat agglomerate wat attapulgië bevat moontlik swakker is as agglomerate wat bentoniet bevat. Die effek van kleibinder-seleksie op die vlak van pre-reduksie wat behaal kon word is ook ondersoek, aangesien dit aansienlike effektiwiteits- en ekonomiese implikasies tot gevolg kan hê. Vir albei kleie het resultate aangetoon dat 'n hoër klei-inhoud die vlak van pre-reduksie verlaag. Dit is relevant tot die industriële proses, omdat die klei-inhoud somtyds verhoog word om die groensterkte van nuutgevormde agglomerate te verbeter. Die gemiddelde vlak van pre-reduksie van agglomerate wat bentoniet bevat het was konstant hoër as agglomerate wat attapulgië bevat het. Weereens is dit betekenisvol, omdat attapulgië tans as binder verkies word. Die resultate van hierdie gevallestudie toon aan dat dit onwaarskynlik is dat die prestasie van 'n spesifieke kleibinder in hierdie relatief komplekse proses voorspel kan word deur slegs die chemiese, oppervlak-chemiese en mineralogiese karakterisering van die klei te oorweeg.

Sleutelwoorde: Chromiet, Ferrochroom, Pre-reduksie, Agglomerasie, Klei binder, Attapulgië, Bentonite

GRAPHICAL OUTLINE OF THE DISSERTATION



CHAPTER 1: MOTIVATION AND OBJECTIVES



1.1. Problem statement and motivation

Chromium is a versatile element that is used in numerous applications in the metallurgical, chemical and refractory industries. It is one of the most fundamentally important metals in the modern steel industry, with no adequate replacement for it in corrosion, oxidation-resistant or high temperature alloys. This, combined with the fact that geographically chromium ore (chromite) reserves are very limited, chromium is regarded as a commodity of critical and strategic importance (Murthy *et al.*, 2011; Ideas 1st Research, 2010; Akyüziü & Eric, 1992).

Mined chromite ore, containing chromium in the characteristic spinel mineral form, is the only commercially viable source of new chromium units (Murthy *et al.*, 2011; Beukes *et al.*, 2010; Cramer *et al.*, 2004). South Africa holds approximately 75% of the world's exploitable chromite resources (Lungu, 2010; Basson *et al.*, 2007; Basson *et al.*, 2007; Cramer *et al.*, 2004; Riekkola-Vanhanen, 1999; Cowey, 1994; Howat, 1986), with other smaller but substantial deposits occurring in Kazakhstan, Zimbabwe, India and Finland (Papp, 2009a). Approximately 90-95% of mined chromite ore is consumed by the metallurgical industry for the production of different grades of ferrochrome (FeCr). The

stainless steel industry consumes 80-90% of FeCr produced, primarily as high-carbon or charge grade (Murthy *et al.*, 2011; CRU, 2010; ICDA, 2010). Stainless steel markets have been growing at a rate of 5% per year on average. This trend is predicted to continue and likely to increase to approximately 8% in 2020, thus further increasing the demand for FeCr. FeCr production levels of 7 million t/y were reached in 2007 and 2008 (ICDA, 2010; Ideas 1st Research, 2010) and are predicted to double by 2020 (CRU, 2010; ENRC, 2008; Holappa & Xiao, 2004).

Most FeCr is produced by means of smelting chromite in submerged arc furnaces (SAF) in the presence of carbonaceous reducing agents (Singh & Mohan Rao, 2008; Sing *et al.*, 2007; Weber & Eric, 2006; Akyüziü & Eric, 1992). Historically, the use of fine chromite (usually < 6mm) in this process is limited, since fine materials increases the tendency of the surface layer of the SAF to sinter. This traps evolving process gas, which can result in so-called bed turnovers and blowing of the furnace that could have disastrous consequences (Beukes *et al.*, 2010; Riekkola-Vanhanen, 1999). The majority of South African chromite ore is relatively friable (Beukes *et al.*, 2010; Glastonbury *et al.*, 2010; Cramer *et al.*, 2004; Gu & Wills, 1988), thus an agglomeration (e.g. pelletisation) step is required, prior to feeding it into the SAF (Beukes *et al.*, 2010; Singh & Mohan Rao, 2008; Pei & Wijk, 1993).

Internationally South Africa is the leading producer of FeCr (ICDA, 2010). There are currently fourteen separate FeCr smelter plants in South Africa, with a combined production capacity of 4.7 million t/y (Beukes *et al.*, 2011; Jones, 2010). The abundant chromite resources and the relatively low historical cost of electricity have contributed to South Africa's dominant position in the FeCr industry (Basson *et al.*, 2007). However, South Africa's electricity demand has caught up with electricity-generating capacity (Baker, 2006). This has led to a dramatic increase in electricity prices that is set to continue for the foreseeable

future (Basson *et al.*, 2007). In the period 1980 to 2005 South Africa's nominal electricity price increased steadily at a rate of roughly 0.58 cents/kWh per year (NERSA, 2009b). According to statistic from the National Energy Regulator of South Africa (NERSA) the nominal price of electricity increased by 174% at a rate of about 4.7 cents/kWh per year from 19 cent/kWh in 2007 to 33.14 cent/kWh in 2010 (NERSA, 2009a; NERSA, 2009b). NERSA has since granted Eskom a three-year rate increase resulting in electricity costs of 41.57 cents/kWh for 2010/11, 52.30 cents/kWh for 2011/12 and 65.85 cents/kWh for 2012/13 (Eskom, 2011; NERSA, 2009a). Considering that electricity consumption is the single largest cost component in FeCr production (Daavittila *et al.*, 2004), the afore-mentioned cost increases are very significant. However, the pressure on South African FeCr producers is not unique, since globally lower specific energy consumption (MWh/t FeCr) and a decreased carbon footprint have become driving factors.

Another cause for concern that has emerged out of the above-mentioned electrical generation capacity limitations is the export of unbeneficiated (raw) chromite ore, in particular to China (Creamer, 2011). This could place South African FeCr producers under additional production cost pressure. When chromite is converted locally into FeCr, significant value addition takes place and employment opportunities are created. Considering South Africa's high unemployment rate, the export of large amounts of raw chromite ore will certainly have a negative impact on South Africa's socioeconomic circumstances (Creamer, 2011; Ideas 1st Research, 2010).

Historically, the specific energy consumption of conventional SAF was 3.9-4.2 MWh/t FeCr (Naiker & Riley, 2006; Weber & Eric, 2006). Several processes have been developed to minimise energy consumption (Outotec, 2009; Pei & Wijk, 1993; Niayesh & Fletcher, 1986). However, the technology that is of interest to this study is the pre-reduction of chromite (Takano *et al.*, 2007; Ding & Warner,

1997a; Lekatou & Walker, 1997; Dawson & Edwards, 1986), which is applied at two FeCr smelter plants in South Africa (Beukes *et al.*, 2010; McCullough *et al.*, 2010; Naiker, 2007; Naiker & Riley, 2006). In this process fine chromite ore, a clay binder and a carbon reductant are dry-milled, pelletised and pre-heated before being fed into a rotary kiln where the chromite is partially pre-reduced. The pre-reduced pellets are then charged hot, immediately after exiting the kiln, into closed SAF (Beukes *et al.*, 2010; Naiker, 2007). The advantages of pelletised pre-reduced feed are observed in all aspects of operation, i.e. ability to consume fine chromite, much lower specific energy consumption of approximately 2.4 MWh/t, chromium recoveries in the order of 90% and the ability to produce a low silicon containing FeCr product (McCullough *et al.*, 2010; Naiker, 2007; Takano *et al.*, 2007; Botha, 2003). It can therefore only be assumed that this process option will become more commonly applied, as pressure on energy consumption and environmental consciousness increase.

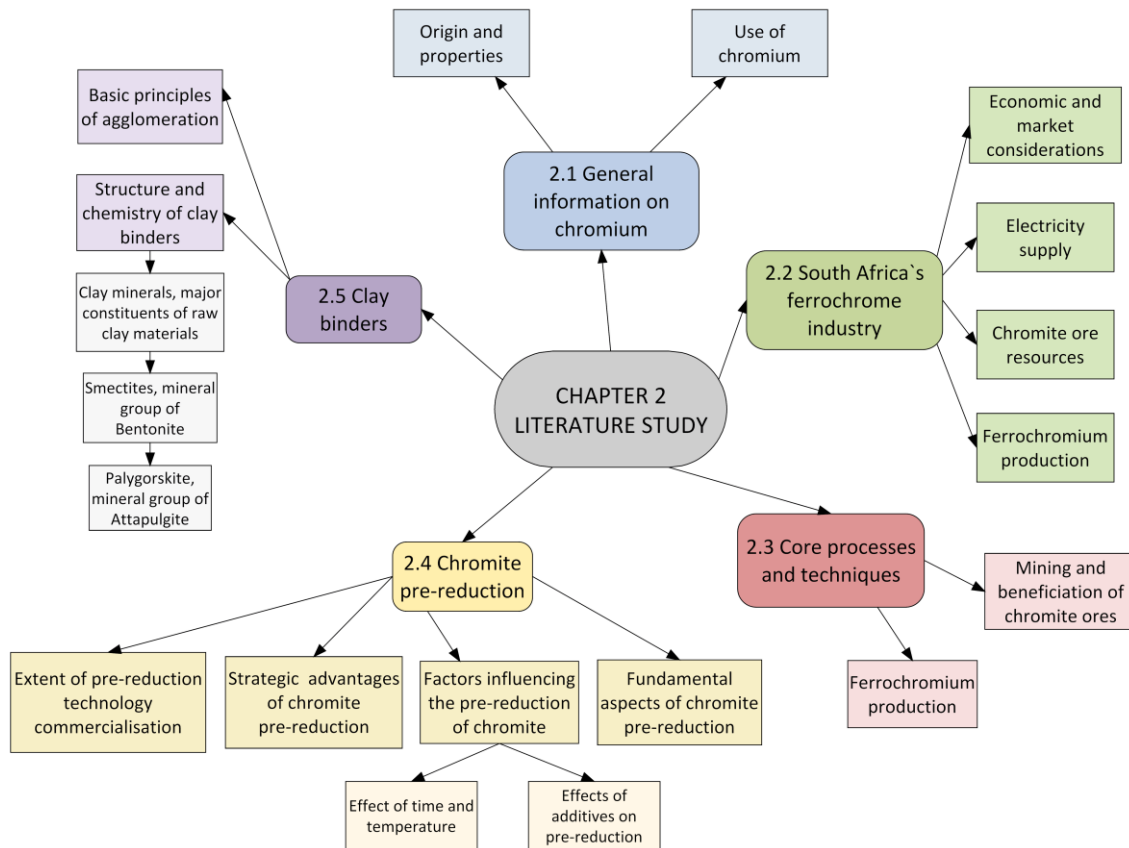
In the pelletised chromite pre-reduction process clay is added to the raw material mixture to act as a binder for the green pellets (newly formed) and to aid in the cured strengths of the pelletised agglomerates. This is not unique, since clay binders also play a similar role in other chromite pelletisation processes. However, due to the unique nature of the pelletised chromite pre-reduction process, there are also other aspects that should be considered during clay selection. In this case study, these unique process considerations of clay binders in the chromite pre-reduced process are highlighted and demonstrated utilising two case study clays.

1.2. Objectives

The specific objectives of this case study are as follows:

- i) The compilation of a comprehensive literature survey in which the importance of the FeCr industry in South Africa, the core processes utilised by this industry, the significance of chromite pre-reduction and a general overview of clay binders utilised in this industry are reported.
- ii) Obtaining and characterisation of typical raw material utilised in the production of pre-reduced pelletised feed, as well as characterisation of typical industrially produced pre-reduced pellets using appropriate techniques.
- iii) Identifying unique process performance requirements that a clay binder has to fulfil in a pelletised chromite pre-reduction process, from the above-mentioned industrially produced pre-reduced pellet characterisation.
- iv) Designing and conducting experimental procedures to test clay performance of two case study clays in terms of the process performance requirements identified in objective (iii).
- v) Analysing the experimental results obtained and making recommendations with regard to the selection of clay binders utilised in the pelletised chromite pre-reduction process.
- vi) Making recommendations with regards to further research work in this field.

CHAPTER 2: LITERATURE STUDY



2.1. General information on chromium

2.1.1. Origin and properties

Chromium is the ninth most abundant compound in the earth's crust and exists in various mineral forms; however chromite is the only source that is economically feasible to exploit commercially (Roza, 2008; IETEG, 2005; Nriagu & Nieboer, 1988). Chromite ore that is commercially produced is found in South Africa, India, Kazakhstan, Turkey, Oman, Russia, Brazil, Finland, Zimbabwe, Pakistan, Australia, Albania, China and Iran. Chromite deposits are also found in many other countries like Madagascar, Vietnam, United Arab Emirates, Sudan,

Cuba, the Philippines, Afghanistan, Greece and the USA (Papp, 2011; Papp, 2009a; Papp, 2008).

Pure chromium has a bluish-silver colour. It is a lustrous, hard but brittle, malleable metal and can take a high polish. It is odourless and tasteless. Chromium has a high melting and boiling point, 1907 °C and 2671 °C respectively. It has a density near room temperature (20 °C) of 7.15 g/cm³ and a liquid density of 6.3 g/cm³ at its melting point. The heat of fusion of chromium is 21 kJ/mol, its heat of vaporisation is 339.5 kJ/mol and it has a specific heat capacity of 23.35 J/mol.K at 25 °C (Lide, 2009; Roza, 2008; IETEG, 2005).

Chromium is a member of the transition metals. The oxidation states of chromium range between Cr²⁺ and Cr⁶⁺, but it most commonly occurs as Cr⁰, Cr²⁺, Cr³⁺ and Cr⁶⁺. Chromium in the 2+ oxidation state is, however, rather unstable and is rapidly oxidised to the 3+ state, thus only the trivalent and hexavalent forms are found in nature. Trivalent chromium is of nutritional importance for a large range of organisms. In trace amounts it influences sugar and lipid metabolism in humans and a shortage is suspected to cause a disease called chromium deficiency. Chromium is found in humans at 30 ppb by body mass. In contrast, airborne hexavalent chromium is considered to be carcinogenic (IETEG, 2005; Anon, 1974).

The oxidation potential of hexavalent to trivalent chromium is strong, and it is highly unlikely that oxidation of the trivalent form could occur *in vivo* (Anon, 1974). The hexavalent form of chromium is almost always linked to oxygen and is a strong oxidising agent. The most important chromium ions are chromates and dichromates. These ions are easily reduced to trivalent chromium (Schroeder, 1970).

The trivalent state is the most stable and important oxidation state of chromium. In this state it forms complexes whose ligand exchange rates are

low. Trivalent chromium forms octahedral complexes of coordination number six. A large number of these complexes are known. It is because of this kinetic inertness that these compounds can persist for long periods in solution, even in conditions that are thermodynamically unstable (Anon, 1974). All hexavalent chromium compounds except chromium hexafluoride, CrF_6 , are oxo-compounds. Acid solutions of dichromate are strong oxidising agents. Chromium metal resists attack by a wide variety of chemicals at normal temperatures, but reacts with many of them at high temperatures. It reacts with several common acids with evolution of hydrogen and it reacts slowly with diluted sulphuric acid. Chromium is soluble in aqueous hydrogen fluoride, hydrogen chloride, hydrogen bromide and hydrogen iodide, and forms Cr^{2+} as long as air is not present. Chromium resists attack from phosphoric acid and many organic acids, including formic, citric and tartaric acid. It is, however, slowly attacked by acetic acid. Chromium is insoluble in nitric acid and aqua regia. These acids as well as many other oxidising agents like chlorine, bromine, solutions of hydrochloric acid and chromium oxide make chromium passive and render it relatively non-reactive. It is also slowly passivated by superficial oxidation in air. Passive chromium can be made active by a reduction process such as treatment with hydrogen gas or by immersion in diluted sulphuric acid while bringing the chromium into contact with zinc below the surface of the acid. Passive chromium acts somewhat like a noble metal and is not attacked by mineral acids but it is very active in the non-passive state. The passivation of chromium is due to the fact that oxygen is absorbed onto the surface that leads to the formation of an oxide coat (Anon, 1974).

2.1.2. Use of chromium

Different forms of chromium are required for different applications. The chromite ore produced globally each year is divided into three principal industrial end-uses, i.e. metallurgical, refractory and chemical applications

(IETEG, 2005; Anon, 1974). Approximately 90-95% of mined chromite is consumed by the metallurgical industry for the production of different grades of FeCr, indicated in Table 2–1. The stainless steel industry consumes 80-90% of FeCr, primarily as high-carbon or charge grade FeCr (Murthy *et al.*, 2011; CRU, 2010; ICDA, 2010; Abubakre *et al.*, 2007).

Table 2–1: The main commercial grades of ferrochromium according to ISO-standard 5448-81 (Lyakishev & Gasik, 1998; Downing *et al.*, 1986)

	% Cr	%C	%Si	%P	%S
High Carbon FeCr (HC FeCr)	45-70	4-10	0-10	< 0.05	< 0.10
Medium Carbon FeCr (MC FeCr)	55-75	0.5-4	< 1.5	< 0.05	< 0.05
Low Carbon FeCr (LC FeCr)	55-95	0.01-0.5	< 1.5	< 0.03	< 0.03
Charge grade	53-58	5-8	3-6		

2.2. South Africa’s ferrochrome industry

2.2.1. Economic and market considerations

Although this dissertation is for the most part technically orientated, a small section is devoted to understanding the economic and market considerations impacting on the local ferrochromium industry.

Chromite ore is mined in over twenty countries, but about 80% of the production originates from four countries, i.e. during 2007-2009 South Africa accounted for 37% of the world’s production, with both India and Kazakhstan accounting for around 16% and Turkey for 8% (ICDA, 2010; Papp, 2009b; Papp, 2008). As previously mentioned (Par. 2.1.2), the majority of chromite is converted into FeCr, which in turn is mostly consumed for stainless steel production (CRU, 2010; ICDA, 2010). It is therefore useful to consider the correlation between chromite, FeCr and stainless steel production volumes.

Figure 2–1 indicates that there is a direct correlation, with some lags, between the production volume trends of these commodities.

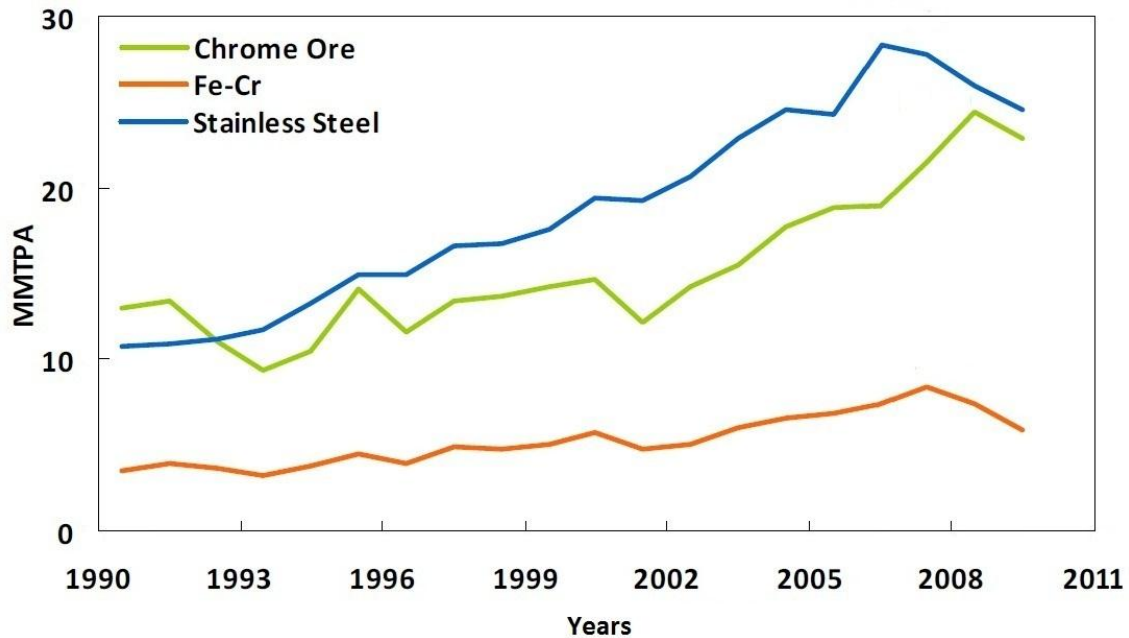


Figure 2–1: World production in million metric tons per annum (MMTPA) for 1990-2009 (Ideas 1st Research, 2010)

From Figure 2–1 it is obvious that if the demand for stainless steel increases the demand for FeCr will automatically follow suit. This will either lead to a supply deficiency and a rise in FeCr prices or an increase in FeCr production, or both. Figure 2–2 indicates the correlation between the stainless steel and FeCr price indexes.

The South African Rand exchange rate is a potentially significant factor in the price of chromite ore and FeCr because South Africa is a leading producer of these materials (Papp, 2008). South Africa is also the largest and second largest exporter of platinum and gold respectively, thus it is expected that these two markets would have a significant influence on South Africa’s currency (Ideas 1st Research, 2010). Figure 2–3 shows the monthly average South African Rand (ZAR) per U.S. Dollar (US\$) exchange rate (Pacific exchange rate service, 2011).

From these exchange rate fluctuations the volatility and possible financial effect on the South African ferrochromium industry are evident.

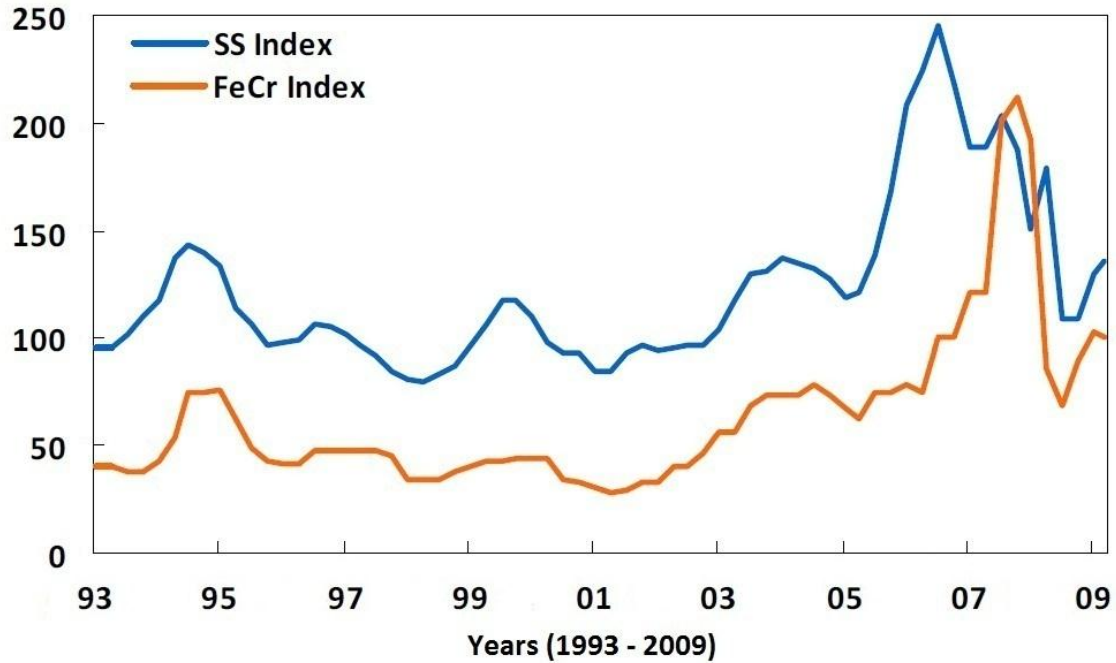


Figure 2-2: Stainless steel (SS) and FeCr price indexes (CRU, 2010; Ideas 1st Research, 2010)

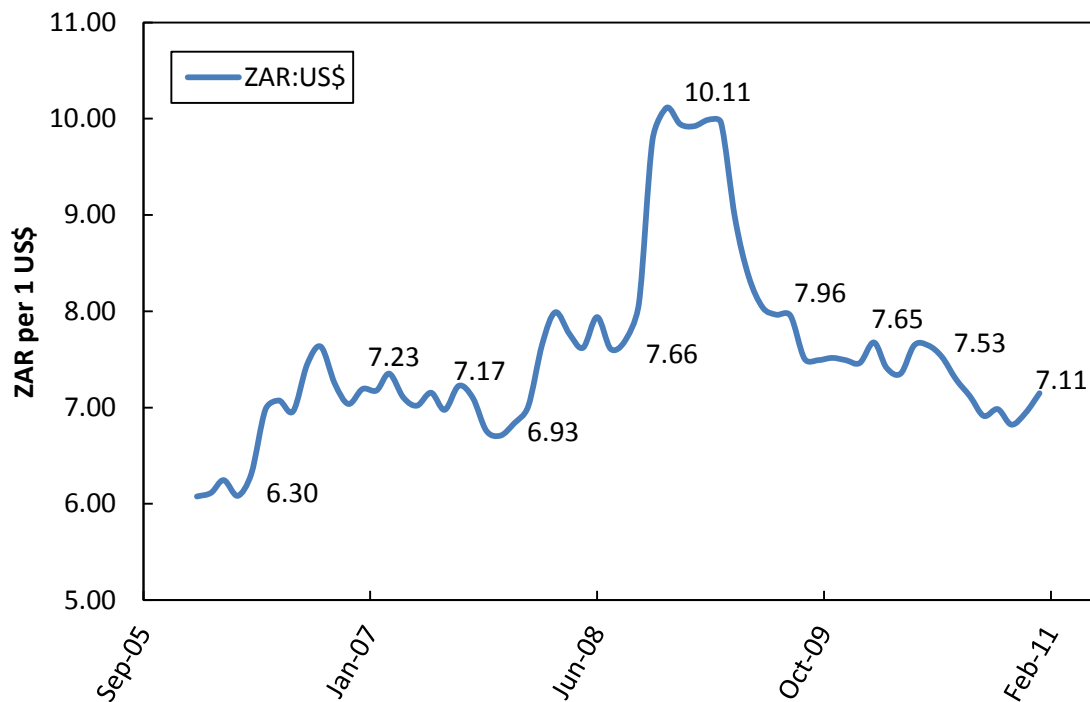


Figure 2-3: Monthly average exchange rates: South African Rand (ZAR) per U.S. Dollar (US\$) (Pacific exchange rate service, 2011)

Another factor that has a significant impact on the South African FeCr industry is the availability of suitable reductants. Coal, anthracite, char and coke are the main sources of carbon (Makhoba & Hurman Eric, 2010). For FeCr production a reductant with a low ash, low phosphorus and low sulphur content is required (Ideas 1st Research, 2010; Makhoba & Hurman Eric, 2010; Basson *et al.*, 2007). Due to the specific properties required, reductant availability is a cause of concern for FeCr producers. Moreover, there is no regulation within reductant markets and therefore over-supply or shortages may occur regularly resulting in enormous price fluctuations. In addition, the steel industry has a major influence on the dynamics of coking coal prices (Ideas 1st Research, 2010; Makhoba & Hurman Eric, 2010).

2.2.2. Electricity supply

Electricity supply is also an economic and market consideration and it could therefore have been discussed in Par. 2.2.1. However, the relevance of it within the context of this study necessitates a separate discussion thereof.

The electricity demand of South Africa has caught up with its electricity generating capacity (Baker, 2006). The historic supply-demand overview of electricity in South Africa up to 2007 is shown in Figure 2–4 (Basson *et al.*, 2007; Pfister, 2006). From this it is clear that the availability of surplus generation capacity has significantly been eroded. Realistically it can be expected that this trend continued beyond 2007, to 2011. The erosion of surplus generation capacity has led to a dramatic increase in electricity prices, indicated in Figure 2–5, that is set to continue in the foreseeable future (Basson *et al.*, 2007). In the period 1980 to 2005 the nominal electricity price in South Africa increased steadily at a rate of roughly 0.58 RSA cents/kWh per year (NERSA, 2009b). According to statistics from the National Energy Regulator of South Africa (NERSA), the nominal price of electricity increased by 174% from 2007 to 2010

(NERSA, 2009a; NERSA, 2009b). NERSA has since granted Eskom a three-year rate increase resulting in electricity costs of 41.57 RSA cents/kWh for 2010/11, 52.30 RSA cents/kWh for 2011/12 and 65.85 RSA cents/kWh for 2012/13 (Eskom, 2011; NERSA, 2009a). Considering that electricity consumption is the single largest cost component in FeCr production (Daavittila *et al.*, 2004), the afore-mentioned cost increases are extremely significant. However, the pressure on South African FeCr producers is not unique, since globally lower specific energy consumption (MWh/t FeCr) and a decreased carbon footprint have become driving factors.

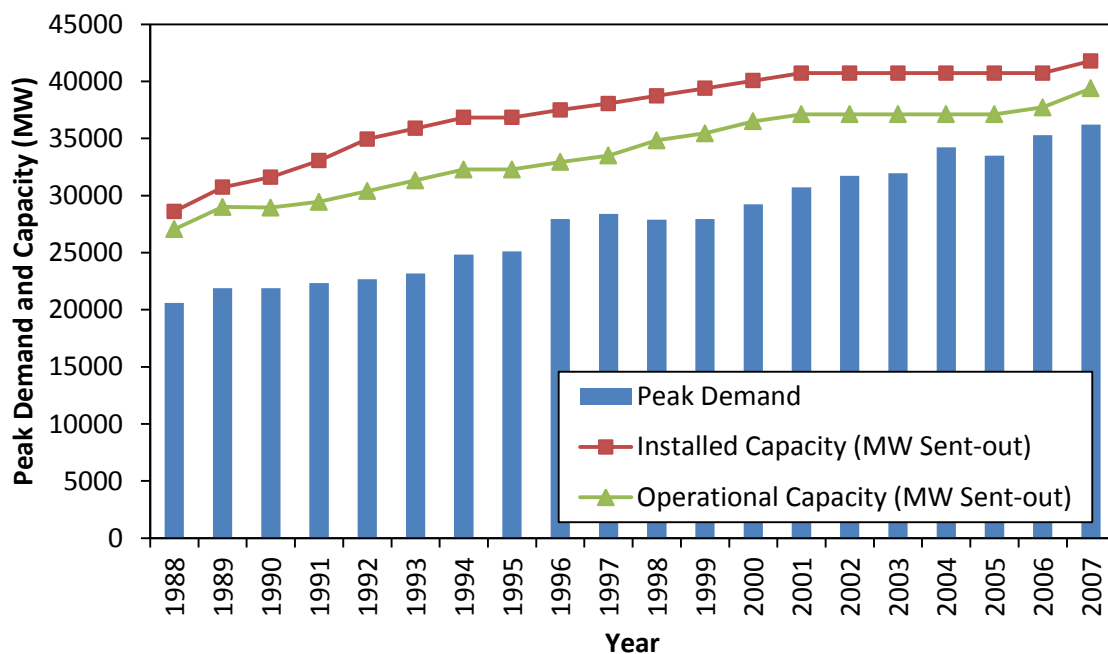


Figure 2-4: Electricity demand overview for South Africa (Basson *et al.*, 2007; Pfister, 2006)

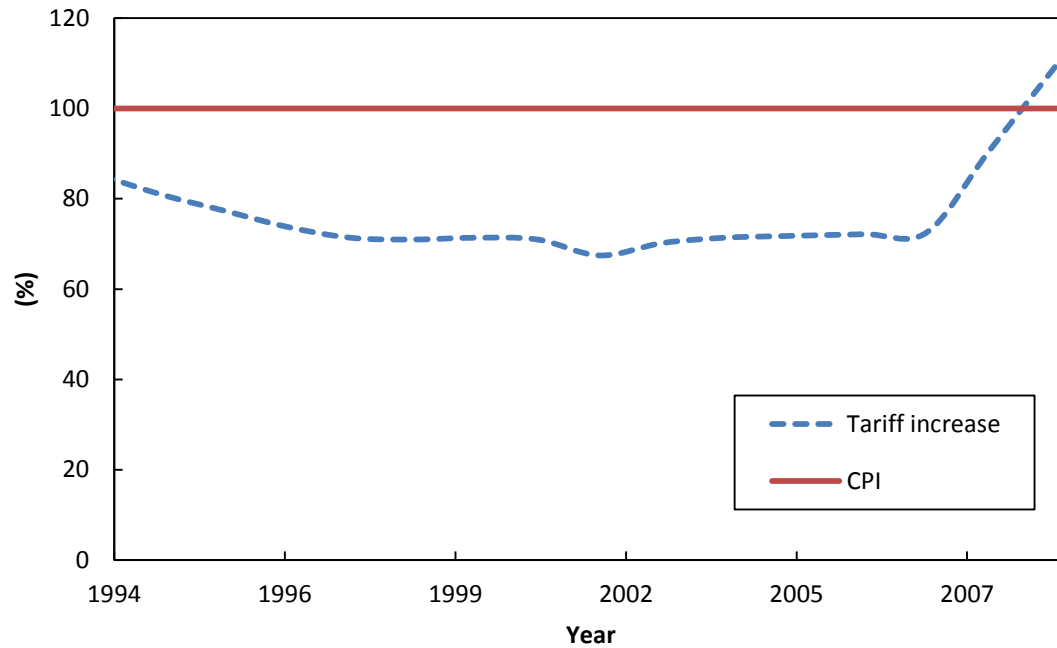


Figure 2–5: Eskom’s tariff adjustment as a percentage of consumer price index (CPI) using 1990 as a basis (Eskom, 2009)

2.2.3. Chromite ore resources

The United States Geological Survey (USGS) define shipping-grade chromite ore as the deposit quantity and grade normalised to 45% Cr₂O₃. The total world shipping-grade chromite ore reserves are estimated by the USGS at around 474 million tonnes (Papp, 2008; Basson *et al.*, 2007). According to various sources South Africa holds from 68% to 80% of the world’s economically viable chromite ore reserves (Lungu, 2010; Basson *et al.*, 2007; Cramer *et al.*, 2004; Riekkola-Vanhanen, 1999; Cowey, 1994; Howat, 1986). Geologically the world’s chromite ore resources are found in either podiform or stratiform deposits. Podiform-type chromite deposits occur in irregular shapes like pods or lenses, while stratiform-type chromite deposits occur as parallel seams in large, layered igneous rock complexes. The layering is regular and there is large lateral continuity. The largest and best example of this type of deposit is the Bushveld Igneous Complex (BIC). South Africa’s entire chromite ore resources are located within the BIC where several chromite seams exist (Cramer *et al.*, 2004). The

economically exploitable seams are the lower group 6 (LG6) with a Cr-to-Fe (Cr/Fe) ratio of 1.5-2, the middle group 1 and 2 (MG1 and MG2) with a Cr/Fe ratio of 1.5-1.8 and the upper group 2 (UG2) with a Cr/Fe ratio of 1.3-1.4. The last of these is not of interest as a source of chromite alone but primarily as a source of platinum group metals (PGMs). Chromite ores in South Africa are therefore associated with PGMs. The major reserves of PGMs are the UG2 and Merensky reefs which are the largest deposits of chromium, vanadium and platinum in the world (Basson *et al.*, 2007; Cramer *et al.*, 2004; Xiao & Laplante, 2004; Cramer, 2001; Howat, 1986). UG2 chromite ore is gaining acceptance as a source for charge chrome (ChCr) production with the utilisation of several technological innovations (Basson *et al.*, 2007). One should take note that South Africa's *in situ* chromites are largely low grade ores (< 45% Cr₂O₃) with low Cr/Fe ratios (< 1.6) and are generally brittle. The resulting alloys produced from these ores are mostly charge grade (ChCr) with a chromium content of < 55%. There is also a general requirement for agglomeration of the ore to render it suitable for efficient ChCr production. The production of ChCr with lower chromium content also influences the transport cost per Cr unit adversely (Basson *et al.*, 2007).

2.2.4. Ferrochromium production

Since the advent of argon-oxygen decarburisation 50 years ago that triggered the expansion of South Africa's FeCr industry, South Africa has become the world leader in FeCr production by some margin (Basson *et al.*, 2007; Featherstone & Barcza, 1982). This can be ascribed to an abundance of good quality raw materials (ore, reductants and fluxes), historically relatively low electricity costs, adequate infrastructure and reasonably low-cost capital (Basson *et al.*, 2007). In 2009 South Africa produced around 2.3 million metric tonnes of the world's ChCr, the most common production grade. This was 38.92% of the 5.9 million metric tonnes produced world-wide. When

considering statistics of the International Chromium Development Association (ICDA) Statistical Bulletin 2010, depicted in Figure 2–6, it is evident that South Africa’s charge grade FeCr production went down by 7.37% from 46.29% in 2007 to 38.92% in 2009. This can be ascribed to the world economic crisis, as well as the situation surrounding South Africa’s electricity supply mentioned previously in Par. 2.2.2. The summarised production capacities of South Africa’s FeCr smelter plants are shown in Table 2–2 (Beukes *et al.*, 2011; Jones, 2010; Bonga, 2009; Basson *et al.*, 2007).

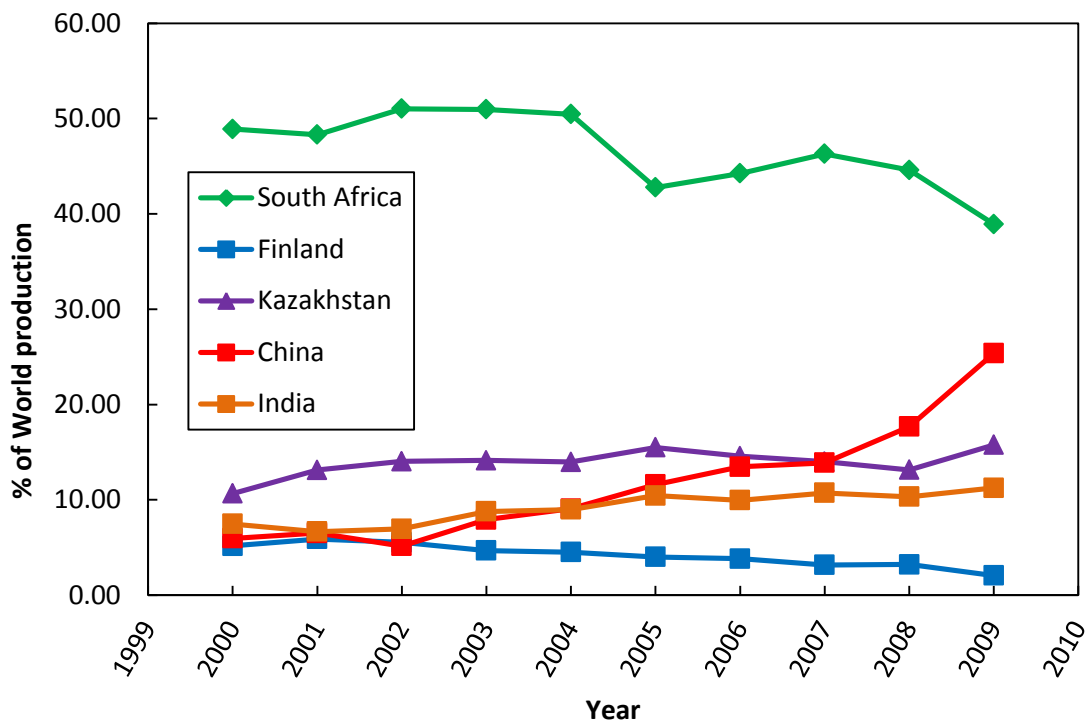


Figure 2–6: High carbon charge grade ferrochromium production 2000-2009 (ICDA, 2010)

Table 2–2: Production capacity of South African FeCr producers adapted from Jones (2010) by Beukes *et al.* (2011)

Plant	Locality	Production capacity (ton/year)
ASA Metals Dilokong	Burgersfort	360 000 [#]
Assmang Chrome	Machadodorp	300 000
Ferrometals	Witbank	550 000
Hernic Ferrochrome	Brits	420 000 [#]
International Ferro-Metals	Rustenburg-Brits	267 000
Middelburg Ferrochrome	Middelburg	285 000
Mogale Alloys	Krugersdorp	130 000
Tata Ferrochrome	Richards Bay	135 000
Tubatse Ferrochrome	Steelpoort	360 000
Xstrata Lydenburg	Lydenburg	400 000
Xstrata-Merafe Boshhoek	Rustenburg-Sun City	240 000
Xstrata-Merafe Lion	Steelpoort	364 000*
Xstrata Rustenburg	Rustenburg	430 000
Xstrata Wonderkop	Rustenburg-Brits	545 000
TOTAL		4 786 000

[#] Production capacities of these facilities in the original reference (Jones, 2010) were updated by Beukes *et al.* (2011), since it did not consider relatively recent capacity enlargement projects

* An expansion project for this facility is currently underway and will double its current capacity (Beukes *et al.*, 2011)

2.3. Core processes and techniques

2.3.1. Mining and beneficiation of chromite ores

Open-cast mining as well as underground mining techniques are used to obtain raw chromite ore. Specific mining techniques vary widely depending on the local resources and materials (Gediga & Russ, 2007; Nafziger, 1982).

The purpose of beneficiation is to render the ore physically (granulometry) and chemically suitable for subsequent treatments. Operations typically serve to separate and concentrate mineral values from waste materials, remove the impurities or prepare the ore for further refinement. Beneficiation activities do not change the mineral values themselves other than by reducing (crushing and grinding) or enlarging (pelletising and briquetting) particle size to facilitate further processes. Chromite ore is beneficiated for processing using several methods. The ore source, end use sector requirements, mineral characteristics of the ore deposits, gangue mineral assemblage and the degree of dissemination of constituent minerals determine the beneficiation practices and methods that are used. A general representation of a chromite ore beneficiation process is shown in Figure 2–7 and consists of two sections, i.e. comminution (preparing the material for subsequent unit operations) and concentration (Murthy *et al.*, 2011; Abubakre *et al.*, 2007).

In the feed preparation section the run-of-mine ore is screened from ± 220 mm to 75 mm. This is followed by a primary and secondary crushing stage separated by screening to produce an offset of less than 3 mm. The secondary crushers offset is recycled back and rescreened. The crushed ore is then further grounded to less than 1 mm. In the concentration section the ore is upgraded using conventional gravity techniques like spiral concentrators and shaking tables (Murthy *et al.*, 2011:377).

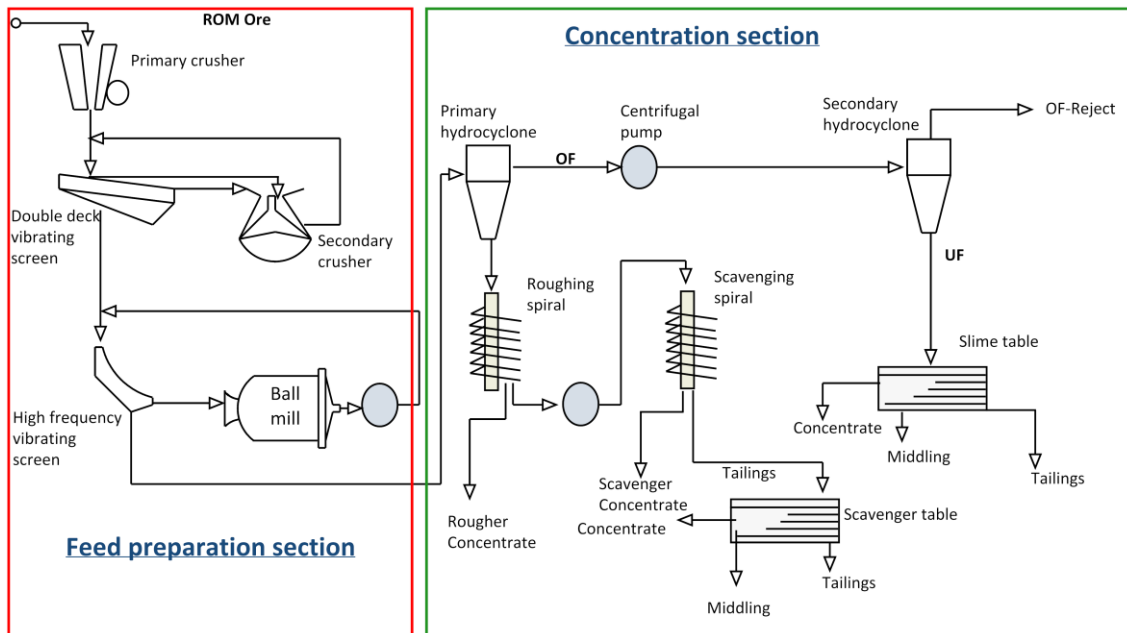


Figure 2–7: General process flow sheet for chromite ore beneficiation (Murthy *et al.*, 2011)

Though gravity techniques are well established and widely accepted for the concentration of chromite ore, such techniques become inefficient and complex while treating fine size particles of less than 75 μm . Recovery is a concern particularly in finely disseminated ores due to its inherent complexities. Each gravity separation technique delivers its maximum efficiency under specific operating conditions and particle size range (Murthy *et al.*, 2011:377).

Heavy medium and gravity concentration methods are the most commonly used beneficiation processes. Heavy medium separation is the most economical method when coarse particles ranging between 10-100 mm need to be treated. In the case of finer particles, jigs, spirals and shaking tables are used. Spirals are, however, the most important among gravity concentrators and are currently the preferred choice. Chrome can be recovered within the range of 80 to 85% when using these processes (Gu & Wills, 1988; Howat, 1986).

Gravity separation methods predominate over flotation techniques (Nafziger, 1982). Flotation is thus not a major method of beneficiation for chromite ores. In some instances fatty acids, such as oleic acid, have been used where flotation

has been adopted as a method of separation. Chromites from different locations exhibit a wide variation in surface properties which is a major difficulty when making use of flotation (Gu & Wills, 1988).

All chromites are paramagnetic at room temperature. Their magnetic capacity is dependent on the Fe^{2+} content (Owada & Harada, 1985). It has been speculated that this ferromagnetism is predominantly present in the sections more concentrated with Fe^{2+} because of the non-uniform distribution of magnetic ions in the crystalline structure. Low-intensity magnetic separation (about 0.1 T) is used to reject the magnetite from paramagnetic chromite material, but is inefficient in separating the chromites that are present in fine intergrowths with other materials. In a high-intensity magnetic field (about 1 T) chromite can be extracted as a magnetic product from the gangue material (Gu & Wills, 1988; Nafziger, 1982).

South African chromite ores are relatively friable and easily break down to the size of the chromite crystals (Gu & Wills, 1988). Due to this friability, it is common to only recover 10-15% lumpy ore (15 mm < typical size range < 150 mm) and 8-12% chip or pebble ores (6 mm < typical size range < 15 mm) during the beneficiation process employed after chromite mining. The remaining ore would typically be in the < 6 mm fraction, which would usually be crushed and/or milled to < 1 mm and then upgraded utilising typical gravity separation techniques (e.g. spiral concentrators) to approximately 45% Cr_2O_3 content. This upgraded < 1 mm ore is commonly known as metallurgical grade chromite ore (Glastonbury *et al.*, 2010).

2.3.2. Ferrochromium production

A generalised process flow diagram, which indicates the most common process steps utilised by South African FeCr producers, is shown in Figure 2–8 (Beukes *et al.*, 2010).

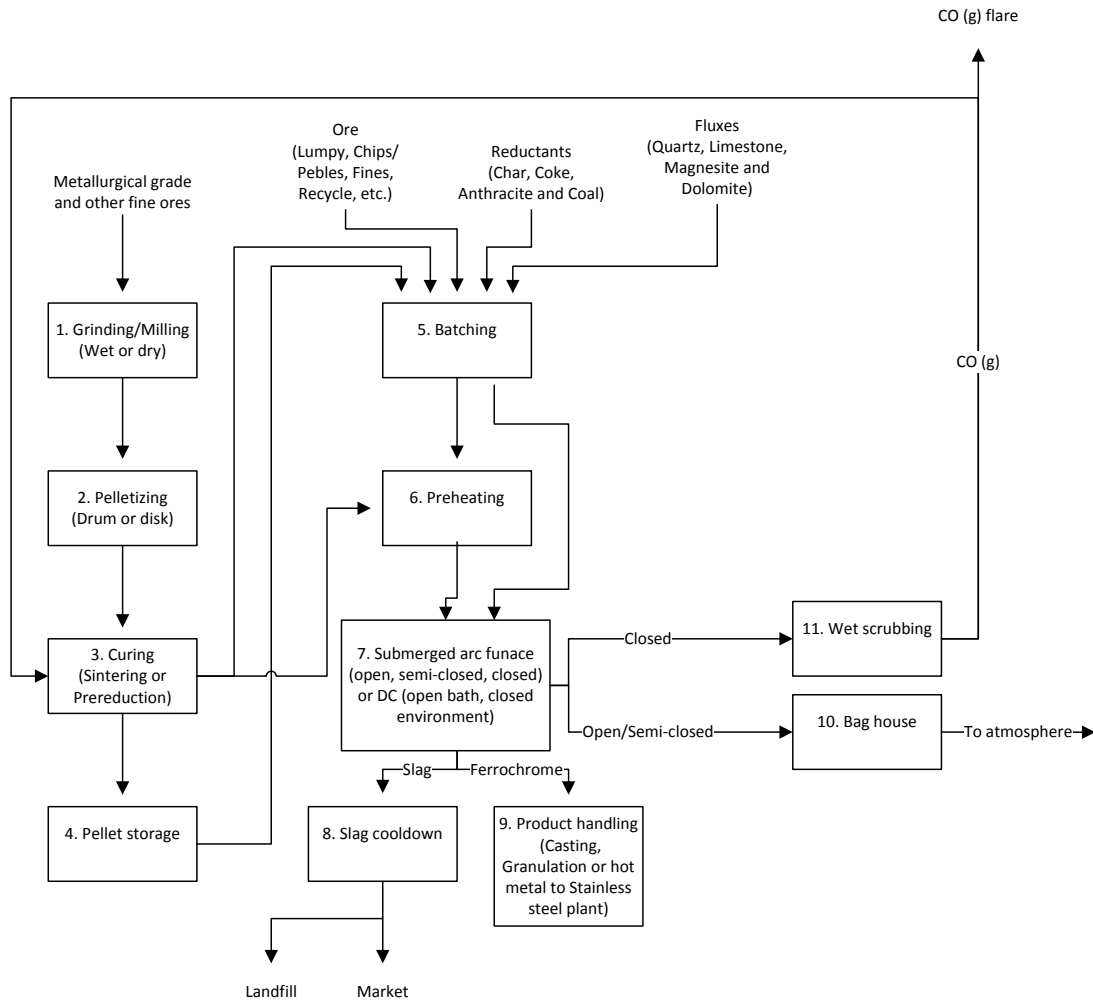


Figure 2–8: A flow diagram adapted by Beukes *et al.* (2010) from Riekkola-Vanhanen (1999), indicating the most common process steps utilised for FeCr production in South Africa

In general, four relatively well-defined process combinations are utilised by South African FeCr producers (Beukes *et al.*, 2010):

1. Conventional semi-closed furnace operations, with bag filter off-gas treatment. This is the oldest technology applied in South Africa, but still

accounts for a substantial fraction of overall production (Gediga & Russ, 2007). In this type of operation, coarse (lumpy and chips/pebble ores) and fine ores can be smelted without an agglomeration process undertaken to increase the size of fine ores. Although it has been stated that fine ores cannot be fed directly into a submerged FeCr arc furnace without causing dangerous blow-outs or bed turnovers (Riekkola-Vanhanen, 1999), substantial amounts of fine ores are in fact fed into some semi-closed furnaces in the South African FeCr industry. With reference to the process flow diagram indicated in Figure 2–8, the process steps followed are 5, 7, 8, 9 and 10. Some semi-closed furnaces do consume pelletized feed, in which case process steps 1-4 would also be included. Most of semi-closed furnaces used in South Africa are operated on an acid slag, with a basicity factor smaller than 1. Equation 2–1 defines the basicity factor (BF) (Beukes *et al.*, 2010):

$$BF = \frac{\%CaO + \%MgO}{\%SiO_2} \quad 2-1$$

Some semi-closed furnaces might operate on $BF > 1$, but these are less common and such operations are sometimes only temporarily undertaken to compensate for refractory linings being in poor condition, or if enhanced sulphur removing capacity by the slag is required (Beukes *et al.*, 2010).

2. Closed furnace operation, usually utilising an oxidative sintered pelletised feed (Outotec, 2011). This has been the technology most commonly employed in South Africa, with the majority of green and brown field expansions utilising this combination of process steps during the last decade. Process steps usually include steps 1, 2, 3, 4, 5, 7, 8, 9 and 11, with or without 6. In all green field FeCr developments the pelletising and sintering (steps 2 and 3) sections were combined with closed furnaces.

However, pelletising and sintering sections have also been constructed at plants where the pelletised feed is utilised by conventional semi-closed furnaces. These furnaces are usually operated on an acid slag ($BF < 1$) (Beukes *et al.*, 2010).

3. Closed furnace operation with pre-reduced pelletised feed (Naiker, 2007; Botha, 2003). The process steps include steps 1, 2, 3, 4, 5, 7, 8, 9, 11. The pelletised feed differs substantially from the oxidative sintered type due to the fact that the pellets are pre-reduced and mostly fed hot, directly after pre-reduction, into the furnaces. The furnaces are closed and operate on a basic slag ($BF > 1$). At present, two South African FeCr smelter plants use this process.
4. DC arc furnace operation (Curr, 2009; Denton *et al.*, 2004). For this type of operation, the feed can consist exclusively of fine material. Currently three such furnaces are in routine commercial operation for FeCr production in SA and typically utilize a basic slag regime ($BF > 1$). Process steps include 5, 7 (with a DC, instead of a SAF), 8, 9 and 11. Drying (process step 6) might also be included.

2.4. Chromite pre-reduction

2.4.1. Extent of pre-reduction technology commercialisation

Pre-reduction technology has been around for a number of years, with the pre-reduction of iron ore being a more commonly utilised process. Remarkably, pre-reduction of chromite has not been widely used on a commercial scale; however, it is a very well-established practice in South African FeCr production and has been utilised since 1975 (McCullough *et al.*, 2010; Basson *et al.*, 2007; Naiker, 2007; Dawson & Edwards, 1986). It is currently the second most commonly employed pelletisation technology in the South African FeCr industry

(Beukes *et al.*, 2010). A number of studies have been conducted on the pre-reduction of chromite ore utilising different reductant sources including coke, anthracite, carbon monoxide, methane and hydrogen. This has led to a few processes being partially developed as well as implemented on a commercial scale.

The solid state reduction of chromite (SRC) process developed by Showa Denko in Japan was the first commercially successful process (Naiker, 2007). In this process, chrome ore fines are milled in a ball mill, pelletised using a clay binder with coke added as reductant, dried in a travelling grate kiln, and fired in a rotary kiln to approximately 1400 °C. The kiln is heated by a burner using pulverised coal, CO or oil as fuel (Riekkola-Vanhanen, 1999). The SRC process has been employed with success at two commercial plant facilities, the Shunan Denko Plant in Japan and the Consolidated Metallurgical Industries (CMI) Plant in Mpumalanga South Africa, and these have proved to be the most energy efficient FeCr production plants at the time (Naiker, 2007). When Xstrata purchased the CMI plant in 1998 from the Johannesburg Consolidated Industries (JCI) group, they wanted to decrease cost structures at the Lydenburg plant. Therefore, between 1998 and 2001, they developed the Premus process, based on the SRC process, mainly by in-plant trials. Xstrata made a key fundamental change in the operating philosophy of the process in that while the original CMI process main objective was to maximize metallisation in the pellets, the Premus process sought to maximize the energy output from the kiln while still achieving the required efficiencies and therefore increasing furnace output (Naiker, 2007). In 2006 third quarter Xstrata increased their FeCr capacity with the commissioning of its Lion FeCr smelter plant which also makes use of a pre-reduction stage utilising Xstrata's Premus technology (McCullough *et al.*, 2010; Basson *et al.*, 2007). In 2010 Xstrata announced the seconded phase expansion of the Lion plant that will involve the construction of a 360 000 t/y capacity smelter, raising their total FeCr production capacity above 2.3 million t/y.

Construction of the smelter was due to begin in the first quarter of 2011, with commissioning planned for the first half of 2013. The expansion will yet again make use of the Premus pre-reduction technology (Wait, 2011; Creamer, 2010).

Alternative processes that have been used or have been partly developed include the Krupp-Codir CDR (Chrome Direct Reduction Process) and Rotary Hearth Furnace (RHF) of originally Krupp in Germany but acquired by Polysius and Outokumpu's pre-treatment process (McCullough *et al.*, 2010). The CDR process uses unagglomerated ore fines. Self-agglomeration of the fines occurs inside the rotary kiln in the high temperature zone. A temperature of approximately 1500 °C is used and the kiln feed consists of chromite concentrate, a siliceous flux, and a large excess of reductant. This is because coal is used as both energy source and reductant (Riekkola-Vanhanen, 1999; Dawson & Edwards, 1986). A big disadvantage of this process is that the excess reductant must be separated from the metal-slag mixture before smelting can commence. To achieve this, the kiln discharge must be cooled which results in a substantial loss of enthalpy (Dawson & Edwards, 1986). SAMANCOR installed the CDR pre-reduction process at its Middelburg FeCr Plant with the process involving the partial fluxing of chrome ore fines (not pellets) and the use of oxygen enrichment to attain temperatures of around 1500 °C, but ran into problems in particular with refractory wear. INMETCO developed its Direct Reduced Iron (DRI) Technology process utilizing a RHF and applied it with great success to stainless steel dust recycling. However, attempts to apply the RHF process to chrome ore pre-reduction were only partly successful, the main problem being the re-oxidation of the pre-reduced chrome pellets (McCullough *et al.*, 2010). Tenova Pyromet in co-operation with its technical partners, Paul Wurth and Tenova LOI Italimpianti, has recently developed a pre-reduction process for FeCr ores based on using Rotary Hearth Furnace technology fired with closed furnace off-gas, but the process has not yet been industrially applied (Dos Santos, 2010).

Outokumpu studied its process for about ten years in the laboratory and on pilot scale as well as for two years in a commercial scale operation. The process consisted of a rotary kiln with a length of 55 m and inner diameter of 2.3 m. The major problem that they encountered was to maintain an even pre-reduction degree. Consequently, plant operation became difficult to maintain and efficiency were not good enough to make the operation viable, so they returned to using the equipment for preheating (Daavittila *et al.*, 2004).

2.4.2. Strategic advantages of chromite pre-reduction

Although various processes are utilised in the production of FeCr (Par. 2.3.2), the use of pelletised pre-reduction chromite has a number of key advantages over other processes:

- a) Pre-reduction's most important advantage is certainly the reduction of the overall process electric energy consumption. At present, high-carbon FeCr is generally produced in electric arc furnaces. A major disadvantage of this process is the amount of electrical energy required for the reduction of the metal oxides to the metallic state. In order to minimize energy consumption and consequently improve cost efficiency, solid state carbothermic pre-reduction of chromite has become a necessary option, since it requires the lowest specific energy for operation of all FeCr production processes (Neizel, 2010; Weber & Eric, 2006). With pre-reduction levels of up to 90% for the iron and 50% achieved for chrome, electrical energy consumption is reduced by approximately 40% from around 3.9 MWh/t required in conventional processes down to 2.4 MWh/t (McCullough *et al.*, 2010). The net specific energy consumption as a function of the degree of chromium pre-reduction achieved and then charged into an arc furnace at different temperatures was reconstructed from Takano *et*

al. (2007) and Niayesh and Fletcher (1986) and is presented in Figure 2–9.

- b) The process utilises 100% fine chromite ore, therefore taking maximum advantage of friable chromite ore available in South Africa (Naiker & Riley, 2006).
- c) Providing an agglomerate feed to furnaces thus reducing the risk of bed turnovers and blowouts occurring (Naiker & Riley, 2006).
- d) Although pre-reduction capital cost is higher than the capital incurred for a conventional process, it is still the lowest capital cost per annualised ton of FeCr and will thus have the lowest cost of production for the foreseeable future when compared to other alternative environmentally acceptable processes available (Naiker, 2007).
- e) High recoveries of metallic oxides (90%).
- f) Production of a low silicon product (< 3%).
- g) The use of lower cost fine reductants instead of lumpy reductants and the use of oxygen as an energy source (Naiker, 2007; Naiker & Riley, 2006; Botha, 2003).

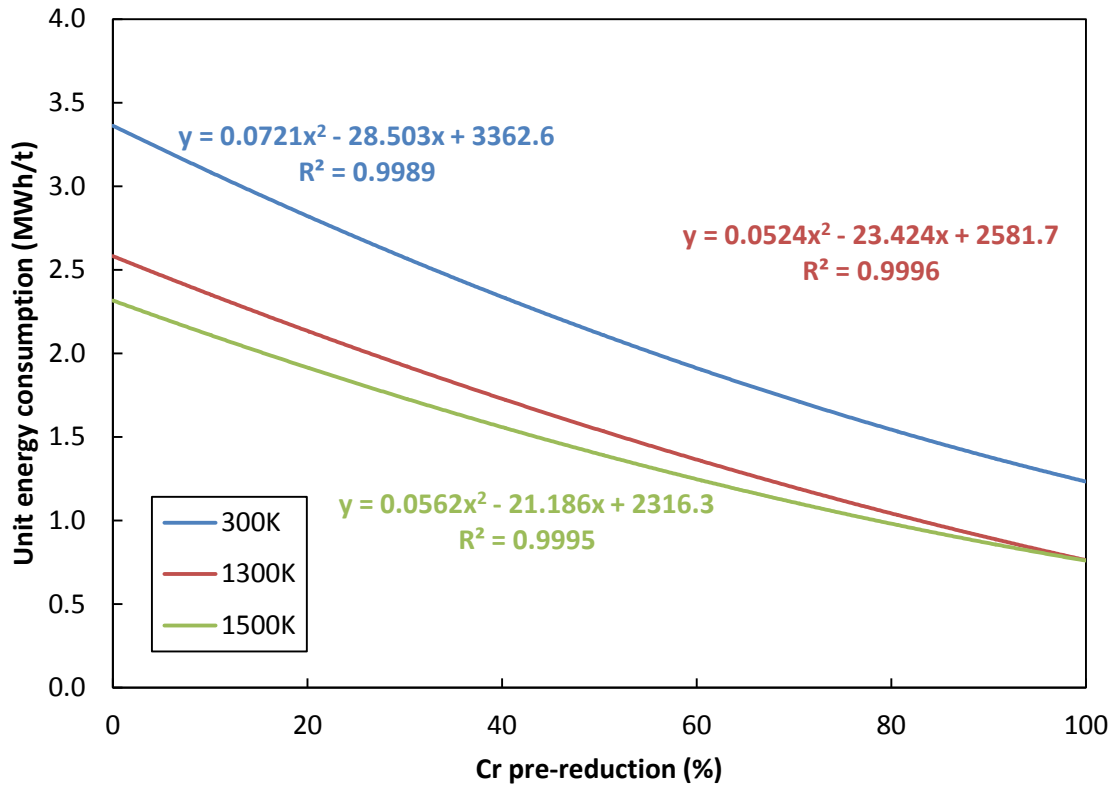


Figure 2–9: Net energy requirement for the production of 1 ton of FeCr as a function of the degree of pre-reduction achieved and charging temperature (Takano *et al.*, 2007; Niayesh & Fletcher, 1986)

2.4.3. Fundamental aspects of chromite pre-reduction

In a chromite pre-reduction process certain terms are used to describe the reduction rate and extent of reduction and metallisation. It is therefore necessary to define these terms before going into further discussions. Barnes *et al.* (1983) proposed definitions for the terms “degree of reduction” and “metallisation” which have since been used by some researchers (Weber & Eric, 2006; Soykan *et al.*, 1991a). Given that the removal of oxygen is associated with reduction, the extent of reduction, R(%), was defined as (Barnes *et al.*, 1983):

$$R(\%) = \frac{\text{Mass of oxygen removed}}{\text{Original removable oxygen}} \times 100 \quad 2-2$$

In the pre-reduction process solid carbon is used as a reductant and CO is thus formed as a reduction reactions product (illustrated in Equation 2–5, Equation 2–6 and Equation 2–7). The extent of reduction can thus also be defined as (Barnes *et al.*, 1983):

$$R(\%) = \frac{\text{Mass of CO evolved}}{28/16 \times \text{Original removable oxygen}} \times 100 \quad 2-3$$

The amount of removable oxygen used to define Equation 2–2 and Equation 2–3 is determined from the oxygen loss associated with the metal oxides Fe₂O₃, FeO and Cr₂O₃.

The extent of metallisation, M(%), is defined as (Barnes *et al.*, 1983):

$$M(\%) = \frac{(\text{Cr}^0 + \text{Fe}^0)}{(\text{Cr}_{\text{tot}} + \text{Fe}_{\text{tot}})} \times 100 \quad 2-4$$

Where: Cr⁰ is the amount of chromium reduced to the metal state

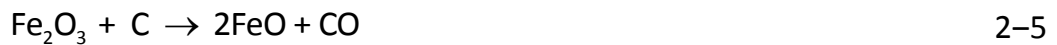
Fe⁰ is the amount of iron reduced to the metal state

Cr_{tot} is the total chromium amount

Fe_{tot} is the total iron amount

Since complete oxygen removal corresponds to complete metallisation, 100% reduction corresponds to 100% metallisation. The relationship between metallisation and reduction is, however, not linear and Barnes *et al.* (1983) attributed this to the following factors:

- 1) In the early stages of reduction, Fe₂O₃ is reduced to FeO without any metallisation:



- 2) FeO is reduced to Fe⁰, producing 1 mol of CO for every mole of Fe⁰ produced:



- 3) Cr₂O₃ is reduced to Cr⁰, producing 1.5 mol of CO per mole of Cr produced:



Dawson and Edwards (1986) illustrated the individual difference in metallisation and reduction of iron and chromium, confirming the above mentioned factors proposed by Barnes *et al.* (1983). A graphic illustration of this relationship between reduction and metallisation were reconstructed for Dawson and Edwards (1986) and shown in Figure 2–10.

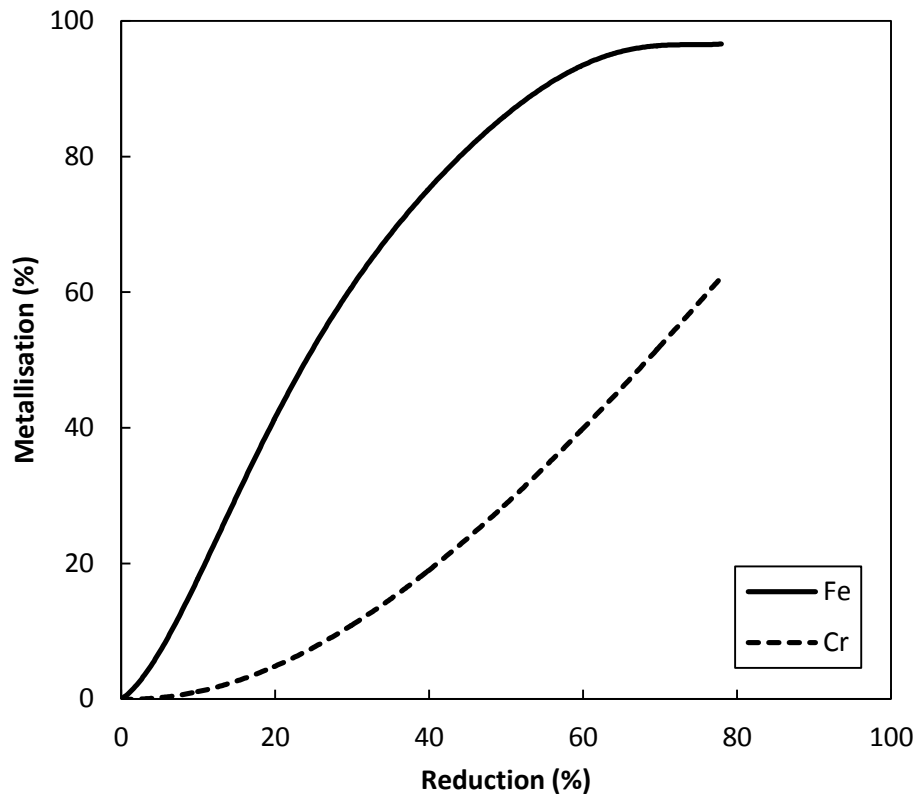
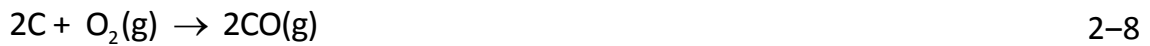


Figure 2–10: The relationship between reduction and metallisation, based on South African LG-6 chromite treated at 1200 °C (Dawson & Edwards, 1986)

Chromite ore is primarily composed of $\text{FeO}\cdot\text{Cr}_2\text{O}_3$, $\text{MgO}\cdot\text{Cr}_2\text{O}_3$, $\text{MgO}\cdot\text{Al}_2\text{O}_3$, $(\text{Cr},\text{Al})_2\text{O}_3$, forming a complex spinel structure and may also hold a certain amount of free iron, not contained inside the spinel (Takano *et al.*, 2007). The general formula for South African chromite ore located in the BIC is $(\text{Fe}_{0.74}^{2+}\text{Mg}_{0.27})_{\Sigma=1.01}(\text{Cr}_{1.42}\text{Al}_{0.40}\text{Fe}_{0.15}^{3+}\text{Ti}_{0.01}\text{V}_{0.01})_{\Sigma=1.99}\text{O}_4$. The reduction mechanism for chromite is therefore much more complex, due to the number of metal oxides, slag components (SiO_2 , TiO_2 , Al_2O_3 , MgO , CaO , including gaseous Mg and SiO) and alkalis contained inside the spinel structure or existing as free compounds (Niemelä *et al.*, 2004).

Takano *et al.* (2007) identified three ways in which high temperature reduction of chromites using a carbon reductant can generally occur, i.e. i) solid chromites is reduced by solid or gaseous reductant; ii) direct reaction at the interface between the slag and metal, where the dissolved chromites in the slag are

reduced by carbon dissolved in the metal phase; and iii) direct reaction between dissolved chromites in the slag and the carbon particles floating on it. In SAF mechanisms ii and iii should be predominant, while in the chromite pre-reduction process a large portion of chromite is expected to reduce by solid or gaseous reductants before liquid phase formation. The reactions required for the carbon based reduction of chromite by a solid or gaseous reductant are indicated in Equation 2–8 and Equation 2–9 (Niemelä *et al.*, 2004).



Niemelä *et al.* (2004) investigated the formation, characterisation and utilisation of CO-gas formed during the carbothermic reduction of chromite. According to the Ellingham diagram calculations they conducted (indicated in Figure 2–11) they showed that solid carbon reduces Fe_2O_3 to FeO at around 250 °C. The reduction of Fe_3O_4 to FeO occurs kinetically at temperatures above approximately 710 °C. FeO is reduced to the Fe^0 state at relatively low temperatures, around 710 °C and above, while the reduction of Cr_2O_3 occurs at higher temperatures of 1250 °C and above. Carbon monoxide reduces Fe_2O_3 to Fe_3O_4 over the whole calculated temperature range, but as mentioned earlier reduction of Fe_3O_4 to FeO occurs kinetically above 710 °C. From the calculations it is evident that the reduction of Cr_2O_3 and $(FeO \cdot Cr_2O_3)$ is not possible with carbon monoxide alone.

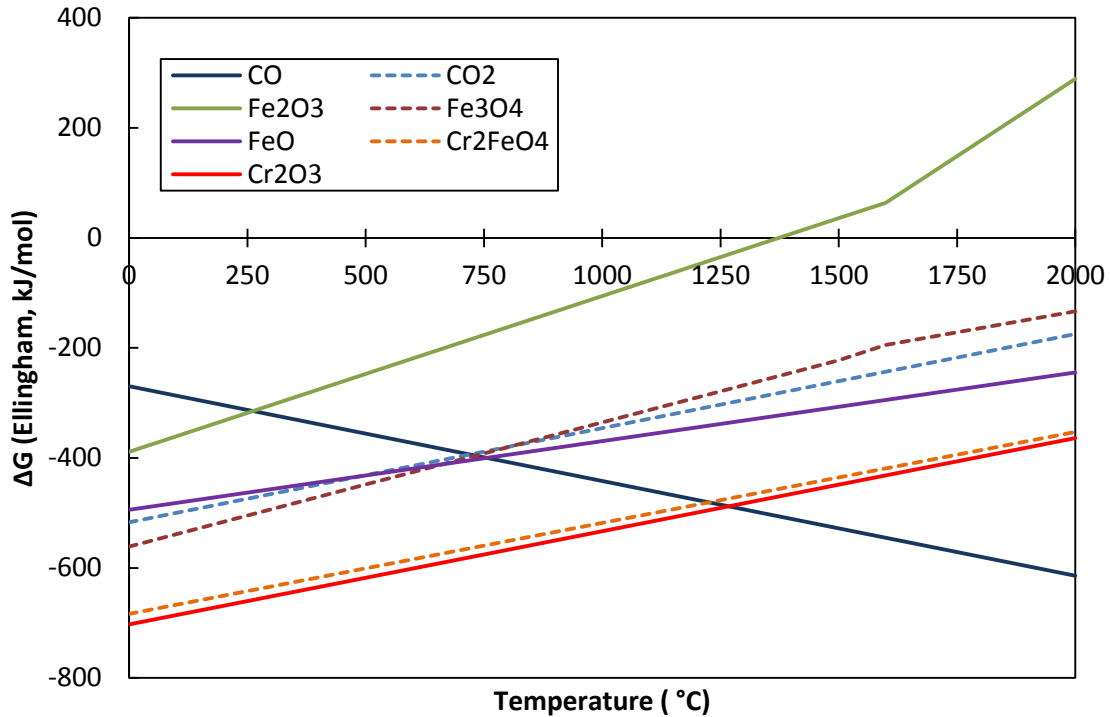


Figure 2–11: Standard free energies of reduction of metal oxides with carbon and carbon monoxide (Niemelä *et al.*, 2004)

The mechanisms and kinetics of the reduction of South African chromite ores have been studied by numerous researchers. A comprehensive reference list of these investigations is given by Hayes (2004). Significant results on the solid-state carbothermic reduction mechanism and kinetics of a chromite from the LG6 layer of the BIC treated at 1400 °C have been published by Soykan *et al.* (Soykan *et al.*, 1991a; Soykan *et al.*, 1991b). Soykan *et al.* proposed a stoichiometric ionic diffuse reduction model involving somewhat complex reactions among the solid carbon reductant, altered chromite spinel phases, and various ionic species. It also included site-exchange mechanisms between Fe²⁺ and Cr³⁺ ions, with the Cr³⁺ being placed in octahedral sites due to its very high affinity for octahedral coordination (Weber & Eric, 2006; Weber & Eric, 1993; Soykan *et al.*, 1991a; Soykan *et al.*, 1991b). The proposed mechanism, furthermore, included a swap mechanism between the Cr²⁺ ions of the surface unit cell and the Fe²⁺ ions of the unit cell just below the surface. Soykan *et al.* (1991a&b) observed that localisation occurred in partially reduced chromites

and that all the oxygen are removed from the surface as iron and chromium is reduced. The inner cores were found to be rich in iron, whereas the outer cores were depleted of iron. A graphic representation, shown in Figure 2–12, of the reduction of chromite was proposed by Ding & Warner (1997b) correlating to the observations of Soykan *et al.* (1991a&b). Soykan *et al.* (1991a&b) revealed that, within the outer core (Reduced area, Figure 2–12), Fe²⁺ and Cr³⁺ ions diffused outward, whereas Cr²⁺, Al³⁺ and Mg²⁺ ions diffused inward. Initially, Fe³⁺ and Fe²⁺ ions at the surface of chromite particle (Interface 1, Figure 2–12) were reduced to the metal state. This was followed immediately by the reduction of Cr³⁺ ions to the 2+ oxidation state. Cr²⁺ ions diffusing toward the inner core of the particle reduced the Fe³⁺ ions in the spinel under the surface of the particle to Fe²⁺ at the interface (Reduced area, Figure 2–12) between the inner and outer cores. Fe²⁺ ions diffuse toward the surface, where they were reduced to metallic iron. After the iron had been completely reduced, Cr³⁺ and any Cr²⁺ that was present were reduced to the metal state, leaving an iron and chromium free spinel, MgAl₂O₄. The metallised iron and chromium carburised during the reduction into (Fe,Cr)₇C₃ according to Equation 2–10 and Equation 2–11.



To conclude this paragraph the ionic diffusion reaction mechanism of chromites in the solid spinel phase by a carbon reductant proposed by Soykan *et al.* (1991a&b) can be summarised into the following reaction sequences (Hayes, 2004):

- 1) Initially, Fe^{3+} and Fe^{2+} at the surface of the chromite particle are reduced to the metal state. This is followed instantaneously by the reduction of Cr^{3+} ions to Cr^{2+} (Interface 1, Figure 2–12).
- 2) Cr^{2+} ions diffusing toward the inner core of the particle reduce the Fe^{3+} ions in the spinel under the surface of the particle to Fe^{2+} at the interface between the inner core (Unreacted chromite core, Figure 2–12) and the surface of the particle. Fe^{2+} ions diffuse towards the surface, where they are reduced to metal iron.
- 3) After the iron has been completely reduced, Cr^{3+} and any Cr^{2+} that is present are reduced to the metal state, leaving an iron and chromium-free spinel, MgAl_2O_4 .

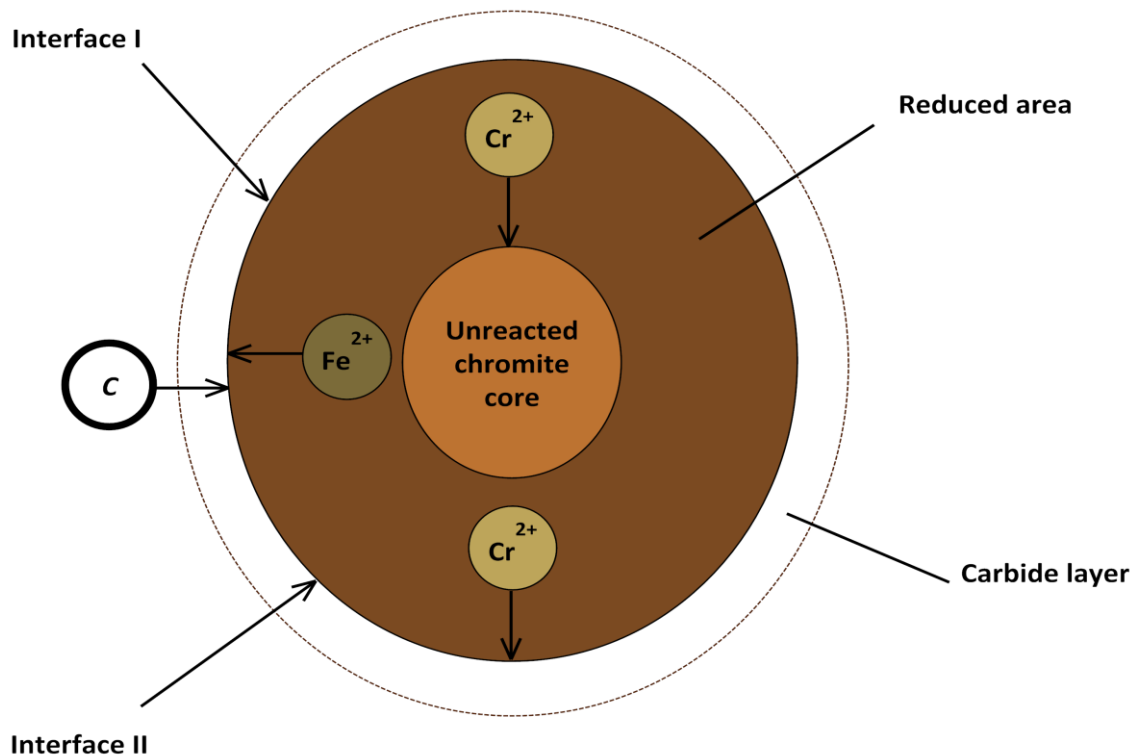


Figure 2–12: Schematic representation of the reduction mechanism of chromite (Ding & Warner, 1997b)

2.4.4. Factors influencing the pre-reduction of chromite

2.4.4.1. Effect of time and temperature

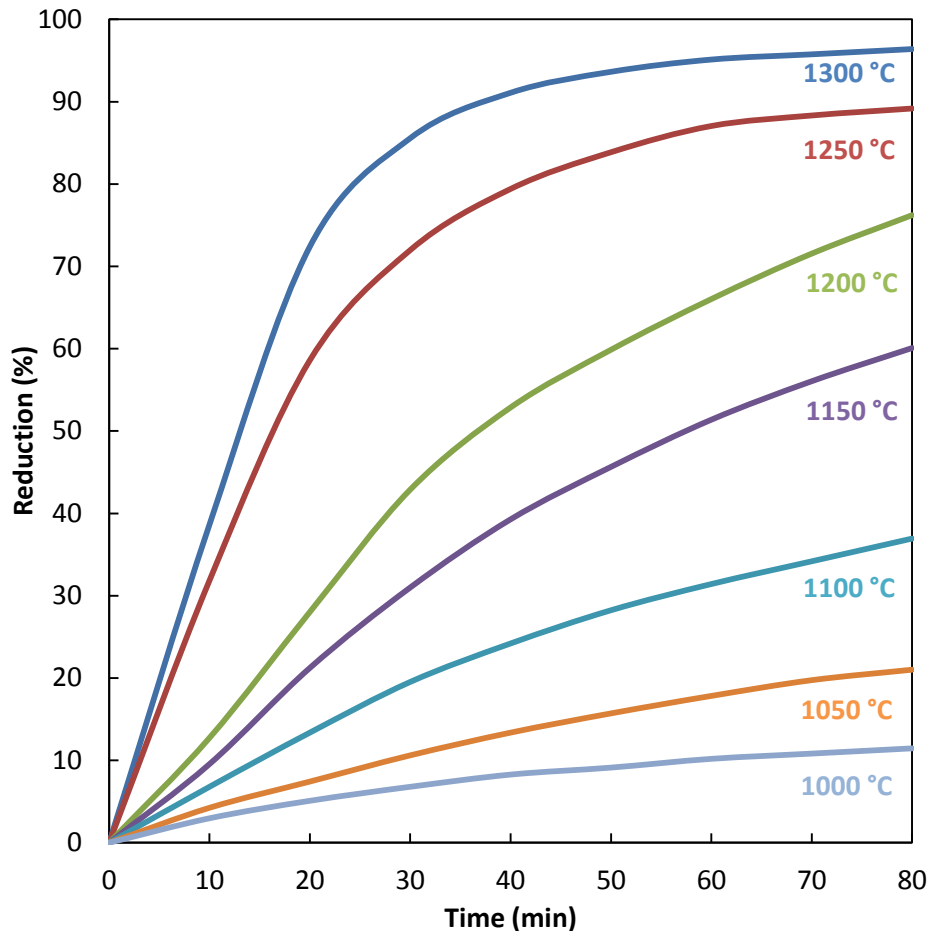


Figure 2–13: The effect of time and temperature on the rate of chromite reduction (Barnes *et al.*, 1983)

The extent of chromite pre-reduction achieved in industrial operations is seldom more than 60%. This involves nearly complete metallisation of the iron and typically less than 30% metallisation of the chromium. The low metallisation of the chromium, therefore, limits the potential further reduction in electrical energy required, as mentioned in Par. 2.4.2. The relatively low degree of reduction obtained in current industrial operations is a result of the slow reduction kinetics of chromium species occurring in the chromite. The kinetics is determined by the temperature of operation, which is limited to a maximum

of about 1350 °C. At temperatures above 1350 °C, partial melting of the pellets occurs, that consequently causes dam-ring formation in the kiln and hence a decrease in operation efficiency (Dawson & Edwards, 1986). The effect of time and temperature on the pre-reduction of chromite concentrates with a low chromium-to-iron ratio, studied by Barnes *et al.* (1983), is indicated in Figure 2–13.

2.4.4.2. *Effects of additives on pre-reduction*

The reduction of chromite in the presence of various additives and fluxes with the aim of improving the pre-reduction of chromite has been a subject of several investigations in recent years.

- Sundar Murti *et al.* (1983) studied the effect of 8% CaO addition on the reduction of synthetic and natural chromites at 1200-1300 °C using graphite as a reductant. They found that the reduction was enhanced by the additive and attributed this to the CaO diffusing into the spinel and then releasing the FeO, thereby increasing the chromite reducibility.
- Katayama *et al.* (1986) proved that 1 wt% addition of Na₂B₄O₇, NaF, NaCl, CaB₄O₇, B₂O₃ and CaF₂ improved the reduction rate of Russian chromium ore; while the same wt% CaCl₂ addition inhibited the reduction rate the longer it was exposed to the experimental temperature of 1200 °C. The effect that these salt additives had on the reduction rate of Russian chromium ore at 1200 °C where reconstructed from Katayama *et al.* (1986) and illustrated in Figure 2–14.
- Dawson and Edwards (1986) investigated the addition of a fluxing agent, CaF₂, and a eutectic mixture, NaF-CaF₂, on the reduction rate of chromite. While a moderate addition of CaF₂ was found to be

beneficial for chromite reduction, the eutectic mixture of NaF-CaF₂ were much more effective than using only CaF₂.

- Van Deventer (1988) studied the effect of K₂CO₃, Na₂O₂, CaO, SiO₂, Fe⁰, Cr⁰, Al₂O₃ and MgO additions on the reduction of Kroondal chromite at 1400 °C by graphite. K₂CO₃, Na₂O₂, CaO, SiO₂ and Fe⁰ were found to enhance the rate of reduction, while Al₂O₃ and MgO inhibited the reaction. Cr⁰ additions had little influence on reduction rates.
- Nunnington and Barcza (1989) found that the addition of granite and fluorospar to act as fluxing agents in the pre-reduction of chromite ore pellets under oxidising conditions improved reduction rates.
- Weber and Eric studied the carbothermic reduction of chromite in the presence of silica flux extensively and found that reduction was enhanced at and above 1400 °C (Weber & Eric, 2006; Weber & Eric, 1993; Weber & Eric, 1992).
- Ding and Warner investigated the catalytic effect of both lime and SiO₂ additions on the reduction of ground South African chromite concentrates. SiO₂ was found to have an enhanced effect on the reduction rate at and above 1380 °C, but only if reduction levels are higher than 40%, constituting the formation of a liquid slag (Ding & Warner, 1997b). Experiments on the catalytic reduction of carbon chromite composite pellets by lime were carried out at 1270-1433 °C and the reduction rate and extent were found to increase with increasing reduction temperature and lime addition (Ding & Warner, 1997a).
- Lekatou & Walker (1997) also researched the effect of SiO₂ additions on the solid state reduction of chromite concentrates.

- Takano *et al.* (2007) utilised Portland cement, hydrated lime and silica as additives and proved that composite pellets containing these compounds had enhanced chromite reduction rates.

The above-mentioned investigations indicate that the addition of certain additive could have an effect on the reduction of chromite, either positive or negative. The list given above are by no mean comprehensive, but it does provide some insight into past research activities.

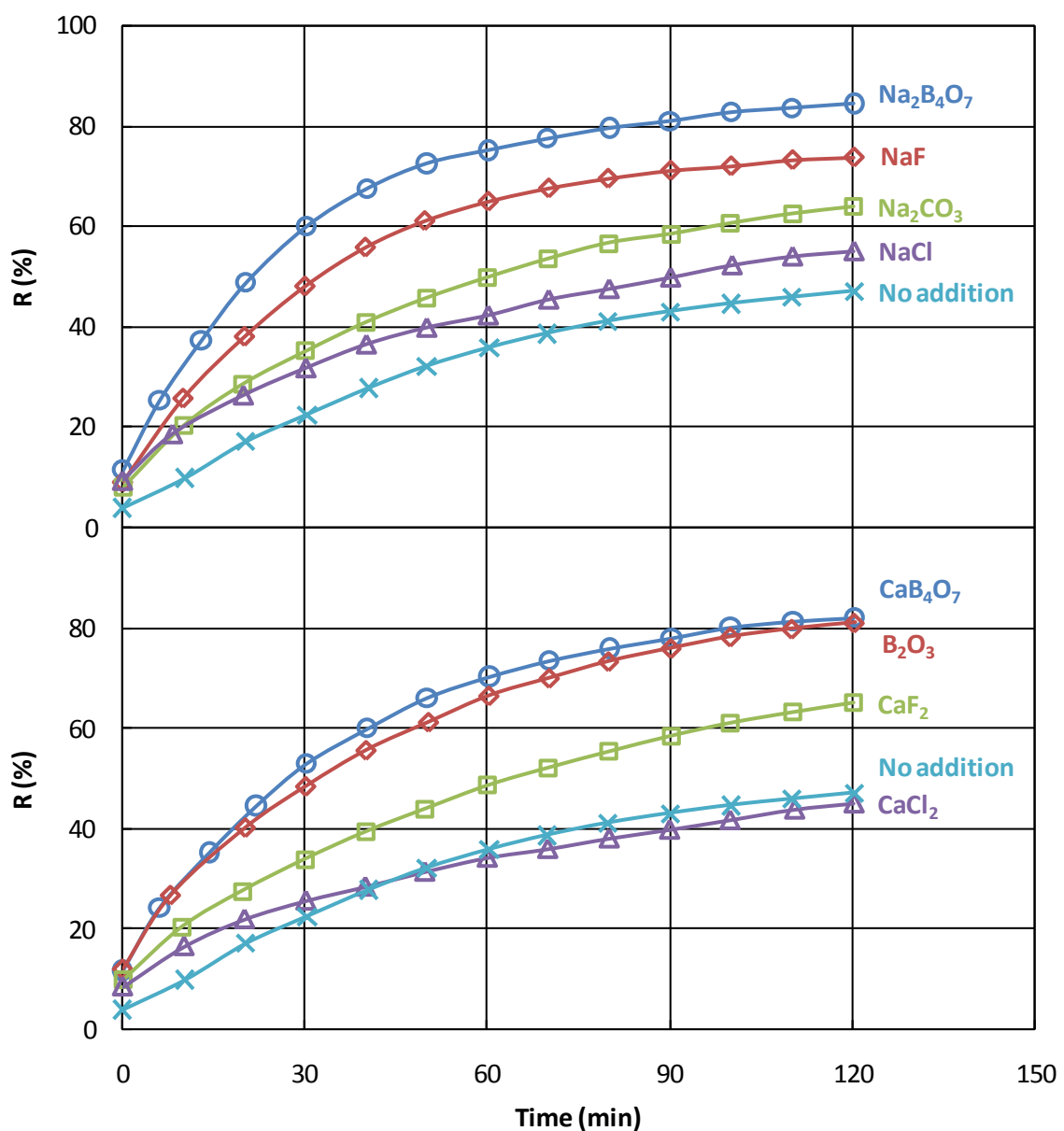


Figure 2-14: The effect of various salt additives (1 wt% addition) on the reduction rate of Russian chromium ore at 1200 °C (Katayama *et al.*, 1986)

2.5. Clay binders

2.5.1. Basic principles of agglomeration

Binders (e.g. clay) accomplish two very important functions in ore agglomeration (e.g. pelletisation) (Eisele & Kawatra, 2003):

- The binder, along with the moisture added, gives the raw materials adhesive properties, so that it will nucleate seeds that can grow at a controlled rate into well-formed good quality pellets.
- During drying, the binder holds the particles in the agglomerates together while the water is removed and continues to bind them together until the pellet is heated sufficiently to sinter the grains together.

Binder selection is therefore determined by how well it can carry out each of these functions while at the same time not causing contamination or efficiency problems. An additional feature of certain clay binders, e.g. bentonite, which is helpful in pelletisation, is its ability to absorb several times its own weight in water. This makes it possible to control the free moisture content of the pelletisation feed and consequently green pellet quality by simply adjusting the clay addition rate. This is an important characteristic because pelletisation works over a fairly narrow range of feed moisture contents. Because not all ore concentrates will filter to the same moisture content, this capability of a clay binder provides a convenient method for making small adjustments to the feed moisture content. The strength of a pellet is dependent on the type of bonding produced by the binder, indicated in Figure 2–15 (Eisele & Kawatra, 2003; Sastry, 1996a; Sastry, 1996b).

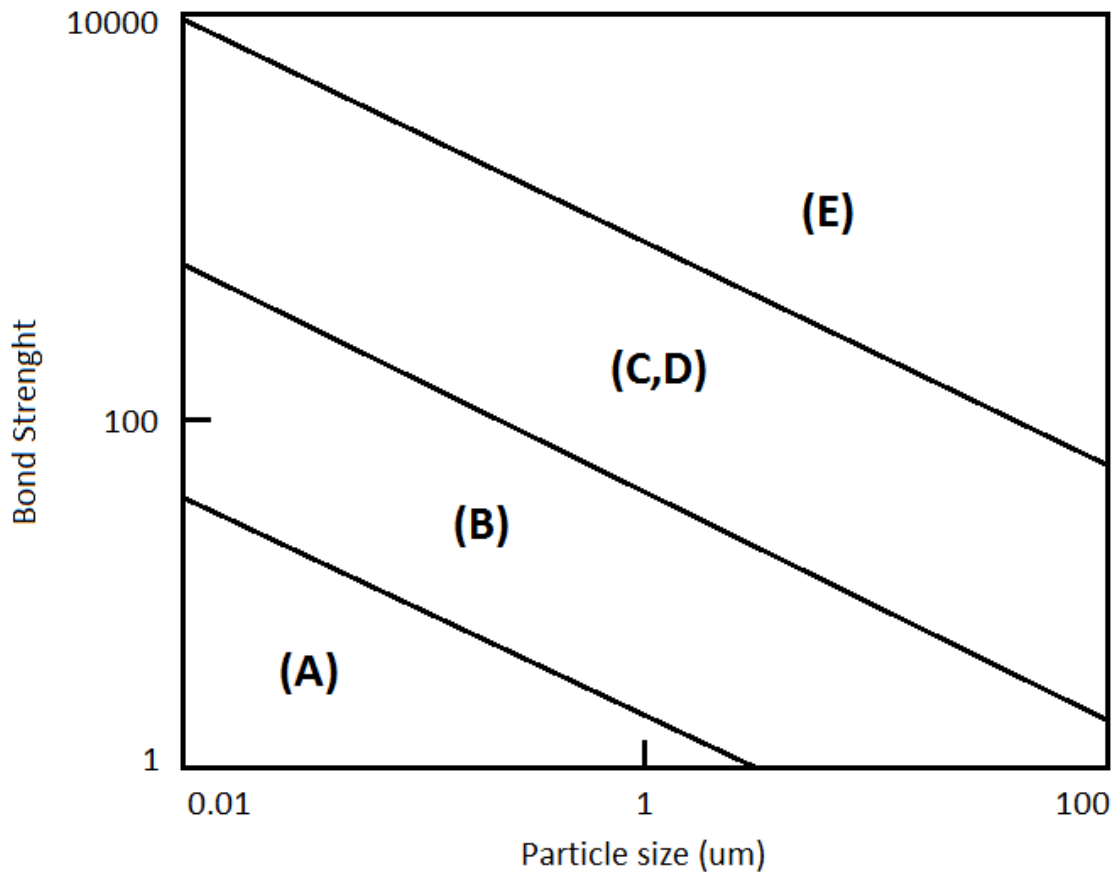


Figure 2-15: Magnitudes of bond strengths for various classes of interparticle bonds in pellets: (A) van der Waals, magnetic, or electrostatic forces; (B) capillary forces from the liquid phase; (C) adhesional and cohesive forces; (D) mechanical interlocking; (E) solid bridges formed by sintering or crystallisation of dissolved materials (Eisele & Kawatra, 2003; Sastry, 1996a; Sastry, 1996b)

Almost any material with a fine consistency can contribute to Van der Waals bonding, however, this bonding type is very weak and of little importance. Capillary forces are stronger but are not adequate in providing adhesive strength to formed pellets as it requires the presence of liquid in the pellet. Binders that can take advantage of adhesional or cohesive forces are therefore needed (Eisele & Kawatra, 2003). It should be noted that, in addition to affecting the unfired strength of the pellets, various additives alter the characteristics of fired pellets. Ball *et al.* (1974) studied the effects of additives such as NaCl, KCl, CaCl₂, MgCl₂, Ca(OH)₂, MgO, Al₂O₃, CaCO₃, CaMg(CO₃)₂, glucose, ferrous sulphate, and bentonite on the fired pellet properties of iron ore pellets. Some of these additives increased strength up to a certain point,

whereas others had no effect or even caused a strength decrease. Microstructural studies conducted by Ball *et al.* (1974) showed that these effects correlated to the degree to which additives cause quartz dissolution and melt formation. In general, electrolytes (NaCl, KCl, CaCl₂) and alkali calcium compounds (Ca(OH)₂, CaCO₃) tended to cause an increase in fired strength, mainly due to an increase in the amount of slag melt that formed; however, over-dosage of any of these additives lead to a decrease in strength. MgO reduced the fired strength, due to reaction with the magnetite to produce a solid mixture solutions of magnetite and magnesioferrite, with relatively little material left over to form a slag. Bentonite tended to increase the pellet strength due to increased amounts of slag whereas glucose reduced the strength by increasing the porosity. Ferrous sulphate had no significant effect on fired pellet strength (Ball *et al.*, 1974). Since it is much more likely that the above mentioned additives, if naturally present in clays, are incorporated into the various mineral phases in forms other than simple oxides and ionic compounds, it would therefore be difficult to be certain in advance whether a particular binder will have undesirable effects on the fired pellet quality.

2.5.2. Structure and chemistry of clay binders

2.5.2.1. Clay minerals, major constituents of raw clay materials

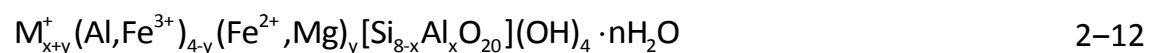
Clay minerals are the fundamental constituents of raw clay materials. Their crystal structure, with some exceptions, consists of sheets, giving rise to the terms sheet silicates or phyllosilicates, firmly arranged in structural layers. The individual layers are composed of two to four sheets that are formed by either tetrahedrons, [SiO₄]⁴⁻, or by octahedrons, e.g. [AlO₃(OH)₃]⁶⁻. The interior of tetrahedrons and octahedrons contains smaller metal cations, their apices being occupied by oxygen from which some are bonded to protons (as OH). All these fundamental structural elements are arranged to form a hexagonal network in each sheet (Velde & Meunier, 2008; Moore & Reynolds, 1997; Konta, 1995).

The crystalline clay minerals are classified into seven groups according to i) the number and the ratio of sheets in a fundamental structural layer, ii) the existing cation substitutions in the tetrahedral and octahedral sub-structures and iii) the resulting charge of the layers. These groups are the kaolinite and serpentine group, micas, vermiculites, smectites, pyrophyllite and talc group, chlorites and the palygorskite and sepiolite group (Konta, 1995; Newman, 1987). For the purpose of this study only the smectite and palygorskite groups will be discussed further, since these correlate with the clays selected in this case study.

2.5.2.2. *Smectites, mineral group of Bentonite*

Smectite is name given to a group of sodium, calcium, magnesium, iron, and lithium aluminum phyllosilicate minerals, both dioctahedral and trioctahedral, all of which are able to expand and contract their structures while maintaining two-dimensional crystallographic integrity. The individual mineral names for these are sodium montmorillonite, calcium montmorillonite, saponite, nontronite, beidellite and hectorite (Moore & Reynolds, 1997; Murry, 1991). These minerals consist of three-sheet phyllosilicates, where the tetrahedron:octahedron ratio is 2:1 and the charge of the three-sheet layer is 0.5-1.2.

Bentonite is formed by hydrothermal alteration of igneous volcanic ash deposits. It is actually a mixture of clay minerals, with the primary component being the smectite class mineral, montmorillonite, which has the ideal composition (Ball *et al.*, 1974):



M^+ represents the absorbed alkali cations in the interlayer space (especially Na^+). Where, however, alkaline earths (Ca^{2+} , Mg^{2+}) occur, they are represented by $M_{x/2}^{2+}$ (Konta, 1995). The basic crystal structure of montmorillonite is shown in Figure 2–16 (Murry, 1991; Grim, 1968).

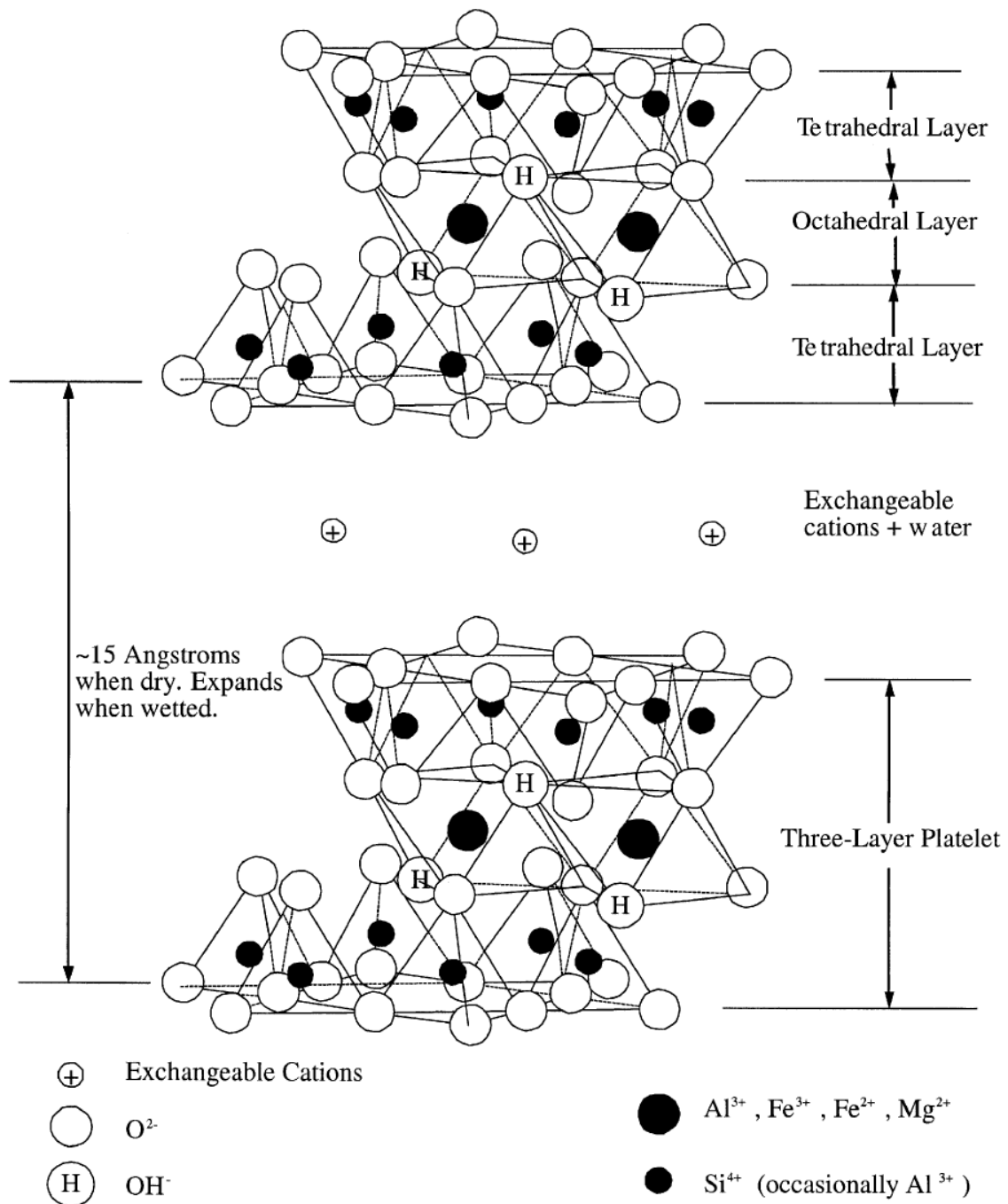


Figure 2–16: Structure of the smectite crystal (Murry, 1991; Grim, 1968)

Isomorphic substitution of Al^{3+} with Mg^{2+} into the $[\text{SiO}_4]^{4-}$ tetrahedrons sheets alters the crystal charge balance and requires surface adsorption of exchangeable cations, normally Na^+ and Ca^{2+} , to balance the charge. When coming into contact with water, illustrated in Figure 2–17, hydration of these exchangeable cations causes the clay mineral to swell. The swelling ability of montmorillonite differs depending on the type of exchangeable cation. Ca^{2+} have a higher charge and smaller diameter than Na^+ , and as a result tend to interact more strongly with the aluminophyllosilicates platelets, making them less susceptible to hydration. As a result, sodium bentonites hydrate and expand readily on contact with water whereas calcium bentonites expand to a much lesser extent (Eisele & Kawatra, 2003; Kawatra & Ripke, 2002; Kawatra & Ripke, 2001; Ripke & Kawatra, 2000c).

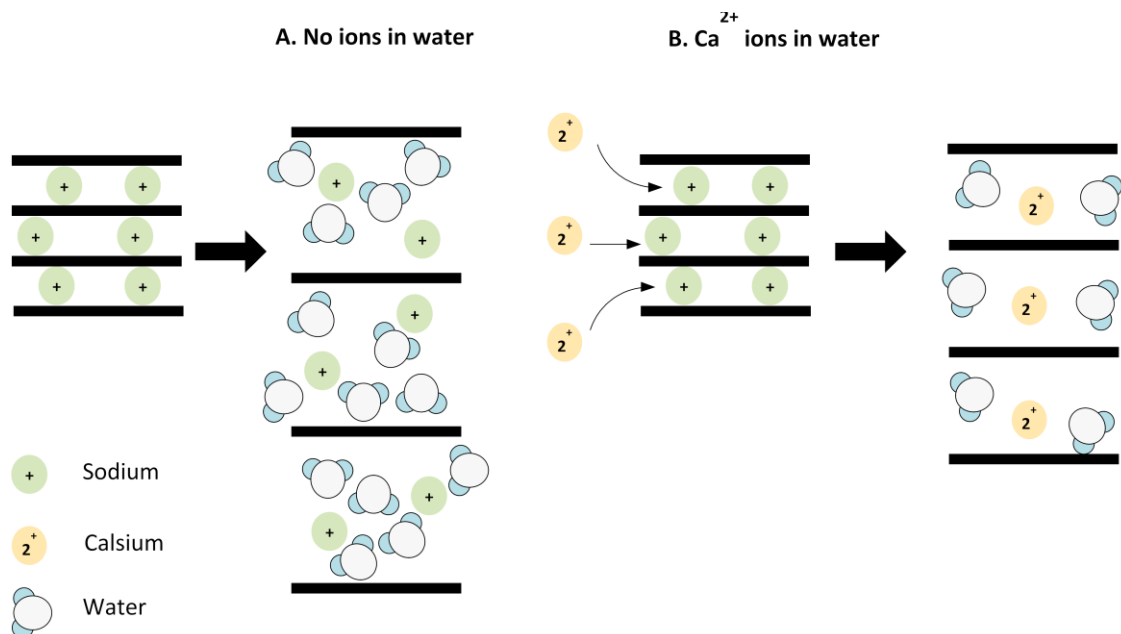


Figure 2–17: Effect of Ca^{2+} ions in water on the expansion of sodium bentonite. (A) Water contains no ions, bentonite expands freely. (B) Calcium in the water can displace sodium and increase the bonding between bentonite platelets so that the expansion is reduced (Kawatra & Ripke, 2003)

The expansion of the clay minerals in bentonite when they come in contact with water has three effects that are of interest in ore pelletisation (Eisele & Kawatra, 2003):

- i) It absorbs water, which can be valuable for controlling the moisture content of the pellets. It also increases the viscosity of the fluid between the mineral grains in the pellet, leading to a well-rounded, elastic pellet that can be conveniently handled and transported in the plant.
- ii) The clay binder is spread exceptionally easily throughout the raw materials upon mixing. During drying, the clay bonds to the mineral grains and to each other, giving excellent dry strength to the pellet. This is an important function of a pellet binder because in the absence of a binder, the pellet will disintegrate after it is dried. The effect of bentonite platelets on pellets during the drying process is presented in Figure 2–18.
- iii) During sintering to produce finished high-strength pellets, the sodium and calcium components of the bentonite act as fluxing agents, reducing the melting point of some of the minerals in the pellet. This allows a portion of the pellet to melt before the sintering temperature is reached. This helps to strengthen the pellets during the preheating stage, allowing dusting and breakage to be minimised during transfer to the final firing step.

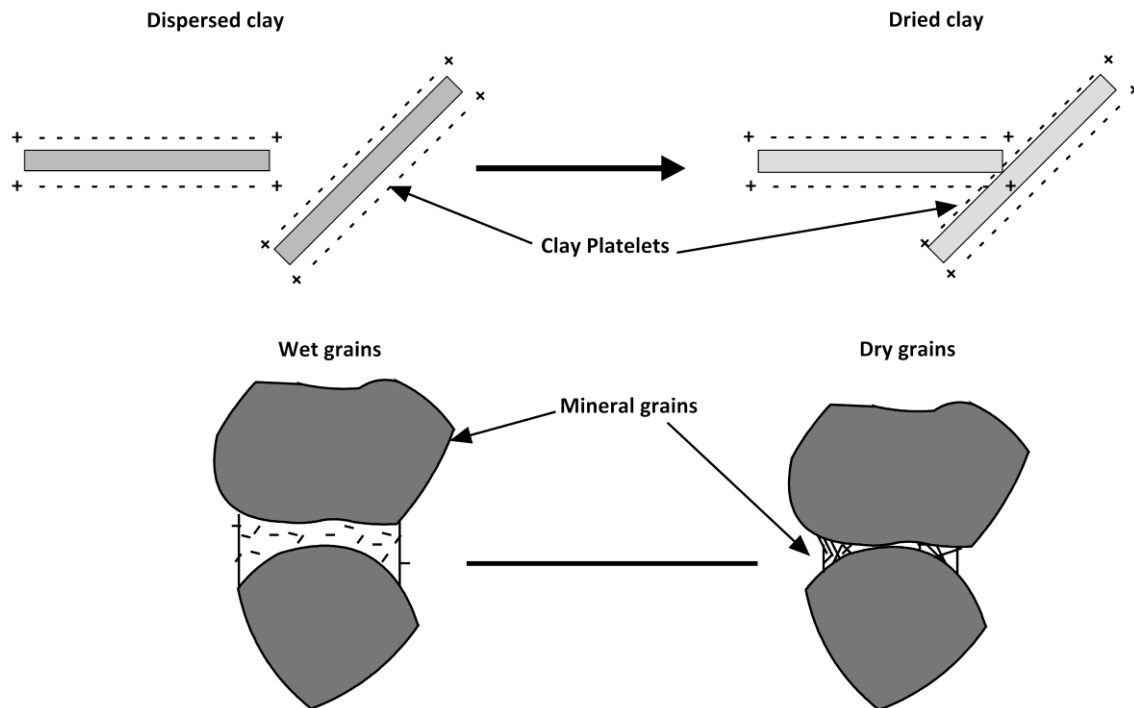


Figure 2–18: Conventional view of how bentonite platelets bind mineral grains in a pellet. Platelets are initially dispersed in the liquid, and the platelets bond to the mineral grains and each other as the liquid dries. Bonding is enhanced by the electrostatic attraction between the platelet faces (which have a negative charge) and the platelet edges (which are positively charged) (Van Olphen, 1987)

The conventional view (Figure 2–18, Figure 2–19 A and B) of the behaviour of clay as a binder is that the expanded clay disaggregates into submicron platelets, which would then adhere to the raw material particles and to each other as they dry. One of the characteristics of clay minerals that helps in this regard is that the edges of the platelets tend to have an electrostatic charge opposite than that of the platelets faces. This causes the clay platelets to bond to each other quite strongly by electrostatic bonding during the drying process (Van Olphen, 1987); however, it appears that this conventional view may not be entirely correct, particularly when the moisture content is not sufficient to completely disband and disperse the bentonite platelets (Eisele & Kawatra, 2003; Kawatra & Ripke, 2002; Kawatra & Ripke, 2001; Wenninger & Green, 1970). Kawatra and Ripke suggested a bentonite fibre bonding mechanism that is quite different from that of the conventional dispersion mechanism of

bentonite binding. They proposed that in low-moisture conditions the clay particles would, rather than disperse, expand into a fibrous matrix (Figure 2–19C) that ties the raw material particles together. These fibres form when a shearing action or force is applied, promoting the bentonite platelets to slide relative to one another, like a deck of cards pushed across a table, forming a fibrous web of strands Figure 2–20. The proposed mechanism is consistent with the fibrous appearance of silica sand grains bonded with bentonite in low moisture conditions, which is shown in the scanning electron micrographs of Figure 2–21.

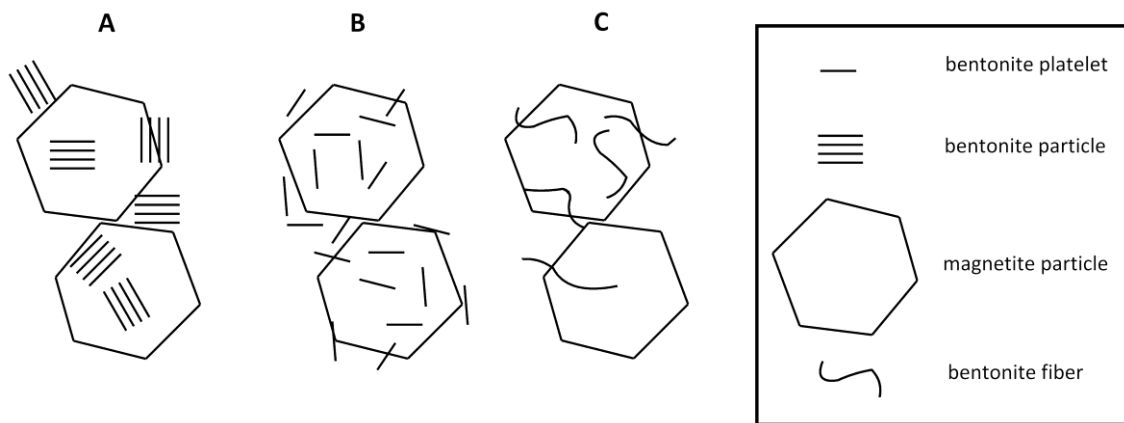


Figure 2–19: Two bonding mechanisms of bentonite on ferrous ore particles. Diagrams A and B show the dispersion mechanism. Diagram C shows the fibre mechanism (Kawatra & Ripke, 2001)

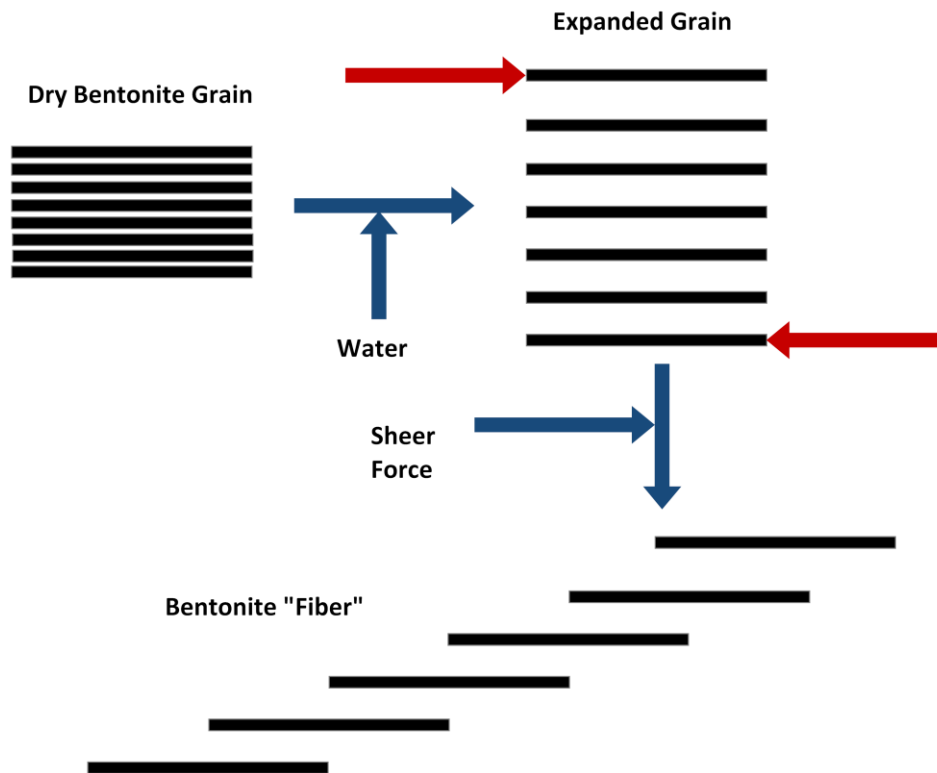


Figure 2–20: Behaviour of bentonite grains that are not completely dispersed in water. The grain expands when moistened and the platelets are lubricated by the interplatelet water. Under shear stress, the grain can then spread into a long fibre in an effect similar to spreading a deck of cards across a table (Eisele & Kawatra, 2003; Kawatra & Ripke, 2001)

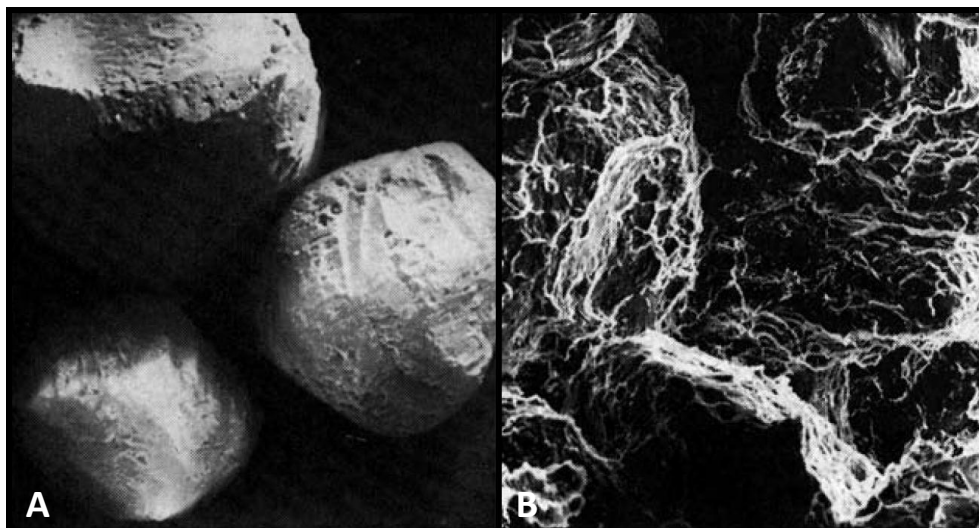


Figure 2–21: Scanning electron micrographs of silica sand (A) and of the same sand after bonding with bentonite (B). The bentonite formed strands stretching over and between grains, which is consistent with the bonding mechanism described by Kawatra and Ripke (2001). (A) Sand grains, AFS Fineness No. 55, taken at 250 times magnification. (B) Sand with 6.0% sodium bentonite, mixed 1.5 minutes with 3.2% water, taken at 250 times magnification (Wenninger & Green, 1970)

2.5.2.3. Palygorskite, mineral group of Attapulgite

Palygorskite and attapulgite are names for the same hydrated magnesium aluminum silicate clay mineral (Murry, 1991). The term attapulgite is largely used industrially even though the international mineral nomenclature committee ruled that palygorskite was first used and therefore the preferred term (Murray, 2002). The general molecular formula for palygorskite is $Mg_3Si_8O_{20}(OH)_2(OH_2)_4 \cdot 4H_2O$, with a small possibility of magnesium substitution by aluminium (Konta, 1995). Palygorskite's crystal shape (Figure 2–22) is typically that of fibres with thin elongate chain type structures because of two particularities of the crystal lattice i.e. i) a discontinuous octahedral sheet; ii) the $[SiO_4]^{4-}$ tetrahedra are periodically reversed (Velde & Meunier, 2008).

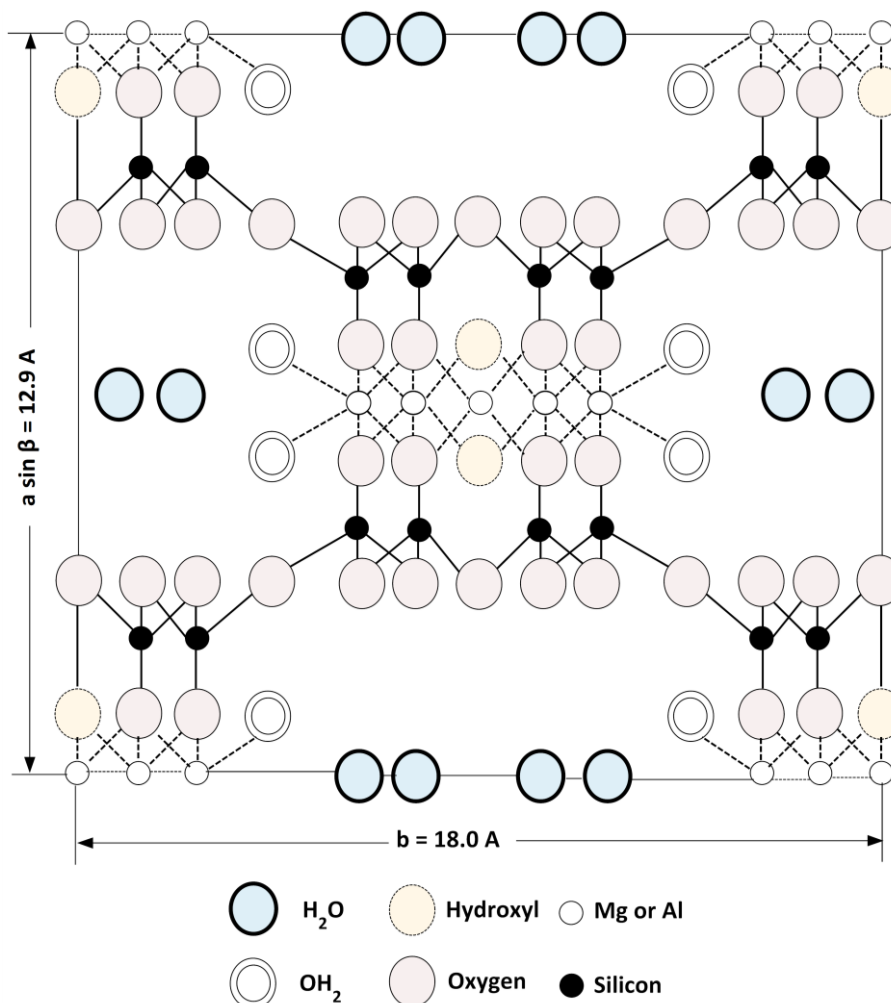
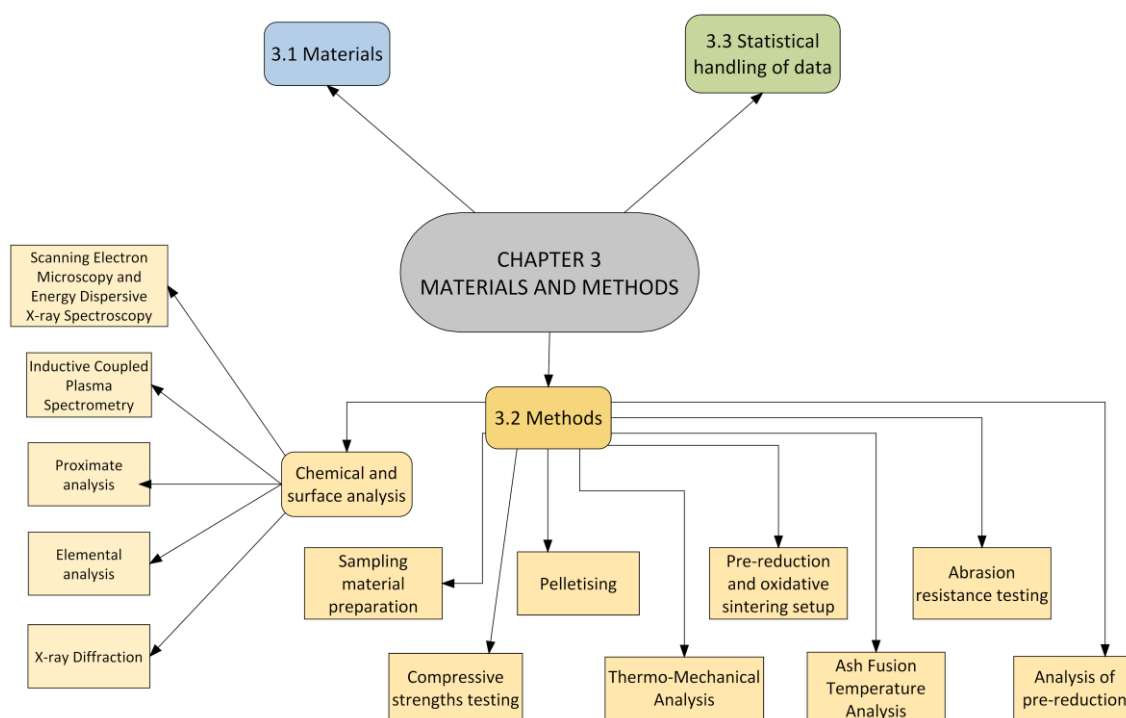


Figure 2–22: Structure of palygorskite (attapulgite) (Murry, 1991)

The silicon tetrahedra form ribbons elongated in one direction and due to periodic interruptions in the octahedral sheet, channels are formed. Therefore, when dispersed in water, these elongate crystals are inert and non-swelling and form a random lattice capable of trapping liquid by attraction due to the unbalanced charge of the cations. These clays do not flocculate with electrolytes and are stable at high temperatures, which make them uniquely applicable for a number of uses. The major uses of palygorskite are in drilling muds, paints, liquid detergents, adhesives, car polish, flexiographic inks, cosmetics, floor absorbents, potting mixes, oil-spill clean-up material, carriers for fertilizers, pesticides, or hazardous chemicals, decolourization of various mineral, vegetable and animal oils, as a receptor coating on carbonless copy paper, and for pet litter. Because these clays are relatively unaffected by electrolytes their viscosity is retained whereas bentonite flocculates and loses its high viscosity (Velde & Meunier, 2008; Murray, 2002; Konta, 1995; Murry, 1991).

Compared to bentonite, very little has been published about the possible binding mechanism of attapulgite during ore agglomeration processes. This makes theoretical comparison of the two different clay groups difficult.

CHAPTER 3: MATERIALS AND METHODS



3.1. Materials

The raw materials utilised in the industrial pelletised chromite pre-reduction process consist of ore, a carbonaceous reducing agent and a clay binder. All the raw materials used in this study, except the bentonite, were collected in bulk during a sampling campaign at the Xstrata Lydenburg FeCr plant (Xstrata, 2011b). The plant is situated in the Mpumalanga Province and is currently applying the pelletised chromite pre-reduction process. Samples of metallurgical grade chromite (< 1 mm), anthracite breeze and attapulgite clay being utilised by this FeCr plant were obtained. The metallurgical-grade chromite originally came from Xstrata's Helena Chrome Mine situated on the Eastern Limb of the BIC (Xstrata, 2011a). The anthracite breeze originated from Nkomati Anthracite (Pty) Ltd's mining operations south of eMangweni in the

Mpumalanga Province (Sentula, 2008). The attapulgite clay (lumpy) was from Atta Clay (Pty) Ltd's mine located in the Maandagshoek District in the Limpopo Province (AttaClay (Pty) Ltd., 2011). At the time this study was undertaken, this specific clay was the preferred choice for a binder at the Lydenburg FeCr plant. The bentonite clay used was from G&W Base and Industrial Minerals (Pty) Ltd (Pel-Bond bentonite grade) mined at their Koppies Bentonite Mine in the Free State Province. The bentonite is a sodium-activated bentonite that is specifically prepared for pelletising of ores (G&W Base (Pty) Ltd., 2011). Industrially produced chromite pre-reduced pellets were also obtained from the Xstrata Lydenburg FeCr plant.

SARM 8 and SARM 18 obtained from Industrial Analytical (Pty) Ltd were used as reference materials in the analysis of carbonaceous reductants and chromite containing materials, respectively. All other chemicals used were analytical grade (AR) reagents, obtained from the different suppliers and used without any further purification. Ultra-pure water (resistivity $18.2 \text{ M}\Omega\cdot\text{cm}^{-1}$), produced by a Milli-Q water purification system, was used for all procedures requiring water. Instrument grade synthetic air and nitrogen gas were supplied by Afrox.

3.2. Methods

3.2.1. Chemical and surface analysis

3.2.1.1. Scanning Electron Microscopy and Energy Dispersive X-ray Spectroscopy

Analyses using scanning electron microscopy incorporated with energy dispersive x-ray spectroscopy (SEM-EDS) were employed to visually and chemically characterise surface properties of samples. Analyses were conducted at both the North-West University and at Mintek (<http://www.mintek.co.za/>). Two different instruments were utilised, i.e. i) a

FEI QUANTA 200 ESEM, integrated with an OXFORD INCA X-Sight 200 EDS system operating with a 15 kV electron beam at a working distance of 10 mm located at the North-West University and ii) a Zeiss MA 15 SEM incorporating a Bruker AXS XFlash[®] 5010 Detector X-ray EDS system operating with a 20 kV electron beam at a working distance of 17.4 mm located at Mintek. Sample materials were mounted on buttons with carbon tape for visual and chemical characterisation at different magnifications. Copper tape instead of carbon tape was used to mount the anthracite sample to avoid carbon contamination when determining the surface chemical composition. For SEM-EDS characterisation of typical industrial pellets, sample pellets were split in half. The one half was polished before analysis, while the other half was left unpolished and analysed as is.

3.2.1.2. Inductively Coupled Plasma Spectrometry

Inductively Coupled Plasma Spectrometry (ICP) analyses of the bentonite and attapulgite clays were performed by SMI Analytical. Samples were microwave digested prior to analysis using a Perkin Elmer Multiwave[™] 3000 microwave sample preparation system. Typically nitric acid is placed in the reaction container with the sample and a combination of other reagents such as hydrochloric and hydrofluoric acid, or hydrogen peroxide is added depending on the sample matrix. Hydrofluoric and hydrochloric acids are used as digestive reagents, especially in the presence of silicates and precious metals respectively. The use of hydrogen peroxide enhances the oxidation properties of nitric acid especially in the digestion of organics. A 0.25 to 1.0 g sample was weighed and placed in the reaction container along with 9 mL of nitric acid. Depending on the sample matrix the appropriate amount of hydrofluoric and/or hydrochloric acid were then added. Finally the hydrogen peroxide was added. The mixture was then allowed to react for approximately one minute prior to sealing the container. The container was then slotted into a rotor and placed

inside the microwave. The sample container was then heated to at least 180 °C over 5.5 minutes and then held at 180 °C for at least 9.5 minutes (Kingston & Walter, 1998; EPA, 1996). The microwave digestion reagents and their specified mixing ratios according to different sample matrixes are indicated in Table 3-1.

Table 3-1: Microwave digestion reagents and their ratios according to sample matrix (EPA, 1996)

Matrix	Reagent and Volume (mL)			
	HNO ₃	HF	HCl	H ₂ O ₂
Soil/Metallurgical	9	3	2	1
Sediment	9	3	2	1
Biological	9	0	1	2
Botanical (e.g. leaves)	9	0.5	0.5	1
Botanical (e.g. wheat)	9	0	0.5	2
Waste oil (e.g. wear metals in lubricating oil)	9	0.5	0.5	2

Inductively coupled plasma mass spectrometry (ICP-MS) and inductively coupled plasma optical emission spectrometry (ICP-OES) of the bentonite and attapulgite clays were performed using a Perkin Elmer Optima 5300 ICP-OES, to determine major components, and a Perkin Elmer Elan 6100 ICP-MS to determine minors and trace elements. All results are as per ISO 17025 standards.

ICP-OES of the metallurgical grade chromite ore, anthracite, as well as the pre-reduced pellets were performed using a SPECTRO CIROS VISION ICP-OES Spectrometer. For the determination of major elements in the anthracite by ICP exactly 1 g of sample and 1 g of SARM 18, used as a reference, was placed on silica dishes and exposed to 815 °C for 1½ hour using a muffle furnace. The ash residues were separately transferred into zirconium crucibles each containing 2 g sodium peroxide and 0.5 g sodium carbonate as fluxes and mixed using a

spatula. The mixtures were then fused over a Bunsen flame until a complete melt was achieved. The crucibles were allowed to cool after which the fusions were taped loose from the crucibles and transferred to 500 mL beakers. The remaining fusion residue was washed out of the crucibles using four parts of 20 mL water. 20 mL 1:1 nitric acid was then added to the beakers. To ensure that the entire fusion residue had been removed, the crucibles were rinsed with 10 mL 1:1 nitric acid. All washings were added to the respective beakers, containing the previously collected solutions. The beakers were then placed on a hot plate and heated until the solutions cleared near boiling point. After clearing the solutions were removed and allowed to cool. The solutions were transferred to 200 mL volumetric flasks and 10 mL yttrium solution was added to each, where after they were diluted. The dilutions were then used for ICP analysis. The yttrium solution was prepared by dissolving 0.635 g yttrium oxide in 50 mL 1:1 water:HNO₃, heating the solution slightly until dissolved. The solution was then diluted to 5 L in a volumetric flask. Analysis of the chromite and pre-reduced pellets by ICP was conducted using the same procedure, except that samples were not reduced to ash at 815 °C. Instead exactly 0.2 g of sample was weighed off as starting material and SARM 8 used as a reference.

3.2.1.3. *Proximate analysis*

Proximate (inherent moisture, ash, volatile contents and fixed carbon) analysis of the anthracite was determined according to ASTM standard method D3172-07A (ASTM, 2007). The moisture content of the anthracite was determined by placing a 1 g sample in a drying oven at 110 °C for 1½ hours and measuring weight loss to determine the inherent moisture. Similarly, the ash content was determined by exposing a 1 g sample to 815 °C for 1½ hour using a muffle furnace. The volatile content of the anthracite was determined by adding 4 drops of methyl isobutyl ketone/acetone to a 1 g sample and exposing it to 900 °C for precisely 7 minutes. The fixed carbon was determined by deducting

the ash, moisture and volatile contents from the total weight (combined total 100%). Additionally the water loss and loss on ignition (LOI) of the clays were also determined at 110 and 1000 °C, respectively.

3.2.1.4. Elemental analysis

Elemental carbon and sulphur contents were determined to characterise the anthracite and to determine the fixed carbon (FC) in the experimentally prepared pre-reduced pellets. The pre-reduced pellets were analysed to confirm an excess of free carbon and ensure the reduction rates were not affected by a lack of reducing agent. This was done by means of IR spectrophotometry utilizing a LECO CS 244. A 1:1 mixture of tungsten and iron chips was used as the accelerator flux. Elemental carbon and sulphur analysis of the two clays was performed by SMI Analytical and similarly determined by using a LECO CS 230 IR spectrophotometer.

3.2.1.5. X-ray Diffraction

X-ray diffraction (XRD) of the clays was performed by XRD Analytical and Consulting cc as well as at the North-West University. The material was prepared for XRD analysis using a back-loading preparation method. Semi-quantitative and qualitative XRD analyses of the compounds in the clays were performed using two different instruments, i.e. i) a PANalytical X'Pert Pro powder diffractometer with Fe filtered Co-K radiation incorporating a X'Celerator detector located at XRD Analytical and Consulting cc and ii) a Philips X-ray diffractometer (PW 3040/60 X'Pert Pro) with Cu-K α radiation located at the North-West University. The measurements were performed between variable divergence- and fixed receiving slits. The phases were identified using X'Pert Highscore plus software. The relative phase amounts were estimated using the Rietveld method (Autoquan programme).

3.2.2. Sample material preparation

A Wenman Williams & Co disc mill was used to grind the lumpy attapulgite clay and the anthracite to < 1 mm. Different mixing ratios of the components present in the pre-reduced (chromite ore, anthracite and clay) and oxidative sintered pellets (chromite ore and clay) were then made up, according to the objectives of specific experiments. At the time when the experiments were conducted 3-4 wt% clay addition was being utilised in the industrial process. It was therefore decided to cover the range 2.5-5 wt% clay addition, but also to include a 10 wt% clay addition to help identify trends that might be difficult to recognize at low clay additions. The anthracite was kept constant at 20 wt% (relating to approximately 15 wt% fixed carbon) in all pre-reduction experiments. Anthracite was not added to the pellet mixtures made up for oxidative sintering experiments. The remainder of the mixtures were made up with the chromite ore. The recipes for a 50 g batch of pre-reduced and oxidative sintered pellet mixtures are indicated in Table 3-2.

All raw material mixtures were dry-milled to the particle size specifications applied for industrial pre-reduction feed material (90% smaller than 75 μm). A Siebtechnik laboratory disc mill with a tungsten carbide grinding chamber, to avoid possible iron contamination, was used for this purpose. A Malvern Mastersizer 2000 was used to determine the particle size distribution of the pulverised material. A very dilute suspension of milled ore was ultrasonicated for 60 s prior to the particle size measurement, in order to disperse the individual particles and to avoid the use of a chemical dispersant. It was determined that for a 50 g mixture of raw materials a milling time of 2 min was required to obtain the desired size specification, hence all raw material mixtures were milled similarly.

Table 3-2: Mixing ratios of the recipes for pre-reduced and oxidative sintered pellet mixtures

Pre-reduction experiments (50 g mixture)					
Clay		Anthracite		Ore	
wt%	g	wt%	g	wt%	g
2.5	1.25	20	10	77.5	38.75
3	1.5	20	10	77	38.5
3.5	1.75	20	10	76.5	38.25
4	2	20	10	76	38
5	2.5	20	10	75	37.5
10	5	20	10	70	35

Oxidative sintering conditions (50 g mixture)					
Clay		Anthracite		Ore	
wt%	g	wt%	g	wt%	g
2.5	1.25	-	-	97.5	48.75
3	1.5	-	-	97	48.5
3.5	1.75	-	-	96.5	48.25
4	2	-	-	96	48
5	2.5	-	-	95	47.5
10	5	-	-	90	45

3.2.3. Pelletising

The milled material was pressed into cylindrical pellets with a LRX Plus strength testing machine equipped with a 5 kN load cell from Ametek Lloyd Instruments and a Specac PT No. 3000 13 mm die set. Pellets were prepared in batches of 10 each. At the time when the experiments were conducted a pre-wet water content of approximately 12 wt% was being utilised in the industrial process. It was observed that water was being pressed out of the pellet mixtures when water contents higher than 9 wt% were used. This could have led to some of the mineral constituents dissolving in the water and thus subsequently being removed from the mixtures. For each batch 50 g of dry mixed raw material was pre-wetted with 5 g of water and mixed thoroughly. This related to the mixture

having a water content of approximately 9 wt%. 3.2 g of pre-wetted material was then placed in the die set and compressed at a rate of 10 mm/min until a load of 1500 N was reached, after which this load was held for 10 s. Although time-consuming (each pellet made individually), this technique was preferred over conventional disc pelletisation, since disk pelletisation on laboratory scale can result in the formation of pellets with different densities, sizes and spherical shapes. Pressing the pellets according to the above procedure ensured consistent density, form and size, making monovariance investigation of other process parameters possible.

3.2.4. Pre-reduction and oxidative sintering procedure

A ceramic tube furnace (Lenton Elite, UK model TSH15/75/610) with a programmable temperature controller was used to conduct all pre-reduction and oxidative sintering experiments. Ceramic heat shields were inserted at both ends of the tube furnace to improve the tube length in which a stable working temperature could be achieved. These heat shields also protected the stainless steel caps, which were fitted onto both side of the ceramic tube to seals the ends. The stainless steel caps had a gas inlet on the one side and an outlet on the other.

The gaseous atmosphere inside the ceramic tube was controlled by either utilising a N₂ flow rate of 1 NL/min, or synthetic air flow rate of 1 NL/min. N₂ was used when pre-reduction experiments were conducted, while synthetic air was used when oxidative sintering conditions were required. An inert (N₂) gaseous atmosphere was preferred for the pre-reduction experiments above a reducing gaseous atmosphere, since pre-reduction due to the presence of the carbonaceous reductant in the material mixture was of interest in this study, not pre-reduction occurring due to external gaseous conditions. For the pre-reducing experiments the tube furnace, already loaded with pellets, was flushed

with N₂ for at least 30 min at a flow rate of 1.25 NL/min at room temperature prior to the commencement of an experiment. This was done to avoid oxidising gasses being present.

Two temperature profiles (illustrated in Figure 3-1) were used in this experimental study. These profiles were compiled to attempt simulating conditions occurring in the industrial pelletised pre-reduction of chromite.

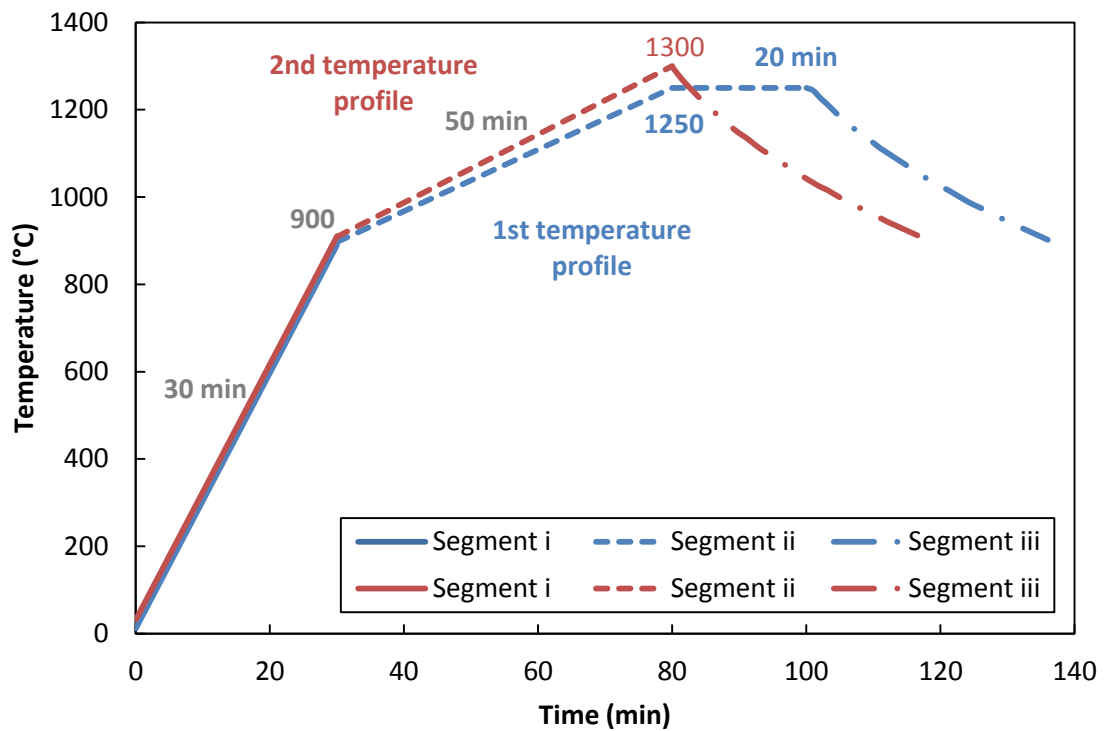


Figure 3-1: Temperature profiles used in pre-reduction and oxidative sintering experiments

Both temperature profiles consisted of three segments, i.e. i) heating up to 900 °C, ii) heating to the final temperature (and soaking if applicable) and iii) cooling down. In the first segment of both temperature profiles, pellets were heated from room temperature to 900 °C over a period of 30 min. In the second segment of the first temperature profile, the temperature was raised from 900 to 1250 °C within a 50 min period and held constant for 20 min, after which the furnace was switched off and allowed to cool down while gas flow

was maintained (segment three). In the second segment of the second temperature profile the temperature was raised from 900 to 1300 °C within a 50 min period, after which the furnace was switched off without any soaking time and allowed to cool down while gas flow was maintained (segment three).

3.2.5. Abrasion resistance testing

The abrasion resistance test apparatus was based on a downscaled version of the European standard EN 15051 rotating drum. The drum was designed according to specifications provided by Schneider and Jensen (2008). The drum was rotated at 44 rpm, which is 4 times faster than that used by Schneider and Jensen (2008). This was done to obtain measurable abrasion on the hardest experimentally prepared pellets. A batch (ten pellets) of the pre-reduced or oxidative sintered pellets was abraded for different time periods, i.e. 1, 2, 4, 8, 16, 32 min. After every time interval the material was screened using 9.5 and 1.18 mm screens. The over and under-sized material was then weighed and the material returned to the drum for further abrasion, until the final abrasion time was achieved.

3.2.6. Compressive strengths testing

Compressive strength is defined as the tensile or compressive load required to fracture a sample. The compressive strength testing method is based on measurements of the mechanical strength that develops in the pellets as sintering takes place. Compressive strengths of the pre-reduced or oxidative sintered pellets (Par. 3.2.4) were tested with an Ametek Lloyd Instruments LRXplus strength tester. A cylindrical pellet was placed on its round side between the compression plates as shown in Figure 3-2. This was done since it is more comparable to the relatively spherical shapes of the industrial pre-reduced pellets.

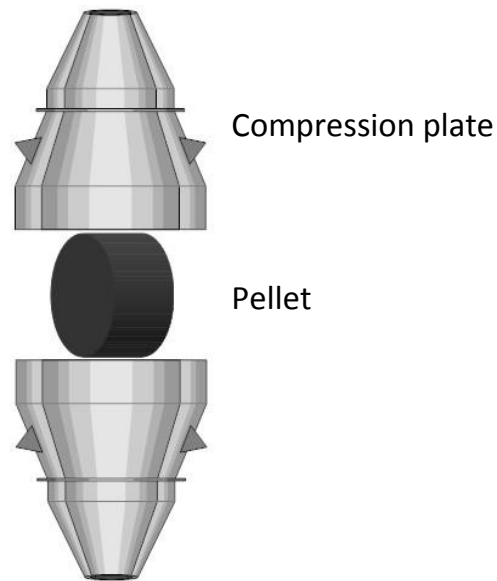


Figure 3-2: Graphic representation of compression strength test

The preload stress and preload speed were set to 0.0056 kN and 22 mm/min respectively. The speed of the compression plates was maintained at 10 mm/min during crushing to apply an increasing force on the pellets. The maximum load/force that each pellet endured before breakage occurred, as shown in Figure 3-3, was recorded.

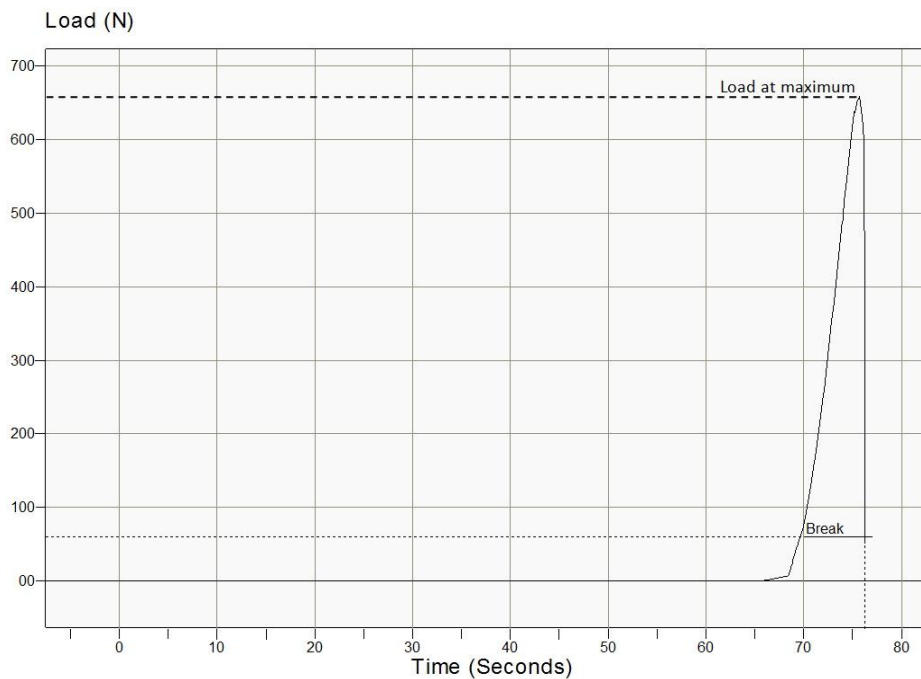


Figure 3-3: An example of a typical compressive strength graph

3.2.7. Thermo-Mechanical Analysis

Pellets were prepared in the same manner as described in Par. 3.2.3 but not pre-reduced or oxidatively sintered as indicated in Par. 3.2.4. A smaller Specac PT No. 3000 10 mm die set was used to pelletise 1 g of material in order for the pellet to fit inside the loading chamber. A single pellet was placed at a time in the Seiko Instruments Inc. TMA/SS 6100 thermal mechanical analyser, interfaced with SII EXSTAR 6000. With this instrument the thermal expansion of the pellets could be measured as a function of temperature up to 1300 °C. The temperature programme was set to ramp at a rate of 5 °C/min from ~22 °C to 1300 °C over a time period of 260 min. All thermo-mechanical analysis (TMA) experiments were conducted in a N₂ atmosphere (1.67 NL/h), since oxidative corrosion of the internal parts of this specific instrument has been detected when operating under atmospheric gaseous conditions. Since the TMA probe was made of alumina, α -alumina coefficients correction was applied to the data as specified in the operational manual of the instrument.

3.2.8. Ash Fusion Temperature Analysis

Ash fusion temperature analysis is usually done to characterise the melting and sintering behaviours of coal ash (Nel *et al.*, 2011). However, it was also applied to the two clays utilised as case study materials in this investigation. The SABS ISO 540:2008 standard method was performed with a Carbolite CAF digital imaging coal ash fusion test furnace by Advanced Coal Technology (<http://www.advancedcoaltech.com/>). In this test a moulded cone of each clay was viewed and the following four temperatures recorded: i) deformation temperature, when the corners of the mould first became rounded; ii) softening temperature, when the top of the mould took on a spherical shape; iii) hemisphere temperature, when the entire mould took on a hemisphere

shape and iv) fluid temperature, when the molten material collapsed to a flattened button on the furnace floor.

3.2.9. Analysis of pre-reduction

This extent of chromite pre-reduction was determined according to the method utilised by laboratories associated with the FeCr smelters in South Africa currently applying the pelletised chromite pre-reduction process, which was based on the methods published by Dinnin (1959).

The % soluble iron and % soluble chrome, required for calculating the % total reduction, is obtained by firstly leaching a pulverised sample in an acidified water solution. Exactly 1 g of pulverised sample material is weighed into a 500 mL Erlenmeyer flask and 50 mL leaching solution is added. The sample is leached under reflux for 1.5 hours at 120 °C on a hot plate. The leaching solution is prepared by adding 100 mL concentrated H_3PO_4 and 400 mL concentrated H_2SO_4 to 500 mL water. The sample solution is then diluted to 250 mL in a volumetric flask where after it is filtrated. Twenty percent of the leachate solution is used for the determination of the soluble chrome and forty percent for soluble iron determination.

A 50 mL (20% aliquot) of the filtrate solution is pipetted into a 250 mL Phillips beaker. 5 mL potassium permanganate solution, 3% w/v (weight by volume), is added and the solution brought to boil for 4 min. 25 mL sodium chloride solution, 20% w/v, is then added and the solution boiled until clear. The solution is removed, allowed to cool and 100 mL water is then added. The % soluble chrome is determined volumetrically by a ferrous ammonium sulphate-potassium dichromate titration, with the titrate value designated as T. 10 mL of a 0.2 M ferrous ammonium sulphate solution is added to the cooled chrome leached solution. 2-3 drops of diphenylamine sulphonate are added as indicator. The indicator is prepared by dissolving 0.5 g diphenylamine

sulphonate in 100 mL water. The solution is then titrated against a 0.1 M potassium dichromate solution till a definite purple colour is reached. The % soluble Cr was determined using Equation 3–1.

$$\% \text{ Sol Cr} = \frac{(E - T) \times F \times 0.1734}{\text{Sample Mass} \times 20\% \text{ (Aliquot mass)}} \quad 3-1$$

The equivalent, E, is obtained by adding 50 mL of the acid leaching solution to 200 mL water. 10 mL of 0.2 M ferrous ammonium sulphate solution and 2-3 drops of diphenylamine sulphonate is added where after the solution is titrated against 0.1 M potassium dichromate solution till a purple colour is reached. The titration value is designated E.

The % soluble iron is determined by pipetting 100 mL (40% aliquot) of the leached filtrate solution into a 500 mL Erlenmeyer flask, adding 2-3 drops of diphenylamine sulphonate indicator and titrating the solution against 0.1 M potassium dichromate. The % soluble Fe was determined using Equation 3–2.

$$\% \text{ Sol Fe} = \frac{T \times F \times 0.5585}{\text{Sample Mass} \times 40\% \text{ (Aliquot mass)}} \quad 3-2$$

The results for % soluble chrome as well as soluble iron obtained by this method are ~1% low when compared with $K_2Cr_2O_7$ taken as the primary standard (Dinnin, 1959). For greater accuracy a correction factor, designated F, is used. F is determined after $K_2Cr_2O_7$ standardisation. 0.2 g $K_2Cr_2O_7$ is weighed into a 500 mL Erlenmeyer flask. 100 mL water followed by 20 mL 1:1 H_2SO_4 and 5 mL phosphoric acid is added to the flask. Using a pipette 40 mL 0.2 M ferrous ammonium sulphate is added to the solution. As an indicator 3-5 drops of diphenylamine sulphonate are added and the solution titrated against the 0.1 M

potassium dichromate solution with the titration value designated T. The factor F was calculated using Equation 3–3.

$$F = \frac{\text{Mass K}_2\text{Cr}_2\text{O}_7 \times 1000}{4.904 \times (E - T)} \quad 3-3$$

The equivalent, E, is determined as described above, however 40 mL of 0.2 M ferrous ammonium sulphate solution and 3-5 drops of diphenylamine sulphonate are used.

The % total pre-reduction was calculated using Equation 3–4.

$$\% \text{ Total Pre-reduction} = \frac{\frac{\% \text{ Sol Cr}}{34.67} + \frac{\% \text{ Sol Fe}}{55.85}}{0.0121} \quad 3-4$$

3.3. Statistical handling of data

Most of the analyses and experiments were performed a number of times. In order to ensure that outliers did not influence statistically calculated values, such as averages and standard deviations, the Q-test as recommended by Skoog *et al.* (2004) was applied to the datasets with the aim of identifying and eliminating outliers. The absolute value of the difference between the questionable result (x_q) and its nearest value (x_n) is divided by the spread (w) of the entire dataset to give the estimated Q-value as indicated in Equation 3–5.

$$Q = \frac{|x_q - x_n|}{w} \quad 3-5$$

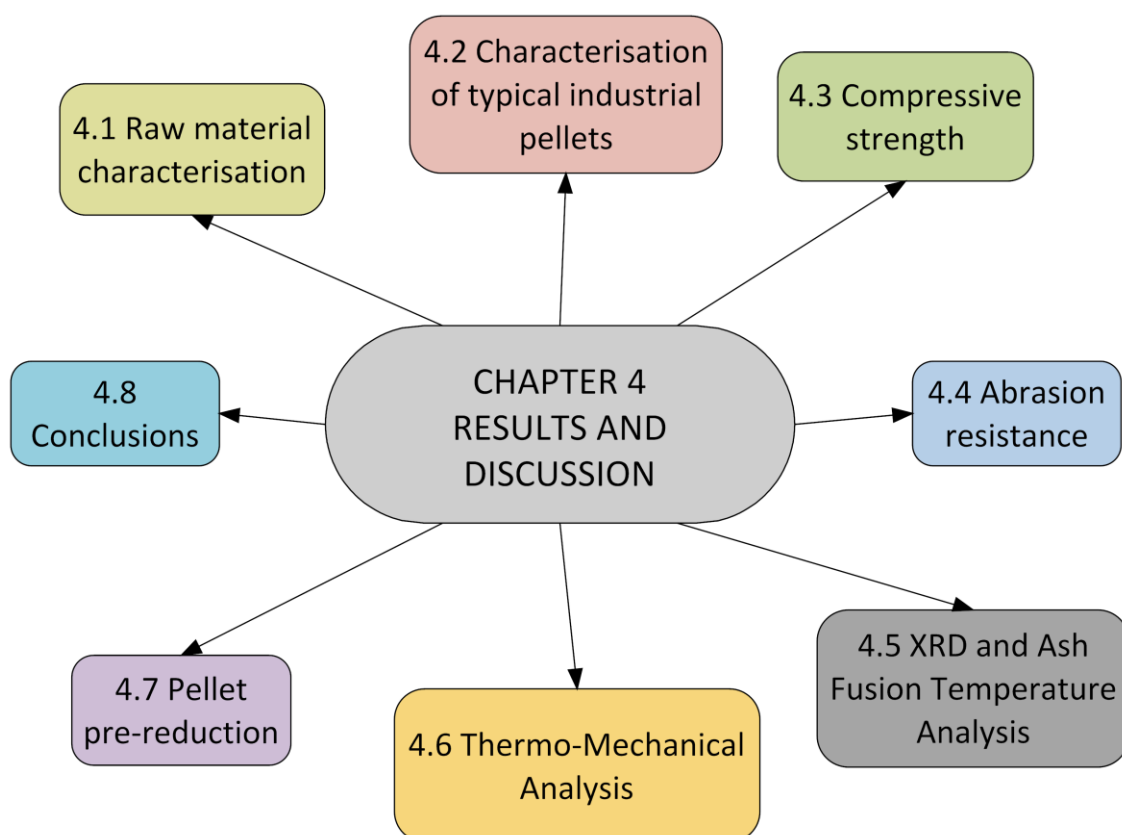
This Q-value is then compared to critical values (Q_{crit}) found in Table 3-3 (Dean & Dixon, 1951). If the value of Q was greater than Q_{crit} , the questionable value was rejected from statistical calculations. During this study, a 95% confidence level, as indicated in Table 3-3, was used.

Table 3-3: Critical values for the rejection of quotient Q (Dean & Dixon, 1951)

Number of observations	Q_{crit} (Reject if $Q > Q_{crit}$)		
	90% Confidence	95% Confidence	99% Confidence
3	0.941	0.97	0.994
4	0.765	0.829	0.926
5	0.642	0.71	0.821
6	0.56	0.625	0.74
7	0.507	0.568	0.68
8	0.468	0.526	0.634
9	0.437	0.493	0.598
10	0.412	0.466	0.568

The compressive strength results were compiled from 20 repetitions for every set of experimental conditions reported, the abrasion resistance strength tests from 3 repetitions, the TMA results from 6 repetitions and the pre-reduction determinations from 5 repetitions of the entire experimental procedure for every experimental condition tested. The mean and standard deviations were calculated for every dataset, after the elimination of possible outliers utilising the Q-test with 95% confidence level. The mean and standard deviations were then used in the presented data shown in Chapter 4.

CHAPTER 4: RESULTS AND DISCUSSION



4.1. Raw material characterisation

Different chemical and physical properties of raw materials (ore, carbon reductant and clay binder) play a crucial role in the various pelletising and pre-reduction sub-processes (drying, grinding, moistening, pelletisation, pellet drying, pre-heating and roasting) and variations in these properties could significantly affect the process as a whole (Singh & Mohan Rao, 2008; Chakraborty *et al.*, 2007; Pistorius, 2002; Dawson & Edwards, 1986). It was therefore very important to not only characterise the two case study clays properly, but the chromite ore and anthracite reductant as well. The visual and chemical characterisation by means of SEM, ICP, SEM-EDS, proximate and

elemental analysis of the raw materials utilised are indicated in Figure 4–1 and Table 4–1.

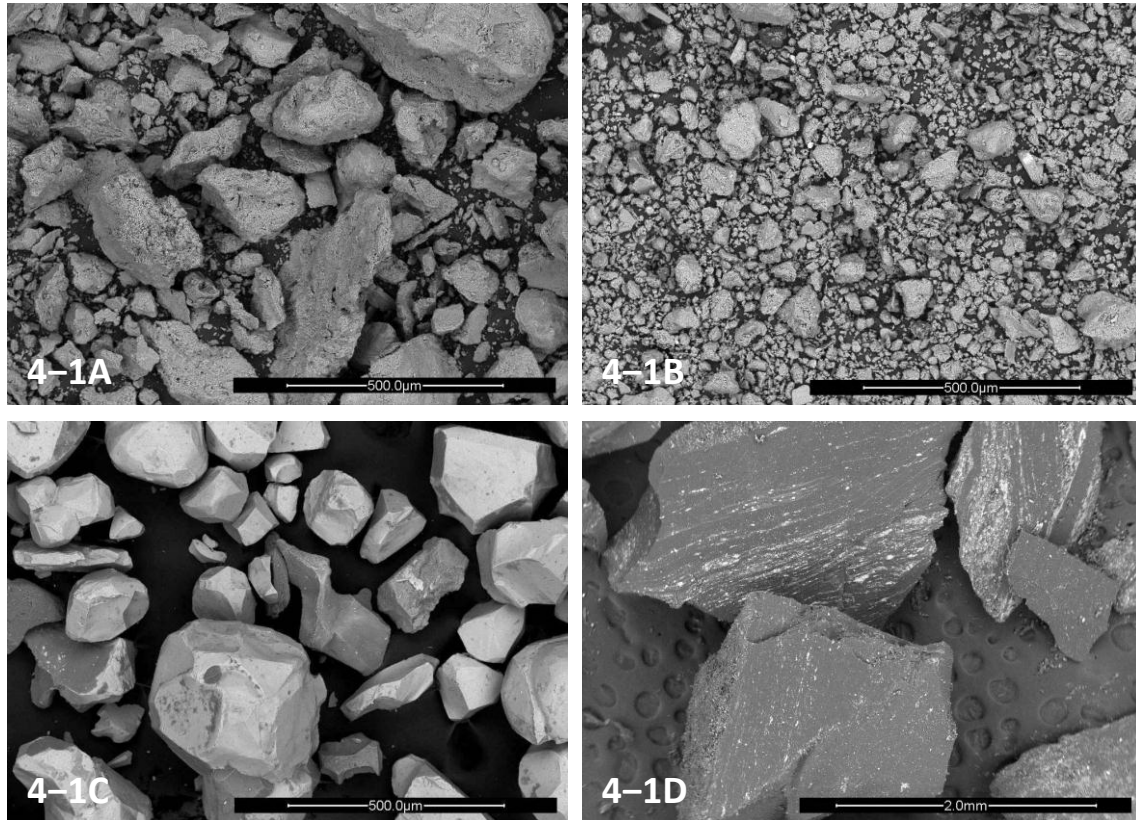


Figure 4–1: SEM micrograph images of the attapulgite clay (4–1A), bentonite clay (4–1B) and chromite ore (4–1C) taken at 200 times magnification as well as the anthracite (4–1D) taken at 60 times magnification

Figure 4–1C is a micrograph of a chromite ore sample taken at 200 times magnification. It can be seen from Figure 4–1C that the majority of ore particles are smaller than 0.5 mm, which is consistent with beneficiated chromite ore commonly known as metallurgical grade (< 1 mm) (Glastonbury *et al.*, 2010). Figure 4–1A and Figure 4–1B is micrographs of an attapulgite and bentonite sample respectively taken at 200 times magnification. It can be seen from Figure 4–1A and Figure 4–1B that the bentonite had a much finer consistency than the attapulgite clay.

Table 4–1: Chemical characterization of the different raw materials utilised, with various techniques

Chromite				Anthracite			
ICP (%)		SEM-EDS (%)		ICP (%)		SEM-EDS (%)	
Cr ₂ O ₃	45.37	Cr	27.21	SiO ₂	10.09	Si	2.53
FeO	25.39	Fe	15.33	Al ₂ O ₃	3.13	Al	0.89
Al ₂ O ₃	15.21	Al	6.39	FeO	1.62	Fe	1.19
MgO	9.83	Mg	6.37	CaO	0.8	Ca	0.18
SiO ₂	1.72	Si	3.70	MgO	0.35	-	-
CaO	0.22	Ca	0.48	P	0.011	-	-
P	< 0.01	Ti	0.37	S	0.59	S	0.68
-	-	O	40.16	-	-	C	76.9
-	-	-	-	-	-	O	17.63
				Proximate analysis (%)			
				FC		75.08	
				Inherent Moisture		0.26	
				Ash		17.79	
				Volatiles		6.87	
Attapulgitite				Bentonite			
ICP (%)		SEM-EDS (%)		ICP (%)		SEM-EDS (%)	
SiO ₂	46.91	Si	21.80	SiO ₂	53.53	Si	23.61
Al ₂ O ₃	14.76	Al	8.11	Al ₂ O ₃	13.17	Al	7.35
Fe ₂ O ₃	6.72	Fe	5.32	Fe ₂ O ₃	5.33	Fe	5.73
Fe	4.70	-	-	Fe	3.73	-	-
CaO	5.63	Ca	3.14	CaO	4.77	Ca	3.37
MgO	5.29	Mg	2.91	MgO	2.64	Mg	1.70
TiO ₂	0.26	Ti	0.15	TiO ₂	0.45	Ti	0.31
-	-	Na	0.12	-	-	Na	2.15
K ₂ O	0.21	K	0.09	K ₂ O	1.14	K	1.10
MnO	0.15	-	-	MnO	0.08	-	-
P	< 0.01	-	-	P	0.02	-	-
-	-	O	58.36	-	-	O	54.69
LECO (%)				LECO (%)			
C		1.47		C		1.14	
S		< 0.001		S		< 0.001	
Water loss (110 °C)		8.73 wt%		Water loss (110 °C)		9.78 wt%	
LOI (1000 °C)		13.04 wt%		LOI (1000 °C)		7.69 wt%	

From the ICP and SEM-EDS results, the Cr-to-Fe ratio of the chromite was calculated as 1.57, which is typical of South African deposits (Cramer *et al.*, 2004; Howat, 1986). The anthracite had a fixed carbon content of approximately 75% and a volatile content of 6.87%. This volatile content was under the maximum acceptable volatile content specification of 7%, as a higher volatile content generally results in pellets bursting while passing through the grate and rotary kiln (Naiker, 2007). The major ash elements in the anthracite were found to be Si, Al, Fe, P, Ca and Mg. As expected the clays were mainly alumina-silicates. The significance of other elements in the clays will be discussed later. Phosphorous and sulphur contents are usually included in the FeCr specifications (Basson *et al.*, 2007), hence they were also measured where applicable.

4.2. Characterisation of typical industrial pellets

In order to illustrate the unique process considerations of clay binders in the pelletised chromite pre-reduced process, SEM backscatter micrograph images of an industrially produced pellet as well as SEM-EDS analysis of different zones occurring in the industrial pellet are shown in Figure 4–2 and Table 4–2 respectively.

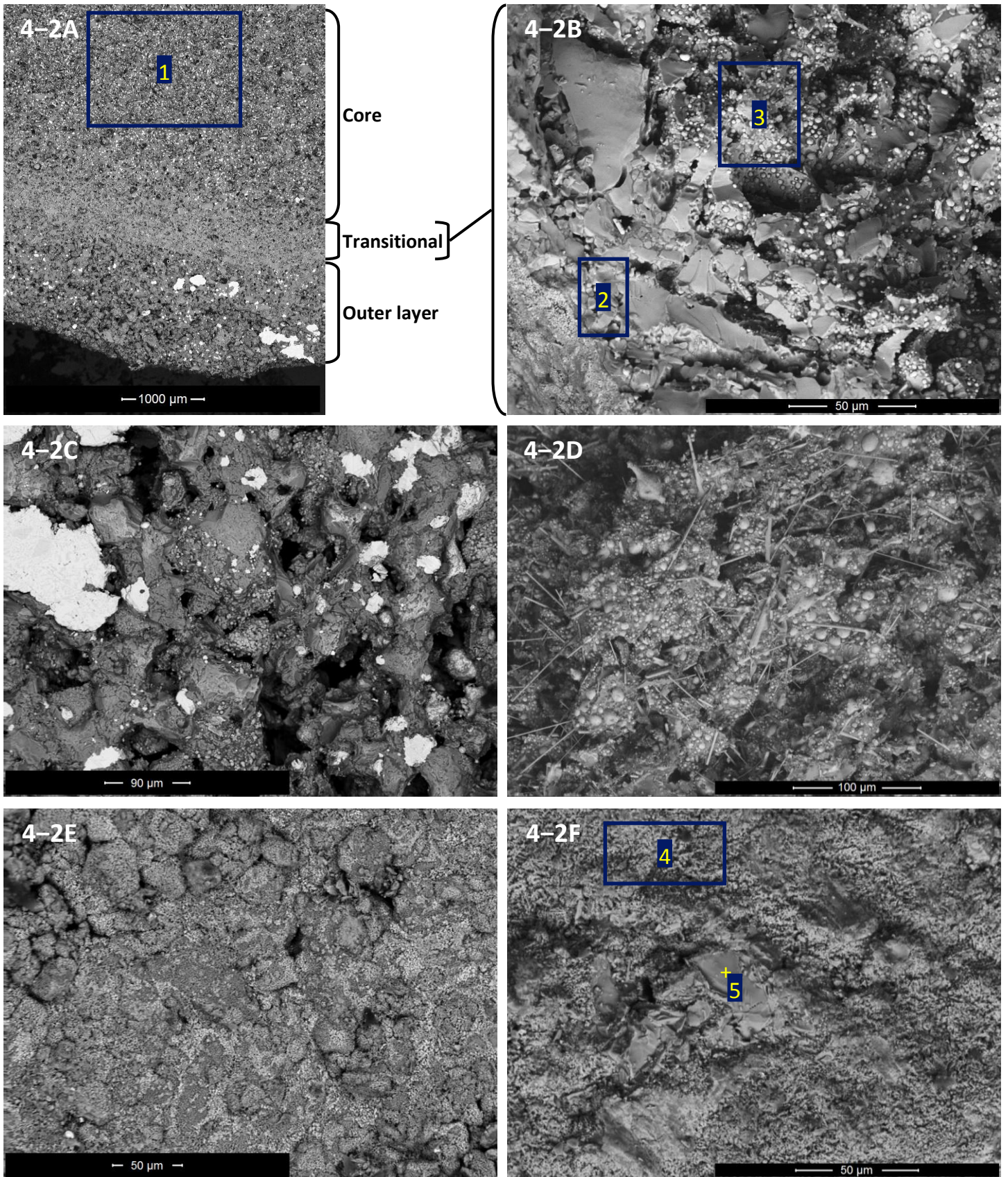


Figure 4-2: Partial SEM micrograph image taken at 45 times magnification of a polished section of an industrial pre-reduced pellet split in two (4-2A), a micrograph of an unpolished section zoomed in (650 times) on the transitional zone and showing part of the core area (4-2B), a micrograph taken at 550 times magnification of the outer layer of a polished section (4-2C), a micrograph taken at 300 times magnification of the inner core of an unpolished section (4-2D) and micrographs of the surface of an industrial pre-reduced pellet taken at 800 times (4-2E) and 650 times (4-2F) magnification

Table 4–2: SEM-EDS analysis performed on selected areas of the industrial pre-reduced pellet

Area	wt%								
	C	Mg	Al	Si	Ca	Ti	Cr	Fe	O
1	7.16	3.85	5.50	3.87	0.88	0.33	21.70	11.83	44.89
2	1.06	5.43	7.71	2.37	0.67	0.40	30.23	16.84	35.28
3	1.91	4.38	6.38	3.34	0.55	0.43	25.32	21.78	35.90
4	1.01	1.03	7.30	8.62	0.17	0.17	31.41	14.00	36.30
5	3.21	0.48	3.77	2.87	9.10	3.65	2.66	36.91	37.37

Figure 4–2A is a partial micrograph of a polished sectional view taken at 45 times magnification of an industrial pre-reduced pellet split in half. As can be seen from Figure 4–2A, it seems as if there are two different zones in such pellets, i.e. the core (Figure 4–2D) and an outer layer (Figure 4–2C), with a transitional zone in between. These two zones correspond to the different conditions to which the pelletised material is exposed during the industrial pre-reduction process. Initially the raw material components (chromite, carbon reductant and clay) are homogeneously spread throughout the pellet. However, as the pellet is exposed to the high temperatures inside the rotary kiln, where the pre-reduction process takes place, the carbon in the outer layer is mostly burned off and a partially oxidised outer layer is formed due to the presence of oxygen at these high temperatures. As the carbon is burned off, pores are formed as well as a network of sintered slag bridges, which can be observed in Figure 4–2C and Figure 4–2E. A small amount of iron reduction might take place before all carbon is consumed in this outer layer, but this can be re-oxidised again. In contrast, oxygen ingress to the core does not take place. At temperatures above 710 °C, reducing reactions of the iron oxides commence (Niemelä *et al.*, 2004), causing reaction gas to escape from within the pellet, thus making it impossible for oxygen to diffuse into the pellet core. Therefore, very little carbon combustion of the core takes place around this

temperature range and higher. The carbon in the core acts as a reductant, resulting in pre-reduction without any oxidation impacting the core. Figure 4–2B indicates the transitional area between these two different zones. In the core area (top right of Figure 4–2B), small globules of pre-reduced metal can be seen, while the transitional zone (bottom left of Figure 4–2B) seems to have a more sintered appearance not indicating any significant metal globules. SEM-EDS analysis was performed in order to chemically characterise the different zones forming within the industrial pellet. Analysis of the core (Figure 4–2A, Area 1) and the outside (Figure 4–2F, Area 4) of the pellet indicated that the surface chemical carbon content of this specific pellet was approximately 7.1 wt% and 1 wt%, respectively. Analysis of the transitional zone (Figure 4–2B, Area 2&3) indicated a surface chemical carbon content of 1-2 wt%. The small amount of carbon still present in the outer layer is most likely due to the formation of iron carbides, prior to complete oxidative combustion of the free carbon in this layer. The thickness of the outer layer is usually less than 1 mm (approximately 0.5 mm in this case), while the overall diameter of the industrial pellets is usually between 12-20 mm.

From the above description it is evident that the functioning of a clay binder within the pelletised chromite pre-reduced process has to be evaluated within two different environments, i.e. performance within an oxidative environment (corresponding to the outer layer of the industrially pre-reduced pellets) and performance within a reducing environment (corresponding to the core of the industrially pre-reduced pellets). This is in contrast with other chromite pelletised processes, e.g. the oxidative sintered pelletised process (Beukes *et al.*, 2010; Outotec, 2009; Outotec, 2008) where only one condition prevails. In the paragraphs that follow, clay binder functioning and characteristics are therefore explored in both environments (reducing and oxidative) in order to fully understand its functioning in the pelletised chromite pre-reduced process. In experiments where the oxidative sintering characteristics were investigated, the

carbonaceous reducing agent, i.e. anthracite, was omitted from the raw material mixture to ensure that reducing behaviour did not influence the results.

4.3. Compressive strength

The compressive strength results for the pellets pre-reduced up to 1250 °C for 20 min (contained anthracite and pre-reduced under N₂), as well as oxidative sintered pellets cured at 1250 °C for 20 min (containing no anthracite and sintered in synthetic air) are shown in Figure 4–3. Figure 4–4 shows similar results, but with the second temperature profile utilised, i.e. maximum temperature of 1300 °C, with no soaking time.

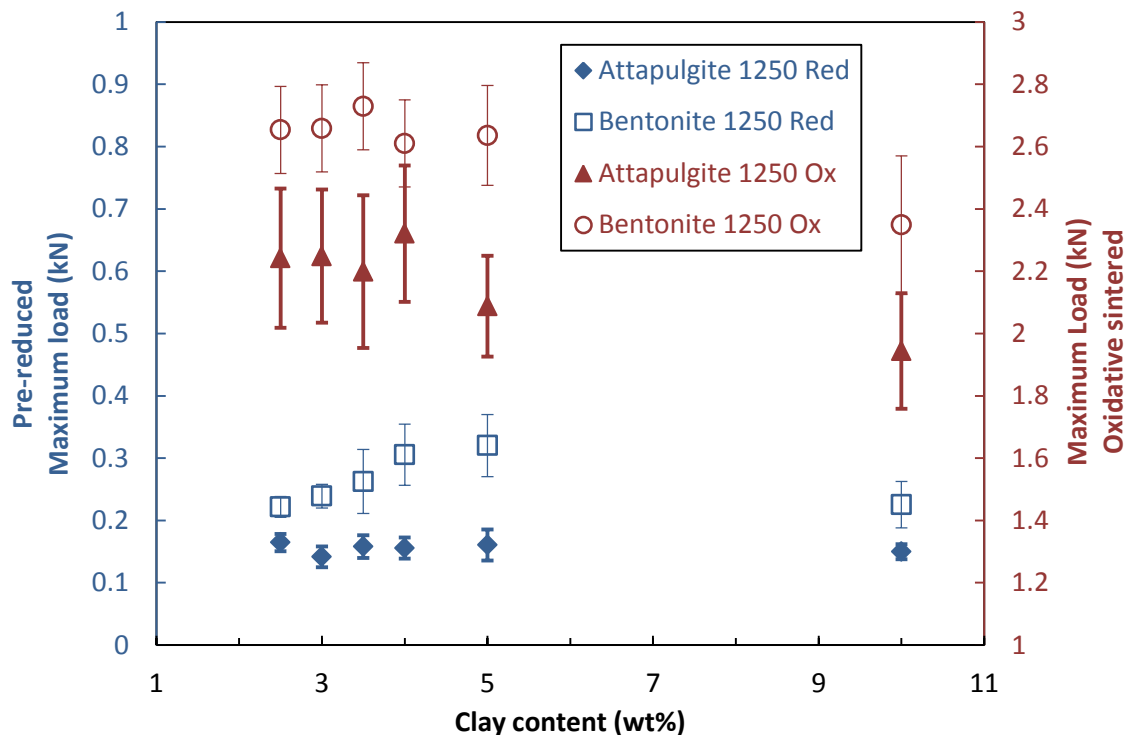


Figure 4–3: Compressive strength (kN) of pre-reduced (primary axis) and oxidative sintered (secondary axis) pellets for the temperature profile up to 1250 °C and hold time of 20 min

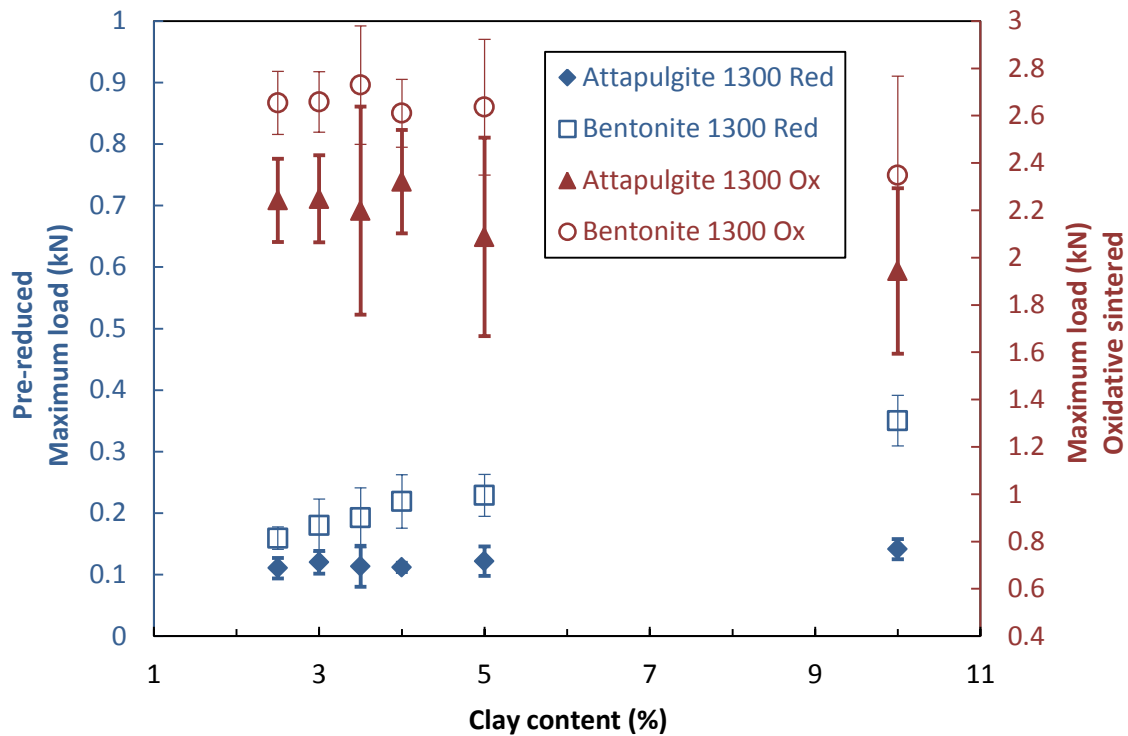


Figure 4-4: Compressive strength (kN) of pre-reduced (primary axis) and oxidative sintered (secondary axis) pellets for the temperature profile up to 1300 °C with no hold time

From both these sets of results several important deductions can be made. The compressive strengths of the oxidative sintered pellets were approximately an order of magnitude higher than that of the pre-reduced pellets. Thus, although the objective of the industrially applied pelletised chromite pre-reduced process is to achieve maximum pre-reduction, the compressive strength of pre-reduced chromite pellets is enhanced significantly by the thin oxidised outer layer (Par. 4.2).

By comparison of the compressive strengths of the two case study clays it is clear that the bentonite clay was superior in both pre-reducing and oxidative sintering environments. This is significant, since the attapulgite clay is currently the preferred option at both South African FeCr smelting plants applying the pelletised chromite pre-reduction process.

The compressive strength of the bentonite-containing pre-reduced pellets generally improved with increased clay content between 2 and 5 wt% additions, which is the industrially relevant addition range. Increased attapulgite content did not, however, result in any significant increased compressive strength of the pre-reduced pellets. Increasing the attapulgite clay content of the industrial pre-reduced pellets might therefore not result in a stronger pellet core (Par. 4.2), although it might aid the green strength, which was not considered in this study.

For both case study clays an increased clay addition resulted in a slightly decreasing trend in compressive strengths of the oxidative sintered pellets. This indicates that clay content addition is not such an important parameter in attaining a strong oxidised outer layer (Par 4.2) on the industrially produced pellets.

4.4. Abrasion resistance

The abrasion resistance strength results for both pre-reduced (contained anthracite and pre-reduced under N₂) and oxidative sintered pellets (containing no anthracite and sintered in synthetic air) cured up to 1300 °C without holding time, for 3.5 and 10% clay contents are shown in Figure 4–5. The results are presented as the percentage weight retained in the size fraction > 9.5 mm. Similar to the compressive strength results, the abrasion resistance strength of the oxidative sintered pellets (indicated on secondary y-axis) was substantially better than that of the pre-reduced pellets (indicated on primary y-axis) with both clay contents. This again confirmed the importance of the oxidised outer layer (Par. 4.2) in imparting strength to the industrially produced pellets. Also, the bentonite outperformed the attapulgite in pre-reduced, as well as oxidative sintered abrasion resistance strength, which again is significant considering that attapulgite is currently the preferred option.

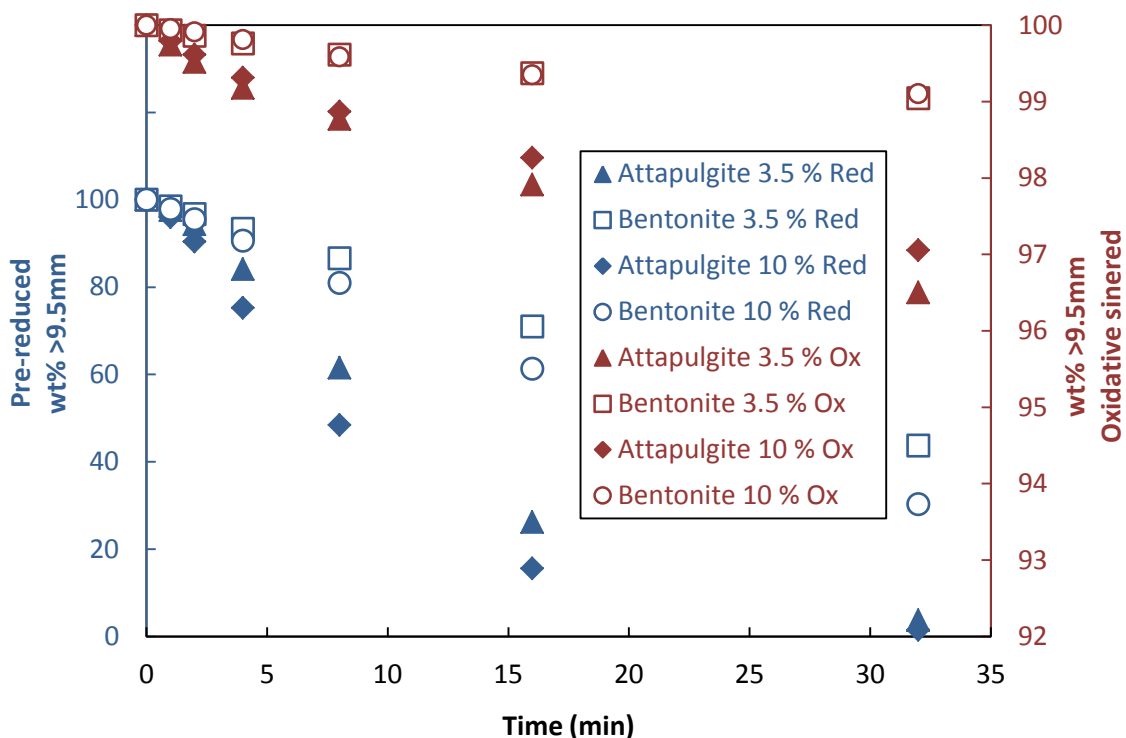


Figure 4–5: Abrasion resistance strength indicated in weight percentage remaining above 9.5 mm versus abrasion time (note error bars were removed, since they were smaller than the markers)

4.5. XRD and Ash Fusion Temperature Analysis

In order to gain some insight into the reasons why the bentonite performed better than the attapulgite in the compressive strength and abrasive resistance tests SEM, SEM-EDS, XRD and ash fusion investigations were performed. Visual investigation with SEM (e.g. observing bridge formations, pore sizes, densities, etc.) and surface chemically analysis with SEM-EDS did not give any conclusive results and are therefore not discussed further.

Quantitative XRD analyses of the two clays are indicated in Table 4–3. Amorphous phases, if present, were not taken into account in the quantification. Due to crystallite size effects the errors may be larger than indicated and the wt% contents may therefore differ. Also, mineral names may not reflect the actual compositions of minerals identified, but rather the mineral group (e.g. “Muscovite” would represent the mineral group “Mica”). As

expected, the smectite clay group minerals were the largest component in both clays. However, the attapulgite clay had considerably higher smectite group content than the bentonite. If only these results were considered, one might wrongly consider the attapulgite clay as the better binder, due to the higher smectite mineral group content.

Table 4–3: Quantitative XRD analysis of the attapulgite and bentonite clays utilised

Attapulgite	wt%	Error	Bentonite	wt%	Error
Augite	1.97	(0.17)	Augite	0.64	(0.09)
Calcite	6.66	(0.08)	Calcite	6.34	(0.09)
Kaolinite	2.45	(0.11)	Kaolinite	0.97	(0.10)
Muscovite	2.23	(0.20)	Muscovite	4.93	(0.16)
Orthoclase	1.78	(0.10)	Orthoclase	4.25	(0.12)
Plagioclase	3.86	(0.11)	Plagioclase	5.98	(0.12)
Quartz	4.22	(0.13)	Quartz	14.39	(0.11)
Smectite	76.8	(1.08)	Smectite	62.51	(0.59)

Limitations of the Rietveld method prevent further breakdown of the smectite group, hence qualitative XRD analyses were also conducted and shown in Figure 4–6 and Figure 4–7. These qualitative results indicated that the attapulgite contains palygroskite, which confirms its status as attapulgite clay, but it did not contain any montmorillonite. In contrast, the bentonite contained montmorillonite, but no palygroskite. It is therefore assumed that the aforementioned quantitative smectite mineral contents (Table 4–3) of the two clays can be ascribed to mainly palygroskite in the attapulgite and montmorillonite in the bentonite.

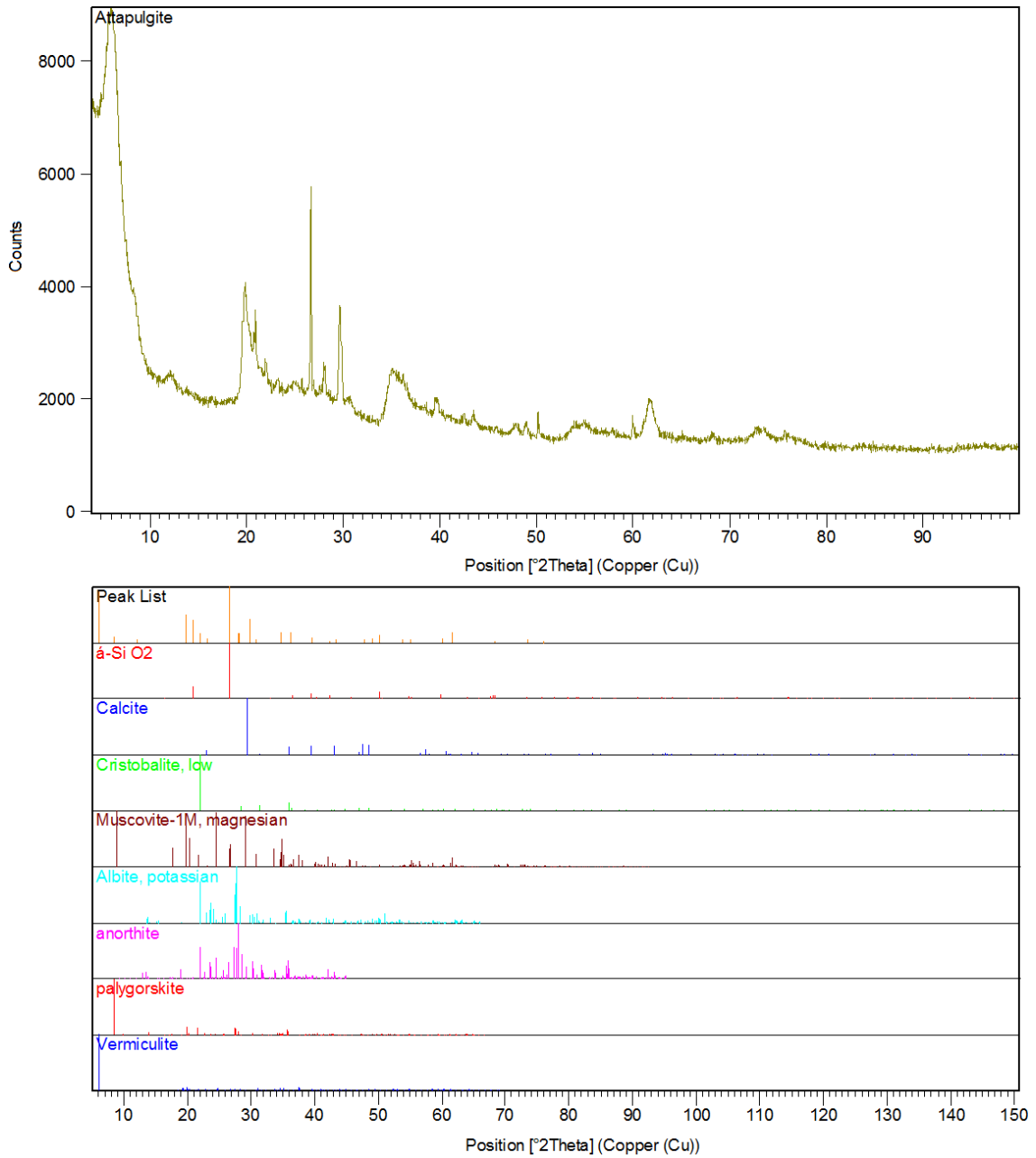


Figure 4–6: Qualitative XRD analysis of the attapulgite clay

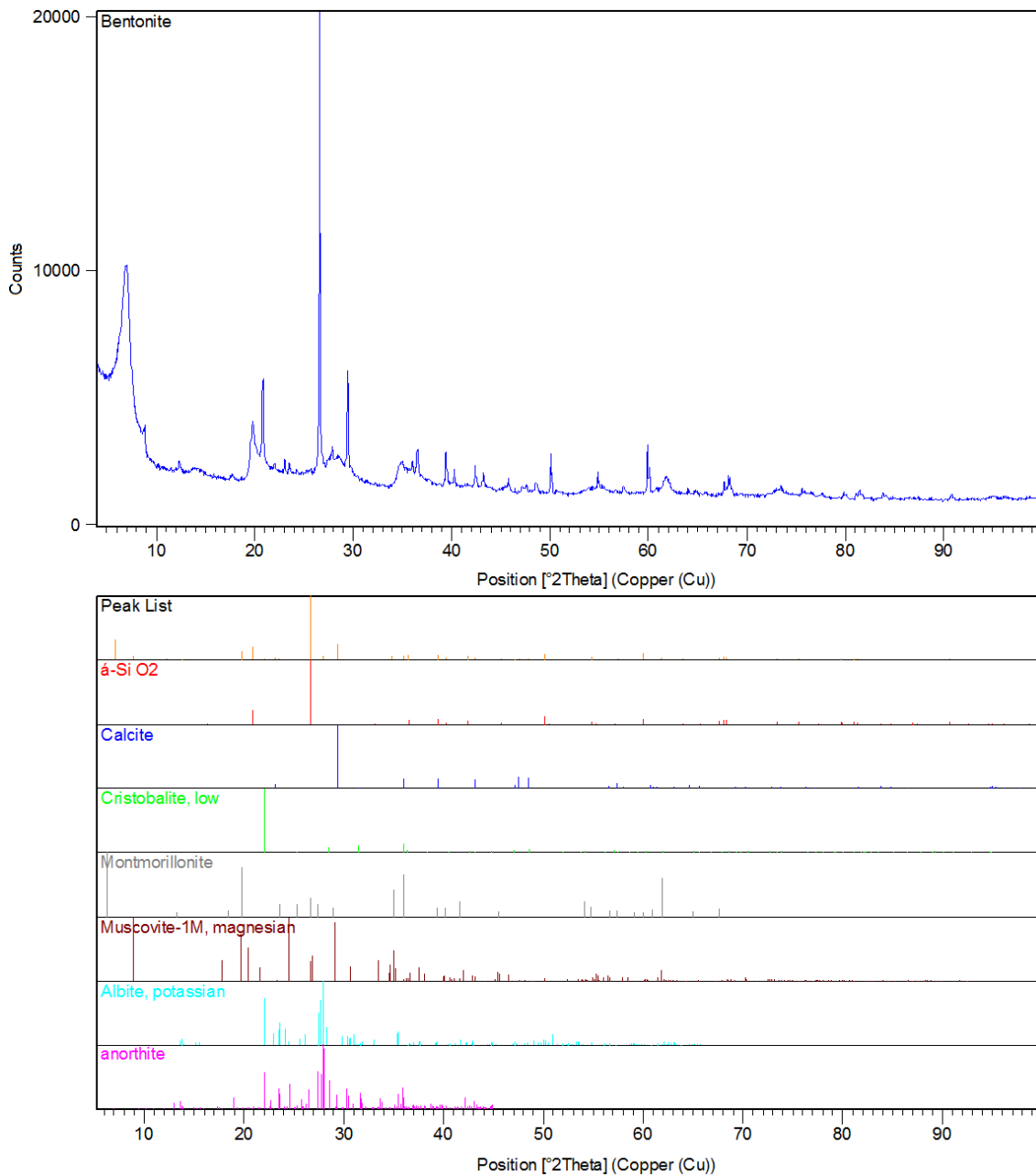


Figure 4–7: Qualitative XRD analysis of the bentonite clay

Bentonite is a blend of layered aluminum hydrosilicate clays with its chemical composition varying between montmorillonite and beidellite (Kawatra & Ripke, 2003; Murry, 1991). The crystalline structure of the smectite minerals present in bentonite consists of three-layer aluminosilicate platelets that are freely held together by electrostatic forces (Kawatra & Ripke, 2003; Murry, 1991; Grim, 1968). Isomorphous substitution of Al^{3+} by Mg^{2+} within the crystal structure alters the charge balance, giving the lattice an overall negative charge. Cations, like

Na^+ and Ca^{2+} , are then absorbed to equilibrate the charge. The hydration of these exchangeable interlayer cations allows for water absorption in between the layered clays, increasing the clay volume by an order of magnitude and thus creating a gel-like viscous fluid (Kawatra & Ripke, 2003; Ripke & Kawatra, 2000c). Kawatra and Ripke (2003) stated that two ways exist in which bentonite promotes dry strength of iron ore pellets, i) it provides a source of colloidal material that decreases interparticle distances, and thus increases van der Waals forces, and ii) it forms a solid bridge of hardened gel that strengthens particle contact points. Several studies have been published proving mechanisms and explanations of bentonite bonding (Kawatra & Ripke, 2002; Kawatra & Ripke, 2001; Ripke & Kawatra, 2000a; Ripke & Kawatra, 2000b; Ripke & Kawatra, 2000c; Elzea & Murray, 1994; Smiernow *et al.*, 1980). Kawatra and Ripke (2000c) identified an interesting bentonite-bonding mechanism and summarised it as follows: when bentonite clay is hydrated, it begins to expand and the electrostatic attraction relaxes, allowing the individual platelets to free up and slip across each other to spread like a deck of cards pushed across a table. When a combination of compression and shear forces is applied, the platelets that make up the clay particles slide to form fibres and sheets over the surface of the material being bonded. Thus, in the pelletising process a high swelling type of clay is desirable. This property is usually associated with sodium-bentonites, whereas calcium-bentonites are associated with low swelling (Naiker, 2007; Konta, 1995). Palygorskite and attapulgite are nomenclature for the same magnesium aluminum hydrosilicate mineral that occur as elongated fibrous lath-like crystals (Murray, 2002; Murry, 1991). Palygorskites constituents are made up of double silica tetrahedral chains linked together by octahedral oxygen and hydroxyl groups containing aluminum and magnesium ions in a chain-like structure. The neto charge on the particles, structural channels and large surface area gives palygorskite a high capacity to absorb and adsorb various materials. The fibrous particles cause high viscosity

when it is added to any liquid (Konta, 1995; Murry, 1991). However, one of palygorskites properties that seem to inhibit its ability to outperform bentonite as a high performance binder is its lattice capability of trapping liquid while the elongate particles remain inert and non-swelling (Reeves *et al.*, 2006; SME, 2006; Murray, 2002; Ciullo, 1996). Considering the bentonite-bonding mechanism identified by Kawatra and Ripke (2000c) it is evident that high-swelling coupled with the hydrous desorption of plate-like particles is an essential characteristics that a clay binder should possess. However, trying to explain why the bentonite seems to be a better binder in this specific application, based only the above-mentioned mineralogical information, would still be presumptuous. Hence ash fusion tests were conducted to derive parameters which could maybe shed more light on this issue. The four ash fusion temperatures recorded for each clay, both in oxidative and reducing conditions, are indicated in Table 4–4.

Table 4–4: Ash fusion temperatures for the attapulgite and bentonite clays utilised

Atmosphere	Ash Fusion Temperatures	Attapulgite	Bentonite
Reducing (N ₂)	Initial deformation temperature	1216	1170
	Softening temperature	1242	1191
	Hemispherical temperature	1294	1251
	Fluid temperature	1337	1301
Oxidising (O ₂)	Initial deformation temperature	1219	1224
	Softening temperature	1256	1255
	Hemispherical temperature	1336	1274
	Fluid temperature	1364	1304

The ash fusion temperatures indicated that in all but one aspect, i.e. initial deformation temperature in an oxidizing environment, the bentonite had a lower deformation, softening, hemispherical and fluid temperatures in both

oxidising and reducing environments. This can possibly give some practical explanation as to why the bentonite performed better in the compressive and abrasion strength tests, for both pre-reduced and oxidative sinter pellets. Having a lower melting point (construed as incorporating all four measured ash fusion temperatures) implies that the bentonite could at lower temperatures than the attapulgite start forming bridges between the particles. It is also notable that the attapulgite's fluid temperatures in both environments were above 1300 °C, implying that it might not have fully liquefied under the experimental conditions.

4.6. Thermo-Mechanical Analysis

Cold compressive and abrasion resistance strength tests give an indication of the cured strength of the pelletised materials after being treated under the different environments. However, the question could be asked what the hot pellet strengths are, since that would influence pellet breakdown in the rotary kiln used in the industrial application. This has relevance to the formation or build-up of damrings (material sticking to inside of the rotary kiln). Unfortunately no instruments that could directly measure high temperature compressive strength or abrasion resistance were available for this investigation. However, a TMA instrument, which measures the thermal expansion of a material as a function of temperature, was available. TMA results for the pre-reduced pellets are shown in Figure 4–8. Oxidative sintering could not be investigated due to instrumental limitation as explained earlier (Par 3.2.7).

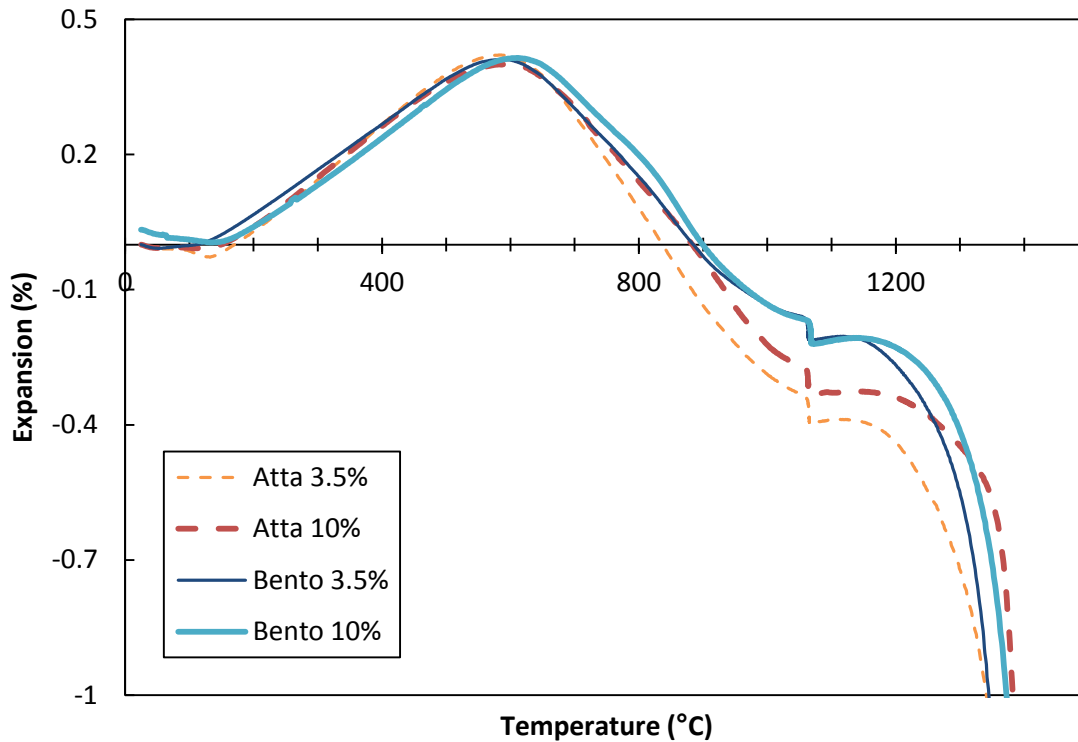


Figure 4–8: Average percentage dimensional changes of *in-situ* pre-reduced of pellets as a function of temperature for both clays investigated at 3.5 and 10% additions

The TMA results of the pellets being pre-reduced *in situ* containing either bentonite or attapulgite, with the different clay additions, all indicate the same initial trends – small shrinkage up to about 120 °C probably due to moisture loss, there after thermal expansion up to approximately 600 °C. However, after 700 °C more significant shrinkage occurred for the attapulgite-containing pellets. In the range 900-1200 °C the attapulgite-containing pellets had shrunk significantly more than the bentonite-containing pellets. This additional shrinkage of the attapulgite can possibly be related to the LOI of the attapulgite (13.04%) measured at 1000 °C as indicated in Table 4–1, which was significantly higher than that of the bentonite (7.69%). Although thermal expansion and shrinkage cannot be related directly to hot pellet strength, more variation in thermal dimensional behaviour could indicate weaker pellets. Thus, although not quantitatively investigated, there is some indication that the hot strength of the attapulgite pellets could be weaker than the bentonite-containing pellets.

4.7. Pellet pre-reduction

The levels of pre-reduction achieved for the two temperature profiles used, as well as clay contents from 2.5 to 10 wt% are shown in Figure 4–9. There are a number of interesting features of this data. Firstly, the pre-reduction levels achieved with 1250 °C and holding times of 20 min were significantly higher than those achieved with 1300 °C without any holding time. According to the Ellingham diagram calculations of Niemelä *et al.* (2004) iron carbon reduction can occur above 710 °C and chromium reduction above 1200 °C. It is therefore not surprising that higher pre-reduction levels were achieved with the lower temperature profile – the maximum temperature of this profile was still above the temperatures required for both Fe and Cr reduction and the increased holding time therefore resulting in higher levels of pre-reduction occurring.

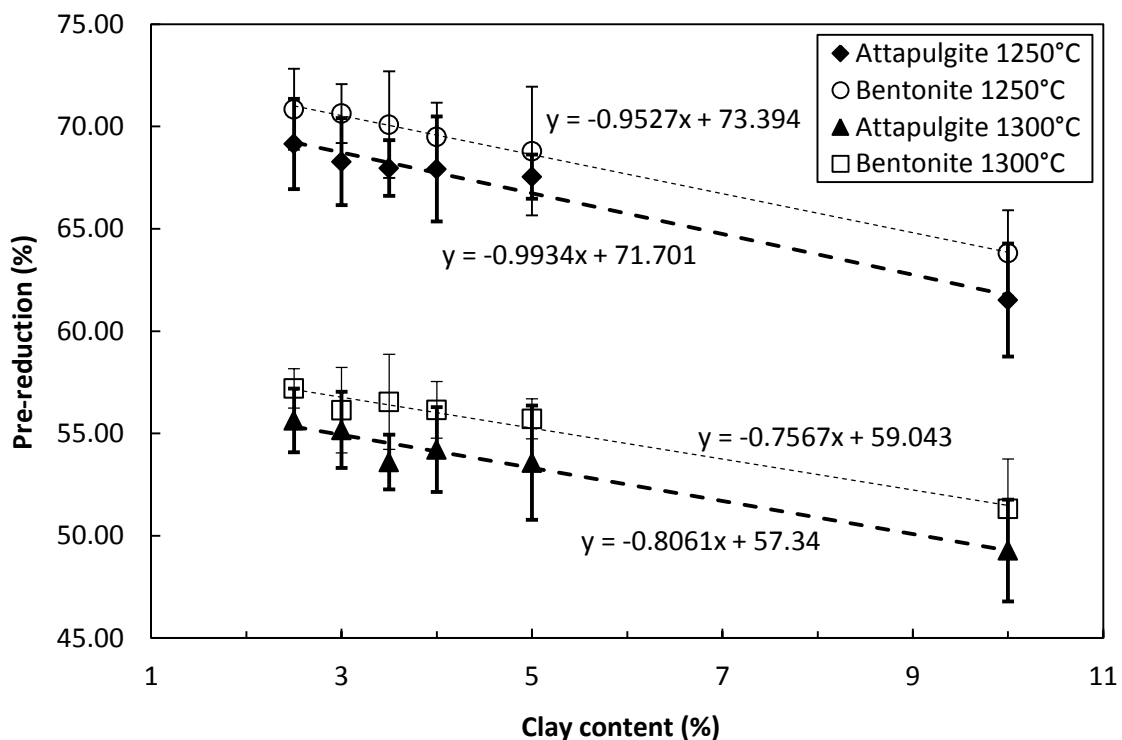


Figure 4–9: Percentage pre-reduction achieved as function of clay content, for both case study clays with both temperature profiles utilised

From the data in Figure 4–9 it is also evident that higher clay contents resulted in lower pre-reduction levels, for both clays and both temperature profiles. This is significant within the industrial process, since higher clay contents are on occasion utilised to achieve improved green strength of the uncured pellets. In order to quantify this observation better, trend lines with associated equations are indicated in Figure 4–9. In the industrial application of pelletised chromite pre-reduction, clay contents of 3 to 4 wt% are utilised. Substituting these values into the equations indicate that 0.76 to 0.99% lower pre-reduction levels can be expected if 4 wt% instead of 3 wt% clay addition is made. Not many references exist in the public domain which can be used to translate these lower pre-reduction values into energy and financial losses. Niayesh and Fletcher (1986) published a graph of chromite pre-reduction as a function of specific energy consumption (kWh/t FeCr produced), for different temperatures of pre-reduced feed material. The graph assuming that the material was fed to the furnace at room temperature of Niayesh and Fletcher (1986) was reconstructed and an empirical fit of the data made. Using this fit and assuming 45% pre-reduction as the base case for an industrial plant, it was calculated that 16.7 kWh/t (for the 0.76% lower pre-reduction) to 21.7 kWh/t (for the 0.99% lower pre-reduction) more electricity would be used for 4 wt% clay, instead of the 3 wt% clay additions. For a FeCr smelting plant producing 300 000 t/y this relates to 5 006 to 6 516 MWh/y more, or R2.62 to R3.41 million using the 52.30 SA cent/kWh price of 2011/2012 (Eskom, 2011; NERSA, 2009c).

The third significant observation for the data in Figure 4–9, is that there seems to be a difference between the performances of the two case study clays with regard to pre-reduction levels achieved. Although there are some overlaps between the error bars, it is clear that the average pre-reduction of the bentonite-containing pellets were consistently higher than that of the attapulgite-containing pellets. Utilising intercept values on the y-axis of the trend lines already indicated, it was calculated that the bentonite-containing

pellets had on average 1.7 % higher pre-reduction levels with both temperature profiles. This is significant, since the attapulgite is currently the preferred industrial option, mostly due to raw material cost considerations. Again using the fitted reconstructed plot of Niayesh and Fletcher (1986) as a guide, the difference in pre-reduction was again converted to possible electricity and financial losses. For a 300 000 t/y smelter, operation at a specific energy consumption of 2.4 MWh/t, this related to 9 163 (1250 °C temperature profile, Par. 3.2.4) to 10 275 MWh/y (1300 °C temperature profile, Par. 3.2.4) more, or R4.79 to R5.37 million using the 52.30 SA cent/kWh price of 2011/2012 (Eskom, 2011; NERSA, 2009c). Considering the compressive strength and abrasion resistance results presented earlier (Par. 4.3), where it was proved that bentonite outperformed attapulgite, it seems possible that lower bentonite pellet additions could be used than attapulgite to obtain the same pellet strength. Again using the trend lines fitted to the data in Figure 4–9, it was calculated that a pre-reduction process utilising 3 wt% bentonite as oppose to 4 wt% attapulgite as a binder, had on average 2.7 % higher pre-reduction levels with both temperature profiles. Using the reconstructed plot of Niayesh and Fletcher (1986) the electricity and financial losses could again be estimated for a 300 000 t/y smelter operation at a specific energy consumption of 2.4 MWh/t. This related to 15 616 (1250 °C temperature profile, Par. 3.2.4) to 16 349 MWh/y (1300 °C temperature profile, Par. 3.2.4) more, or R8.17 to R8.55 million using the 52.30 SA cent/kWh price of 2011/2012 (Eskom, 2011; NERSA, 2009c).

The reason why the bentonite-containing pellets performed better with regard to pre-reduction could be due to two reasons:

- i) The case study bentonite had a lower melting point (Par. 4.5) than the case study attapulgite, thus it might already melt during the pre-reduction process, and hence serve as a flux in promoting metal reduction.

ii) The minerals present in the two different clays could contain materials that could serve to catalyse or inhibit the pre-reduction of chromite. Several studies have been published proving that various substances could have catalytic or inhibiting pre-reduction effects (Takano *et al.*, 2007; Weber & Eric, 2006; Ding & Warner, 1997b; Lekatou & Walker, 1997; Pei & Wijk, 1993; Weber & Eric, 1993; Nunnington & Barcza, 1989; Van Deventer, 1988; Dawson & Edwards, 1986; Katayama *et al.*, 1986). As an example, both clays contain CaO and SiO₂ (Table 4–1), which have been proven to have catalytic effects on chromite pre-reduction (Par. 2.4.4.2). On the other hand, both clays also contained Al₂O₃ (Table 4–1) that has an inhibiting effect (Par. 2.4.4.2). However, these statements are not entirely true, since the chemical composition of the clays was presented (Table 4–1) according to common practice, i.e. as simple oxides, but in fact it cannot be stated categorically that the elements occur as these compounds. It is much more likely that the elements are incorporated into the various mineral phases in forms other than simple oxides. To quantify the catalytic and/or inhibiting effect of each constituent of the two different clays on chromite pre-reduction would constitute a study on its own. This was, however, beyond the scope of this study.

4.8. Conclusions

Several important conclusions could be made from the results presented in this chapter:

- i) From a SEM-EDS investigation (Par. 4.2) of industrially produced pre-reduced pellets it became evident that the functioning of a clay binder within the pelletised chromite pre-reduced process has to be evaluated within two different environments, i.e. performance within

an oxidative environment (corresponding to the outer layer of the industrially pre-reduced pellets) and performance within a reducing environment (corresponding to the core of the industrially pre-reduced pellets). This is in contrast with other chromite pelletised processes, e.g. the oxidative sintered pelletised process (Beukes *et al.*, 2010; Outotec, 2009; Outotec, 2008) where only one condition prevails.

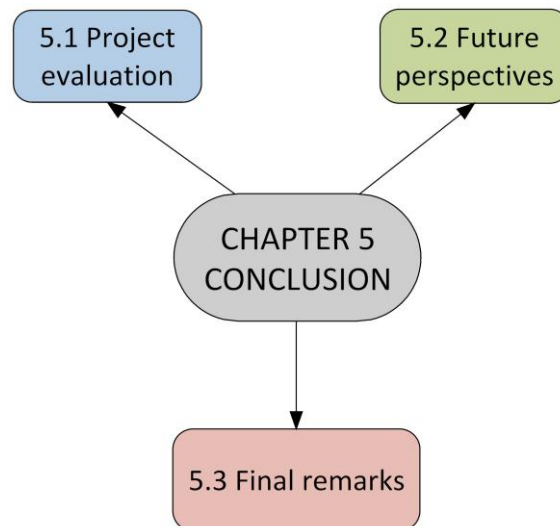
- ii) The compressive strengths of the oxidative sintered pellets were approximately an order of magnitude higher than that of the pre-reduced pellets (Par. 4.3). Similarly, the abrasion resistance strength of the oxidative sintered pellets was also substantially better than that of the pre-reduced pellets (Par. 4.4). Thus, although the objective of the industrially applied pelletised chromite pre-reduced process is to achieve maximum pre-reduction, the strength (compressive and abrasion) of pre-reduced chromite pellets is significantly enhanced by the thin oxidised outer layer.
- iii) From compressive strengths (Par. 4.3) and abrasion resistance (Par. 4.4) tests of the two case study clays it was clear that the bentonite clay was superior in both pre-reducing and oxidative sintering environments. This is significant, since the attapulgite clay is currently the preferred option at both South African FeCr smelting plants applying the pelletised chromite pre-reduction process.
- iv) The compressive strength of the bentonite-containing pre-reduced pellets generally improved with increased clay content; however, increased attapulgite content did not result in any significant increased compressive strength of the pre-reduced pellets (Par. 4.3). Increasing the attapulgite clay content of the industrial pre-reduced pellets might therefore not result in a stronger pellet core, although it might aid the green strength, which was not considered in this study.

- v) For both the case study clays an increased clay addition resulted in a slightly decreasing trend in compressive strengths of the oxidative sintered pellets (Par. 4.3). This indicates that clay content addition is not such an important parameter in attaining a strong oxidised outer layer on the industrially produced pellets.
- vi) It became apparent that predicting the performance, i.e. compressive and abrasion strength, of a clay binder in the pelletised chromite pre-reduction process based on chemical and mineralogical analyses of the clays is unlikely, even if such analyses are done in considerable detail, as presented in Par. 4.1.
- vii) Ash fusion analysis, both in oxidative and reducing conditions, of the two case study clays (Par. 4.5) gave some insight into the possible reason why the specific bentonite considered outperformed the specific attapulgite considered. The bentonite had a lower melting point (construed as incorporating all four measured ash fusion temperatures) implying that it could at lower temperature than the attapulgite start forming bridges between the particles. The attapulgite's fluid temperatures in both oxidative and reducing environments were above 1300 °C, implying that it might not have fully liquefied under the experimental conditions.
- viii) Although not quantitatively investigated, TMA analysis indicated that the hot strength of the attapulgite pellets could be weaker than the bentonite-containing pellets (Par. 4.6).
- ix) Higher clay contents resulted in lower pre-reduction levels for both clays and both temperature profiles investigated (Par. 4.7). This is significant within the industrial process, since higher clay contents are on occasion utilised to achieve improved green strength of the uncured pellets. Results indicated that 0.76 to 0.99% lower pre-reduction levels can be expected if 4 wt% instead of 3 wt% clay

addition is made. Using data published by Niayesh and Fletcher (1986) it was indicated that this related to significant additional electricity consumption and financial loss.

- x) The average pre-reduction of the bentonite-containing pellets were consistently higher than that of the attapulgite-containing pellets (Par. 4.7). It was calculated that the bentonite-containing pellets had on average 1.7 % higher pre-reduction levels with both temperature profiles. This is significant, since the attapulgite is currently the preferred industrial option, mostly due to raw material cost considerations. Again using data of Niayesh and Fletcher (1986) as a guide, the difference in pre-reduction was again converted to possible electricity and financial losses that were significant.
- xi) The reason why the bentonite-containing pellets performed better with regard to pre-reduction was attributed to two possibilities: i) the case study bentonite had a lower melting point (Par. 4.5) than the case study attapulgite, thus it might already melt during the pre-reduction process, hence serve as a flux in promoting metal reduction or ii) the minerals present in the two different clays could contain materials that could serve to catalyse or inhibit the pre-reduction of chromite

CHAPTER 5: PROJECT EVALUATION AND FUTURE PERSPECTIVES



5.1. Project evaluation

The project was evaluated using the objectives set in Chapter 1. The points listed below therefore correlate with the objectives set in Par. 1.2:

- i) A comprehensive literature survey was conducted (Chapter 2). The importance of South Africa's ferrochrome industry was justified in terms of chromite resources (Par. 2.2.3) and ferrochrome production (Par. 2.2.4). Factors influencing this industry were discussed in the light of economic and market considerations (Par. 2.2.1) and electricity supply, as one of these factors, was highlighted (Par. 2.2.2). From the core processes and techniques discussed in Par. 2.3 it was evident that, although various processes are utilised for the production of FeCr, pre-reduction seem to be the most viable option to reduce a FeCr smelter plant's specific energy consumption.

Chromite pre-reduction was found to be a well-established practice in the South African FeCr production industry (Par. 2.4.1). The use thereof poses numerous advantages for FeCr producers (Par. 2.4.2). Numerous studies have been conducted on the effect of additives on chromite pre-reduction (Par. 2.4.4.2). It was therefore clear that apart for the clay acting as a binding agent, it could also be considered as an additive of which the effect on chromite pre-reduction needs to be established. In a general overview of clay binders utilised for the agglomeration of ore (Par. 2.5), the functions and requirements that a clay binder need to fulfil was established (Par. 2.5.1). In general bentonite seems to be the preferred choice for an ore binding agent, as a number of researches have been conducted on bentonite as binder and its mechanism for ore agglomeration (Par. 2.5.2.2). In contrast, very little has been published on the possible utilisation of attapulgite as a binder for ore pelletisation.

- ii) In order to draw comparisons between experimental results and the industry, typical raw materials were obtained from a local FeCr producer actually applying the chromite pre-reduction process. These materials were extensively characterised (Par. 4.1). Industrially produced chromite pre-reduced pellets were also obtained from the same FeCr producer and visually (SEM), as well as surface-chemically characterised (SEM-EDS).
- iii) SEM-EDS analysis showed that chromite pre-reduced pellets consisted of an oxidised outer layer containing small amounts of carbon and a pre-reduced core containing a substantial amount of carbon (Par. 4.2). It was thus decided to distinguish between these two zones and test the two case study clays performances in oxidative sintered and pre-reduced environment.

- iv) Various experiments were designed and conducted to test the performance of the two case study clays (Par. 4.3-4.7).
- v) Apart from making an academic contribution in this study, various industrial relevant recommendations dealing with the selection of clay binder for chromite pre-reduction could be made (Par. 4.8).
- vi) The final objective concerning recommendations with regard to further research work is discussed in Par. 5.2.

5.2. Future perspectives

From the literature survey and results three recommendations can be made with regard to further work related to this research area:

- i) The catalytic and/or inhibiting effect of clay binders on pre-reduction needs to be investigated in more detail in future, as to identify the mineral species present in clay binders responsible for catalytic/inhibiting effects. This would aid industry in selecting the most appropriate clay binders.
- ii) From studies conducted by Ripke & Kawatra it was found that bentonite clay formed fibres when prepared under proper moisture and mechanical mixing conditions. Bentonite also became more effective as a binder when mixed in a manner that promoted fibre formation. Considering the above mentioned results, could it be possible to improve the strength of chromite pre-reduced pellets or minimise the clay addition needed to produce good quality pellets by developing bentonite into a fibrous matrix by manipulating conditions to promoted fibre formation. This would be advantageous as it was shown in Par. 4.7 that an increase in clay content resulted in lower pre-reduction levels. It should also be established if a bentonite clay's characteristics would have an effect on fibre development.

- iii) From the literature study conducted it became evident that little has been published on the attapulgite agglomeration mechanism. Considering the current use of attapulgite by the FeCr industry, more work in the field is required.

5.3. Final remarks

In conclusion, the author (the candidate) would like to assess this MSc dissertation using the exit level outcomes prescribe for a Master Scientiae degree by the North-West University. In short, the exit level outcomes to which an MSc dissertation should comply are listed:

- i) Identification and formulation of a problem statement.
- ii) Setting specific objective that are relevant to the problem, that is both measurable and achievable.
- iii) Thorough investigation of existing knowledge as reflected in appropriate scientific literature.
- iv) Appropriate research to solve the problem.
- v) Scientific evaluation of the results in the context of the problem statement.
- vi) Scientific communication of the results in the form of a dissertation.

From the candidate's point of view these exit level requirements were successfully achieved. Additionally a meaningful scientific contribution was made in understanding the role and unique challenges of a clay binder in a pelletised chromite pre-reduction process. As the true measure of scientific research is the acknowledgment of the work by peers, the candidate intends on publishing the results obtained. Since it is not required at MSc level to make a significantly new scientific contribution, the abovementioned contribution can therefore be

regarded as sufficient proof that this study surpassed the requirements of an MSc.

BIBLIOGRAPHY

ABUBAKRE, O.K., MURIANA, R.A. & NWOKIKE, P.N. 2007. Characterization and beneficiation of Anka chromite ore using magnetic separation process. *Journal of Minerals & Materials Characterization & Engineering*, 6(2):143-150.

AKYÜZÜ, M. & ERIC, R.H. 1992. Slag-metal equilibrium in the smelting of high-carbon ferrochromium. *Journal of the South African Institute of Mining and Metallurgy*, 92(4):101-110.

ANON. 1974. Chromium. Medical and Biologic Effects of Environmental Pollutants. Washington D.C., USA: National Academy of Sciences. 155p.

ASTM. 2007. D3172-07A Standard Practice for Proximate Analysis of Coal and Coke. In: *American Society for Testing and Materials (ASTM), Book of Standards v 05.06-Gaseous Fuels; Coal and Coke*, West Conshohocken, USA.

ATTA CLAY (PTY) LTD. 2011. Product info. <http://www.attaclay.co.za> Date of access: 20 June 2011.

BAKER, R. 2006. Poor planning. *Business Day*, 3 May.

BALL, D.F., FITTON, J.T., DAWSON, P.R. & GOLDRING, D.C. 1974. Effect of Additives on the Strength of Fired Iron Ore Pellets. *Transactions of the Institution of Mining and Metallurgy*, 83C(808):47-58.

BARNES, A.R., FINN, C.W.P. & ALGIE, S.H. 1983. The prereduction and smelting of chromite concentrate of low chromium-to-iron ratio. *Journal of the South African Institute of Mining and Metallurgy*:49-54. March.

BASSON, J., CURR, T.R. & GERICKE, W.A. 2007. South Africa's Ferro Alloy Industry-Present Status and Future Outlook. (*In Proceedings of The 11th International Ferro Alloys Conference. New Delhi, India: Indian Ferro Alloy Producers' Association (IFAPA). p. 3-24.*)

BEUKES, J.P., DAWSON, N.F. & VAN ZYL, P.G. 2010. Theoretical and practical aspects of Cr(VI) in the South African ferrochrome industry. *The Journal of The Southern African Institute of Mining and Metallurgy*, 110(12):743-750.

BEUKES, J.P., VAN ZYL, P.G. & RAS, M. 2011. Treatment of Cr(VI) containing wastes in the South African ferrochrome industry - A review of currently applied methods. *Submitted to The Journal of The Southern African Institute of Mining and Metallurgy*

BONGA, M. 2009. Ferrous mineral commodities produced in the Republic of South Africa 2009. Directorate: Mineral Economics, Department: Minerals and Energy, Republic of South Africa. Date of access: 5 March 2011. <http://www.dmr.gov.za/Mineral_Information/New/D8%202009.pdf>

BOTHA, W. 2003. Ferrochrome production through the SRC process at Xstrata, Lydenburg Works. *Journal of the South African Institute of Mining and Metallurgy*, 103(6):373-389.

CHAKRABORTY, D., RANGANATHAN, S. & SINHA, S.N. 2007. Influence of temperature and particle size on reduction of chromite ore. (*In Proceedings of The 11th International Ferro Alloys Conference. New Delhi, India. p. 144-152.*)

CIULLO, P.A. 1996. Industrial minerals and their uses: a handbook and formulary. New Jersey, USA: Noyes Publications.

COWEY, A. 1994. *Mining and Metallurgy in South Africa - A Pictorial History*. Randburg, South Africa.

- CRAMER, L.A. 2001. The Extractive Metallurgy of South Africa's Platinum Ores. *Journal of the Minerals, metals, and Materials Society*:14-18. October.
- CRAMER, L.A., BASSON, J. & NELSON, L.R. 2004. The impact of platinum production from UG2 ore on ferrochrome production in South Africa. *The Journal of The South African Institute of Mining and Metallurgy*, 104(9):517-527. October.
- CREAMER, M. 2010. Energy for Xstrata's R4,9bn Lion ferrochrome add-on, plus new R700m mine. *Mining Weekly*, 20 October.
- CREAMER, M. 2011. Merafe lobbying 2011 curb on raw chrome exports – CEO. *Mining Weekly*, 1 March.
- CRU. 2010. *Ferrochrome cost and market service*. Mount Pleasant, London.
- CURR, T. 2009. History of DC arc furnace process development. (*In Mintek 75 - A celebration of technology*. Randburg, South Africa. [online]. [Accessed 13 May 2011]. Available from World Wide Web: <http://www.mintek.co.za/Mintek75/Proceedings.>)
- DAAVITTILA, J., HONKANIEMI, M. & JOKINEN, P. 2004. The transformation of ferrochromium smelting technologies during the last decades. *The Journal of The South African Institute of Mining and Metallurgy*:541-549. October.
- DAWSON, N.F. & EDWARDS, R.I. 1986. Factors Affecting the Reduction Rate of Chromite. (*In Proceedings of the 4th International Ferro-alloys Congress*. Sao Paulo, Brazil. p. 105-113.)
- DEAN, R.B. & DIXON, W.J. 1951. Simplified statistics for small numbers of observations. *Analytical Chemistry*, 23(4):636-638.

DENTON, G.M., BENNIE, J.P.W. & GE JONG, A. 2004. An improved DC-arc process for chromite smelting. (*In Proceedings of The 10th International Ferroalloys Congress. Cape Town, South Africa. p. 60-67.*)

DING, Y.L. & WARNER, N.A. 1997a. Catalytic reduction of carbon-chromite composite pellets by lime. *Thermochimica Acta*, 292:85-94.

DING, Y.L. & WARNER, N.A. 1997b. Reduction of carbon-chromite composite pellets with silica flux. *Ironmaking and Steelmaking*, 24(4):283-287.

DINNIN, J.I. 1959. Rapid Analysis of Chromite and Chrome Ore. Washington: United States Government Printing Office.

DOS SANTOS, M. 2010. Meeting the challenges of sustainability through technology development and intergration in ferroalloy submerged arc furnace plant desing. (*In The12th International Ferroalloys Congress. Helsinki, Finland. p. 71-80.*)

DOWNING, J.H., DEELEY, P.D. & FICHTE, R.M. 1986. A7 vols. Chromium and chromium alloys. *In: Ullmans Encyclopedia of industrial chemistry*, Weinheim, Germany: VCH, Verlagsgeschellschaft mbH. 43-65 p.

EISELE, T. C. & KAWATRA, S. K. 2003. A review of binders in iron ore pelletization. *Mineral Processing and Extractive Metallurgy Review*, 24(1):1-90.

ELZEA, J. & MURRAY, H.H. 1994. Bentonite. *In: CARR, D.D., ed. Industrial Minerals and Rocks*, 6th Edition ed. Littleton, Colorado, USA: Society for Mining, Metallurgy, and Exploration Inc. 223-246 p.

ENRC. 2008. An Introduction to Ferrochrome. Date of access: 12 June 2010. <<http://www.enrc.com/PageFiles/1748/ENRC%20-%20Ferrochrome%20presentation%208%20May%20FINAL%20PRINT%20V3.pdf>>

- EPA. 1996. *EPA Method 3052, SW-846*. Environmental Protection Agency (EPA).
- ESKOM. 2009. Average Price Increases. http://www.eskom.co.za/live/content.php?Item_ID=188 Date of access: 2 February 2011.
- ESKOM. 2011. Eskom retail tariff adjustment for 2011/2012. Date of access: 13 October 2011. <<http://www.eskom.co.za/content/priceincrease2011.pdf>>
- FEATHERSTONE, R.A. & BARCZA, N.A. 1982. The growth of ferro-alloy production in South Africa. Date of access: 2 February 2011. <<http://www.mintek.co.za/Pyromet/Files/1982FeatherstoneBarcza.pdf>>
- G&W BASE (PTY) LTD. 2011. Bentonite Ocean MD. Date of access: 20 June 2011. <<http://www.gwbase.co.za/pdfs/Pel-Bond.pdf>>
- GEDIGA, J. & RUSS, M. 2007. *Life cycle inventory (LCI) update of primary ferrochrome production*. Leinfelden-Echterdingen.
- GLASTONBURY, R.A., VAN DER MERWE, W., BEUKES, J.P., VAN ZYL, P.G., LACHMANN, G., STEENKAMP, CJH, DAWSON, N.F. & STEWART, H.M. 2010. Cr(VI) generation during sample preparation of solid samples - A chromite ore case study. *Water SA*, 36(1):105-109.
- GRIM, R.E. 1968. *Clay Mineralogy*, 2nd ed. New York, USA: McGraw-Hill.
- GU, F. & WILLS, B.A. 1988. Chromite- Mineralogy and Processing. *Minerals Engineering*, 1(3):235-240.
- HAYES, P.C. 2004. Aspects of SAF smelting of ferrochrome. (*In Proceedings of the 10th International Ferroalloys Congress. Cape Town, South Africa.*)
- HOLAPPA, L. & XIAO, Y. 2004. Slags in ferroalloys production—review of present knowledge. *The Journal of The South African Institute of Mining and Metallurgy*, 104(7):429-437. August.

HOWAT, D.D. 1986. Chromium in South Africa. *Journal of The South African Institute of Mining and Metallurgy*, 86(2):37-50, Feb.

ICDA. 2010. *Statistical Bulletin*. Paris, France.

IDEAS 1ST RESEARCH. 2010. Ferrochrome March 2010. Date of access: 2 February 2011. <http://ideasfirst.in/Admin/Downloads/Reports/1720868194_Chrome-Ferrochrome%20-%20Final%20-%2031Mar20101.pdf>

IETEG. 2005. Chromium(VI) Handbook. Boca Raton, USA: CRC Press. 784p.

JONES, R. 2010. Pyrometallurgy in South Africa. Date of access: 3 March 2011. <<http://www.pyrometallurgy.co.za/PyroSA/index.htm> >

KATAYAMA, H.G., TOKUDA, M. & OHTANI, M. 1986. Promotion of the Carbothermic Reduction of Chromium Ore by the Addition of Borates. *The Iron and Steel Institute of Japan*, 72(10):1513-1520.

KAWATRA, S.K. & RIPKE, S.J. 2001. Developing and understanding the bentonite fiber bonding mechanism. *Minerals Engineering*, 14(6):647-659.

KAWATRA, S.K. & RIPKE, S.J. 2002. Effects of bentonite fiber formation in iron ore pelletization. *International Journal of Mineral Processing*, 65(3-4):141-149.

KAWATRA, S.K. & RIPKE, S.J. 2003. Laboratory studies for improving green ball strength in bentonite-bonded magnetite concentrate pellets. *International Journal of Mineral Processing*, 72:429-441.

KINGSTON, H.M. & WALTER, P.J. 1998. The Art and Science of Microwave Sample Preparations for Trace and Ultratrace Elemental Analysis. *In*: MONTASER, A., ed. *In Inductively Coupled Mass Spectrometry*, New York, USA: Wiley-VCH. 964 p.

- KONTA, J. 1995. Clay and man: Clay raw materials in the service of man. *Applied Clay Science*, 10:275-335.
- LEKATOU, A. & WALKER, R.D. 1997. Effect of SiO₂ addition on solid state reduction of chromite concentrates. *Ironmaking and Steelmaking*, 24(2):133-143.
- LIDE, D.R., *ed.* 2009. CRC Handbook of Chemistry and Physics, 89th edition (Internet Version). Boca Raton, USA: CRC Press/Taylor and Francis. 2692p.
- LUNGU, J. 2010. Mining and the impact of the recession in the southern African development community states. Date of access: 2 February 2010. <http://www.sarwatch.org/sarwadocs/john_lungu/module1_SARW_Importance_of_mining_in_SADC.pdf>
- LYAKISHEV, N.P. & GASIK, M.I. 1998. Metallurgy of Chromium. New York, USA: Allerton Press Inc.
- MAKHOBBA, G. & HURMAN ERIC, R. 2010. Reductant characterization and selection for ferrochromium production. (*In* Proceedings of The 12th International Ferroalloys Congress. Helsinki, Finland: Outotec Oyj. p. 359-365.)
- MCCULLOUGH, S., HOCKADAY, S., JOHNSON, C. & BARCZA, N.A. 2010. Pre-reduction and smelting characteristics of Kazakhstan ore samples. (*In* Proceedings of The 12th International Ferroalloys Congress. Helsinki: Outotec Oyj. p. 249-262.)
- MOORE, D.M. & REYNOLDS, R.C. 1997. X-Ray Diffraction and the Identification and Analysis of Clay Minerals. New York, USA: Oxford University Press.

MURRAY, H.H. 2002. Industrial Clays Case Study. Mining, Minerals and Sustainable Development project No. 64 of the International Institute for Environment and Development (IIED). Date of access: 19 October 2011. <<http://pubs.iied.org/pubs/pdfs/G00556.pdf>>

MURRY, H.H. 1991. Overview - clay mineral applications. *Applied Clay Science*, 5:379-395.

MURTHY, Y.R., TRIPATHY, S.K. & KUMAR, C.R. 2011. Chrome ore beneficiation challenges & opportunities – A review. *Minerals Engineering*, 24(5):375-380.

NAFZIGER, R.H. 1982. A review of the deposits and beneficiation of lower-grade chromite. *Journal of The South African Institute of Mining and Metallurgy*:205-226, Aug. August.

NAIKER, O. 2007. The development and advantages of Xstrata's Premus Process. (In Proceedings of The 11th International Ferroalloys Congress. New Delhi, India. p. 112-119.)

NAIKER, O. & RILEY, T. 2006. Xstrata Alloys in Profile. (In Southern African Pyrometallurgy. Johannesburg, South Africa: South African Institute of Mining and Metallurgy. p. 297-306.)

NEIZEL, B.W. 2010. Alteration of chrome-to-iron ratio in chromite ore by chlorination. Potchefstroom: North-West University (Dissertation - M.Sc.). 90 p.

NEL, M.V., STRYDOM, C.A., SCHOBERT, H.H., BEUKES, J.P. & BUNT, J.R. 2011. Comparison of sintering and compressive strength tendencies of a model coal mineral mixture heat-treated in inert and oxidizing atmospheres. *Fuel Processing Technology*, 92(5):1042-1051.

NERSA. 2009a. Eskom price increase application 2009. Date of access: 8 September 2011. <<http://www.nersa.org.za/Admin/Document/Editor/file/Electricity/PricingandTariffs/Eskom%20Current%20Price%202009-10.pdf>>

NERSA. 2009b. Historic Eskom Average Selling Price. Date of access: 8 September 2011. <<http://www.nersa.org.za/Admin/Document/Editor/file/Electricity/PricingandTariffs/Eskom%20Historic%20Prices.pdf>>

NERSA. 2009c. Inductive Future Eskom Price Direction. Date of access: 8 September 2011. <<http://www.nersa.org.za/Admin/Document/Editor/file/Electricity/PricingandTariffs/Eskom%20Future%20Pricepath.pdf>>

NEWMAN, A.C.D., *ed.* 1987. Chemistry of clays and clay minerals. Essex, England: Longman Scientific & Technical.

NIAYESH, M.J. & FLETCHER, G.W. 1986. An assessment of Smelting Reduction Processes in the Production of Fe-Cr-C Alloys. (*In Proceedings of the 4th International Ferro-alloys Congress. Sao Paulo, Brazil. p. 115-123.*)

NIEMELÄ, P., KROGERUS, H. & OIKARINEN, P. 2004. Formation, characterization and utilization of CO-gas formed in ferrochrome smelting. (*In Proceedings of The 12th International Ferroalloys Congress. Cape Town, South Africa. p. 68-77.*)

NRIAGU, O.J. & NIEBOER, E. 1988. Chromium in the Natural and Human Environments, Volume 20 of Advances in environmental science and technology. New York, USA: Wiley-Interscience. 571p.

NUNNINGTON, R.C. & BARCZA, N.A. 1989. Pre-reduction of fluxed chromite-ore pellets under oxidizing conditions. (*In Proceedings of The 5th International Ferroalloys Congress. New Orleans, USA. p. 55-68.*)

OUTOTEC. 2008. Outotec. http://www.outotec.com/default_6764.aspx?epslanguage=EN Date of access: 21 October 2008.

OUTOTEC. 2009. Ferrochrome smelting with OPK™ Preheating Kiln. Date of access: 19 October 2011. <<http://www.outotec.com/37992.epibrw>>

OUTOTEC. 2011. Preheating and smelting. http://www.outotec.com/pages/Page____38387.aspx?epslanguage=EN Date of access: 3 May 2011.

OWADA, S. & HARADA, T. 1985. Grindability and magnetic properties of chromites. *Journal of The Mining and Metallurgical Institute of Japan*, 101:781.

PACIFIC EXCHANGE RATE SERVICE. 2011. The University of British Columbia, Vancouver BC, Canada, Sander School of Business, Database retrieval system. <http://fx.sauder.ubc.ca/data.html>. Date of access: 2 February 2011.

PAPP, J.F. 2008. Chromium. Minerals Yearbook–2008 (Chromium – Advance release). Date of access: 2 February 2011. <<http://minerals.usgs.gov/minerals/pubs/commodity/chromium/myb1-2008-chrom.pdf>>

PAPP, J.F. 2009a. 2009 Minerals Yearbook Chromium [Advance Release]. Date of access: 19 October 2011. <<http://minerals.usgs.gov/minerals/pubs/commodity/chromium/myb1-2009-chrom.pdf>>

PAPP, J.F. 2009b. Chromium. Date of access: 2 February 2011. <<http://minerals.usgs.gov/minerals/pubs/commodity/chromium/mcs-2009-chrom.pdf>>

PAPP, J.F. 2011. Chromium. Date of access: 19 October 2011. <<http://minerals.usgs.gov/minerals/pubs/commodity/chromium/mcs-2011-chrom.pdf>>

PEI, W. & WIJK, O. 1993. A kinetic study on chromite ore smelting reduction. *Scandinavian Journal of Metallurgy*, 22:38-44.

PFISTER, J. 2006. *The Eskom plan to meet Government's 6% GDP aspiration*. Eskom, 27 March.

PISTORIUS, P.C. 2002. Reductant selection in ferro-alloy production: The case for the importance of dissolution in the metal. *The Journal of The South African Institute of Mining and Metallurgy*:33-36. January/February.

REEVES, G.M., SIMS, I. & CRIPPS, J.C., eds. 2006. Clay materials used in construction. Bath, UK: The Geological Society Publishing House.

RIEKKOLA-VANHANEN, M. 1999. *Finnish expert report on best available techniques in ferrochromium production*. Helsinki.

RIPKE, S.J. & KAWATRA, S.K. 2000a. Can fly-ash extend bentonite binder for iron ore agglomeration? *International Journal of Mineral Processing*, 60:181-198. Desember.

RIPKE, S.J. & KAWATRA, S.K. 2000b. Iron ore pellet binding mechanisms pozzolanic vs. physical binders. (*In Proceedings of the 21st International Mineral Processing Congress*. Rome, Italy: Elsevier Press. p. A4 120- A4 127.)

RIPKE, S.J. & KAWATRA, S.K. 2000c. Fibrous bonding mechanisms for reducing bentonite dosage. *American Foundry Society Transactions*, 108:101-104.

ROZA, G. 2008. Understanding the Elements of the Periodic Table – Chromium. New York, USA: The Rosen Publishing Group, Inc. 49p.

SASTRY, K. V. S. 1996a. *Role of Bentonite in the Balling of Iron Ore Concentrates*. Presentation given at the Bentonite Task Force Meeting of the Empire Pellet Plant, January 17.

SASTRY, K.V.S. 1996b. *Process Engineering Principles of Iron Ore Balling Circuits*. Presentation to Cliffs Mining Services Co., April 3.

SCHNEIDER, T. & JENSEN, K.A. 2008. Combined single-drop and rotating drum dustiness test of fine to nanosize powders. *Annals of Occupational Hygiene*, 52(1):23-34.

SCHROEDER, H.A. 1970. Chromium. Air Quality Monograph #70-15. Washington D.C., USA: American Petroleum Institute. 28p.

SENTULA. 2008. Nkomati Anthracite (Pty) Ltd. Date of access: 19 June 2011. <<http://www.sentula.co.za/pdf/Presentation%20Nkomati%20Site%20Visit%2010-09-2008.pdf>>

SINGH, V. & MOHAN RAO, S. 2008. Study the effect of chromite ore properties on pelletisation process. *International Journal of Mineral Processing*, 88:13-17.

SING, V., TATHAVADKAR, V., MOHAN RAO, S. & RAJU, K.S. 2007. Predicting the performance of submerged arc furnace with varied raw material combinations using artificial neural network. *Journal of Materials Processing Technology*, 183:111-116.

SME. 2006. Industrial minerals & rocks: commodities, markets, and uses, 7th ed. Littleton, Colorado, USA: Society for Mining, Metallurgy, and Exploration (SME) Inc.

SMIERNOW, G.A., DOHENY, E.L. & KAY, J.G. 1980. Bonding mechanisms in sand aggregates. (*In* AFS Transactions, Proceedings of the 84th Annual Meeting. p. 659-682.)

SOYKAN, O, ERIC, R.H. & KING, R.P. 1991a. The reduction mechanism of a natural Chromite at 1416 C. *Metallurgical Transactions B*, 22B:53-63.

SOYKAN, O, ERIC, R.H. & KING, R.P. 1991b. Kinetics of the reduction of Bushveld Complex chromite ore at 1416 C. *Metallurgical Transactions B*, 22B:801-810.

- TAKANO, C., ZAMBRANO, A.P., NOGUEIRA, A.E.A., MOURAO, M.B. & IGUCHI, Y. 2007. Chromites Reduction Reaction Mechanisms in Carbon–Chromites Composite Agglomerates at 1 773 K. *ISIJ International*, 47(11):1585-1589.
- VAN DEVENTER, J.S.J. 1988. The effect of additives on the reduction of chromite by graphite. *Thermochimica Acta*, 127:25-35.
- VAN OLPHEN, H. 1987. Dispersion and Flocculation. *In*: NEWMAN, A.C.D., ed. *Chemistry of Clays and Clay Minerals*, Mineralogical Society Monograph No. 6 ed. Essex, England: Longman Scientific and Technical.
- VELDE, B. & MEUNIER, A. 2008. The Origin of Clay Minerals in Soils and Weathered Rocks. Berlin Heidelberg, Germany: Springer.
- WAIT, M. 2011. Xstrata opens new mining complex in Steelpoort. *Mining Weekly*, 4 March.
- WEBER, P. & ERIC, R.H. 1992. Solid-state Fluxed Reduction of LG-6 Chromite from the Bushveld Complex. (*In* Proceedings of The 6th International Ferroalloys Congress. Cape Town, South Africa. p. 71-77.)
- WEBER, P. & ERIC, R.H. 1993. The Reduction Mechanism of Chromite in the Presence of a Silica Flux. *Metallurgical Transactions B*, 24B:987-995. December.
- WEBER, P. & ERIC, R.H. 2006. The reduction of chromite in the presence of silica flux. *Minerals Engineering*, 19:318-324.
- WENNINGER, C.E. & GREEN, R.A. 1970. Water-Clay Entities on Grain Surfaces as Defined by a Scanning-Type Electron Microscope. *Transactions of the American Foundrymen's Society*, 78:40-44.
- XIAO, Z & LAPLANTE, A. 2004. Characterizing and recovering the platinum group minerals – a review. *Minerals Engineering*, 17:961-979.

XSTRATA. 2011a. Helena mine. Date of access: 19 June 2011.
<<http://www.xstrataalloys.com/EN/Operations/Pages/HelenaMine.aspx>>

XSTRATA. 2011b. Lydenburg plant. Date of access: 19 June 2011.
<<http://www.xstrataalloys.com/EN/Operations/Pages/LydenburgPlant.aspx>>